Behaviour of Beam Lap Splices Under Seismic Loading

A thesis

submitted in partial fulfilment

of the requirements for the Degree

of

Master of Civil Engineering

in the

University of Canterbury

by

J. L. Wallace

University of Canterbury

1996

ABSTRACT

The results of an investigation into the performance of reinforced concrete beam-column subassemblages containing lap spliced reinforcement in the potential plastic hinge region of a beam are presented. Two specimens were tested with simulated seismic loading.

One specimen complied with the New Zealand Concrete Design Code, NZS 3101:1982, except for the placement of the lap splices. The second specimen contained beam reinforcement details from a building constructed in the early 1960s.

Current concrete design codes specify lap splices should not be placed in beam potential plastic hinge regions where inelastic reversing stresses are possible during seismic events. During testing the transverse steel specified for the confinement of the lap splices was unable to prevent bond deterioration between the spliced bars once inelastic bar strains had developed at one end of the splice. The failure of the lap splices led to a loss of lateral load capacity and a low level of ductility from the specimen.

Reinforced concrete buildings designed to pre-1970s codes may be considered inadequate when viewed in light of the provisions in current codes for seismic design. The testing of beam details taken from one such building indicates insufficient anchorage existed for the plain longitudinal beam bars in the joint. The loss of bond for the plain bars began in the initial load cycles of the test and led to a lack of specimen stiffness and lateral load capacity. The presence of the lap splices is considered to have accelerated the loss of bond from the bars.

Testing investigating the performance available from plain bar reinforced subassemblages should use anchorage for the bars that represent the conditions in the existing structure. The rapid loss of bond from the bars during cyclic loading can lead to the member end connections influencing the test results.

Acknowledgments

The author would like to thank the Earthquake and War Damage Commission for the EQC research funding used to complete the testing.

The efforts of the technicians Mr Norrie Hickey and Mr Gavin Hill during the construction and testing of the specimens were appreciated.

Post-graduate student Mr S Hakuto was helpful during the testing programme with advice and for information on the test rig.

Supervisors Mr Bull and Professor Park kindly gave their time to discuss aspects of the project and reviewed the chapters of the thesis. Their contribution to the project is gratefully acknowledged.

I would like to thank my family for their encouragement during the project.

CONTENTS

NOTATION

A_b area of an individual bar, mm^2

Ag gross area of section, mm^2

A_s area of non-prestressed tension reinforcement, mm^2

A_{sp} area of flexural reinforcement provided, mm^2

A_{sr} area of required flexural reinforcement, mm^2

A_{tr} smaller of area of transverse reinforcement within a spacing s crossing plane of splitting normal to concrete surface containing extreme tension fibres, or total area of transverse reinforcement normal to the layer of bars within a spacing, s, divided by n, mm^2

c the smaller of c_C or c_S, mm (NZS 3101:1982)

c_C distance measured from extreme tension fibre to the centre of the bar, mm (NZS 3101:1982)

c_m the smaller of the concrete cover or the clear distance between bars, mm

c_S the smaller of the distance from the face of the concrete to the centre of the bar, or half the centre-to-centre distance of bars in the layer, mm (NZS 3101:1982)

For splices, c_S was the smaller of the distance from the concrete side face to the centre of the outside bar, or one half the clear spacing of bars spliced at the same location plus a half bar diameter, mm

d_b nominal diameter of bar, wire or prestressing strand, or in a bundle, the diameter of a bar of equivalent area, mm

f'_c specified compressive strength of concrete, MPa

f_y lower characteristic yield strength of non-prestressed reinforcement, MPa

f_{yt} lower characteristic yield strength of transverse reinforcement, MPa

h_b beam depth, mm

h_c column depth parallel to longitudinal beam bars being considered, mm

k_{tr} an index of the transverse reinorcement provided along the anchored bar, $A_{tr}f_{yt}/10s$, expressed as mm (NZS 3101:1982)

L_d development length, mm (l_d, NZS 3101:1982)

L_{db} basic development length of a straight bar, mm (l_{db}, NZS 3101:1982)

n number of bars in a layer

n_L number of ties provided within L_d

s maximum spacing of transverse reinforcement within L_d, or spacing of stirrups or ties or spacing of successive turns of a spiral, all measured from centre-to-centre, mm

V_i ideal horizontal load capacity of the specimen

$\alpha_a, \alpha_b, \alpha_c, \alpha_d, \alpha_e$ parameters used in determining development lengths for straight reinforcing bars

μ displacement ductility factor

CHAPTER ONE

INTRODUCTION

The limited lengths in which reinforcing bars are available make it necessary to link the bars for the construction of most reinforced concrete structures. Reinforcing bars may be welded together or use a form of mechanical coupling, but for economic reasons two bars are often simply overlapped for a distance to create a lap splice. The transfer of forces from one bar to the other is completed through the concrete surrounding the bars.

In earthquake-resistant reinforced concrete structures, sections of members may have to endure large deformations during severe seismic events. In these sections, known as potential plastic hinge regions, damage to the concrete will be inevitable.

As the performance of lap splices is dependent on the condition of the surrounding concrete, present building codes require lap splices to be placed in regions where the integrity of the concrete will be maintained. Previous codes were not as strict on the placement of lap splices and in older reinforced concrete buildings they may have been placed in areas now recognised as potential plastic hinge regions.

This project examined the behaviour of two beam-column subassemblages containing lap spliced reinforcement in a beam potential plastic hinge region. These specimens were constructed for simulated seismic loading tests to investigate the performance of the specimens and the lap splices.

The first specimen complied with the New Zealand Concrete Design Code, NZS 3101:1982, except that the lap splices for the deformed longitudinal bars were placed in a beam potential plastic hinge region. The behaviour of the lap splices and their influence on an otherwise ductile reinforced concrete design are presented.

Seismic design procedures have developed significantly in New Zealand since about 1970. This has led to an awareness that the design of reinforced concrete buildings before this period may be inadequate in several areas. One area of concern is that the anchorage for longitudinal bars in existing structures may not be sufficient according to current code requirements. This

deficiency may be found in early structures reinforced with plain round bars. Present design codes specify plain bar anchorage lengths to be twice that for deformed bars.

The object of the second specimen was to review the seismic capacity of beam details from a building constructed in the early 1960's. Two details of concern were: plain round longitudinal bars lap spliced in the potential plastic hinge region of one beam; a relatively small column depth in comparision to the ratios required in recent design codes for the column depth to longitudinal beam bar diameter. The effect of these on the behaviour of the specimen is discussed.

Research describing the response of plain longitudinal bars to simulated seismic loading is limited. The results from the testing of the second specimen provide additional information on their behaviour during this form of loading.

CHAPTER TWO

LITERATURE REVIEW

2.1 INTRODUCTION

The relationship between steel and concrete in reinforced concrete members is examined with a discussion of anchorage, bond and bar slip. These factors are reviewed as they have a role in lap splice behaviour.

Previous research on lap splices is surveyed with particular reference to loading conditions simulating seismic actions.

2.2 BOND AND ANCHORAGE

2.2.1 General

Satisfactory performance of reinforced concrete structures requires composite action between the reinforcing steel and the surrounding concrete. Bond stresses along the concrete-steel interface modify the steel stress along the bar length by transferring force between the bar and the surrounding concrete [6]. Two distinct situations lead to the formation of bond stresses in reinforced concrete members:

(a) Anchorage or development bond stresses are required in the end region of bars to transmit the bar force to the concrete.
(b) Flexural bond stresses occur along a bar due to the change in bar force as a result of variation in bending moment along a member.

2.2.2 Bond Resistance

Classic bond theory describes three components that contribute to the bond stresses on an embedded bar:

(a) Chemical adhesion
(b) Friction
(c) Mechanical interaction between concrete and steel.

Bond for plain round bars depends primarily on the first two elements. Once sufficient force is applied to break the adhesion, the bar slips relative to the surrounding concrete. Further bond can be developed only by friction between concrete and steel and the wedging action of small dislodged particles.

Deformed bars depend primarily on the mechanical interlocking of the ribs or deformations, that stand proud above the surface of the bar, with the surrounding concrete to provide bond capacity. The bond capacity of deformed bars is typically superior to that of plain round bars. Figure 2.1 shows three types of stress associated with the bond strength of deformed bars:

(a) Shear stresses v_a developed through adhesion along the surface of the bar.
(b) Bearing stresses f_b against the face of the rib.
(c) Shear stresses v_c acting on the cylindrical concrete surface between adjacent ribs.

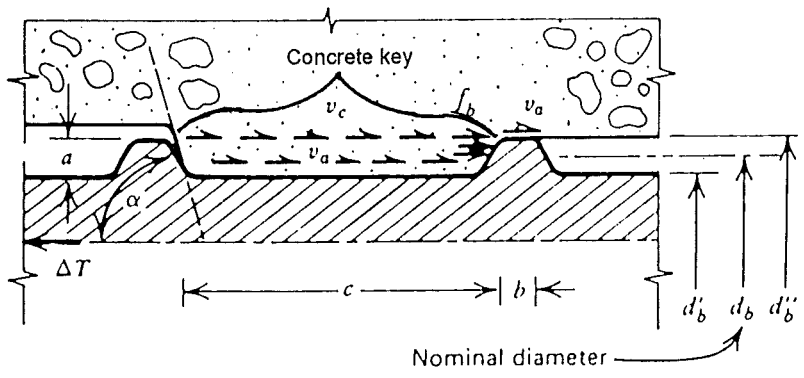

Figure 2.1 The Stresses Between Two Ribs of a Deformed Bar [1].

Experimental evidence indicates that the nature and distribution of bond stresses is far more complex than classical theory suggests. Lutz and Gergely completed a finite element analysis of bond stresses and supported their theoretical analysis with experimentation [4]. A cylinder of concrete with a concentrically embedded deformed reinforcing bar was analysed. The model represented the situation existing between two flexural cracks near a reinforcing bar in a concrete member. The bond stress distribution resulting from the analysis is shown in Figure 2.2.

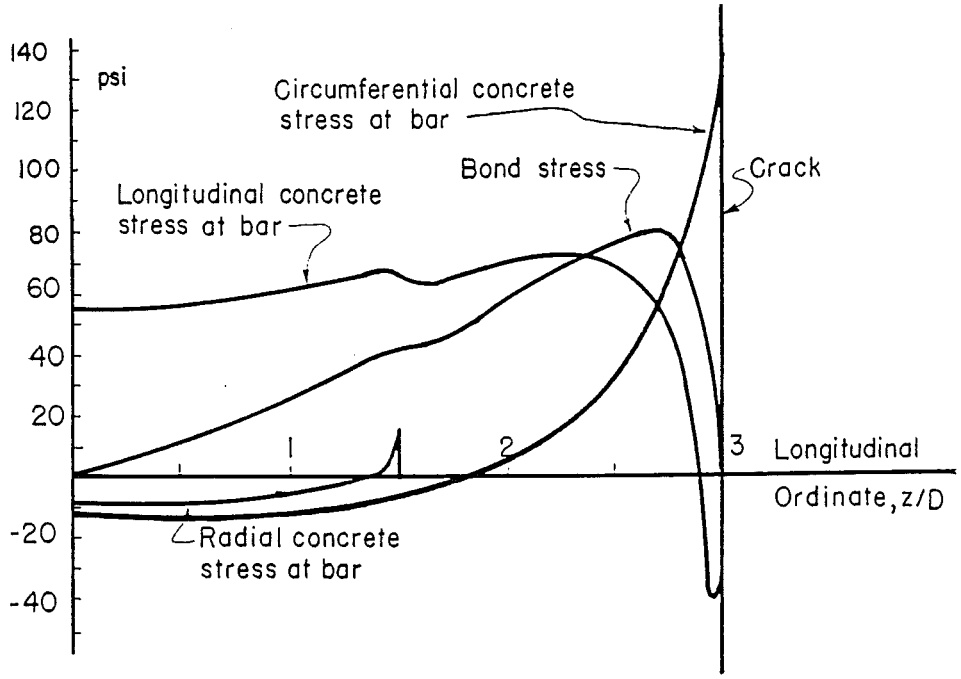

Figure 2.2 Longitudinal Variation of Stresses in a Concentric Pull-out Specimen, at f_s = 6.9 MPa [4].

The following three effects were noted:

(a) Circumferential tensile stresses caused by bonding forces near transverse cracks can start radial (splitting) cracks.

(b) Longitudinal tensile stresses at the concrete-steel interface can form internal transverse cracks.

(c) Radial tensile stresses resulting from dowell action of flexural reinforcement can prevent contact near the crack and allow separation and slip of the bar.

Bond strength is affected by the quality of the concrete immediately surrounding the reinforcing bar, which can be influenced by its placement relative to the reinforcing bars. Water gain, sedimentation and aggregate segregation under bars results in a localised zone of concrete that has compression and tension strengths reduced below that of the main body of the concrete. Bars in the top of concrete elements with more than 300mm of fresh concrete cast beneath [2] are expected to gain greater amounts of air and water beneath them. Their bond strength will be less than that for bars placed lower in an element. This effect is offset in codes of practice by requiring an increase in the anchorage length for bars in these conditions [2,3].

2.2.3 Anchorage

Stress from a deformed bar is transferred by a combination of direct bearing and wedging action between the reinforcement ribs and the concrete. The resultant force can be broken into components parallel and perpendicular to the reinforcing bar axis as shown in Figure 2.3.

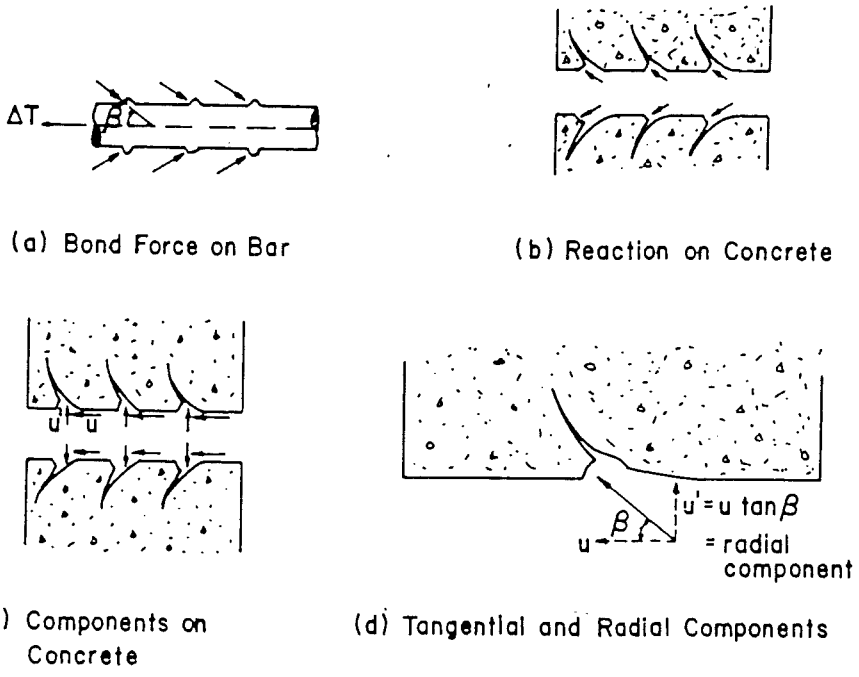

Figure 2.3 Forces Between a Reinforcing Bar and the Surrounding Concrete [5].

The bond component is responsible for the change in bar force. The radial component induces a circumferential tensile stress field in the surrounding concrete. Longitudinal cracks form along the axis of the bar when the tensile stress exceeds the tensile capacity of the surrounding concrete. If splitting of the concrete cover occurs and spalling results, effective anchorage of the reinforcement is prevented and a bond splitting failure follows [16].

When reinforcement is discontinued in a member, the length of embedment between the free end and a critical section is called the 'anchorage length'. Anchorage of straight lengths of deformed reinforcement can fail in one of two ways:

(a) The concrete key (see Figure 2.1) between the rib deformations can fail in shear (often called 'pullout').
(b) The concrete surrounding the bar, can split longitudinally, parallel to the bar axis, leading to loss of effective anchorage.

The first failure mode usually occurs with relatively short anchorage lengths or when significant confinement or volume of concrete around the bar is present. The second failure mode is called bond splitting [16] and is the most common for anchored bars with usual transverse steel contents, concrete cover thicknesses and anchorage lengths.

2.3 BOND STRESS-SLIP RELATIONSHIPS

2.3.1 General

Unless the strain of the concrete and steel is the same and constant over a length, a deformed bar will attempt to move or slip in relation to the surrounding concrete. Initially chemical adhesion and mechanical interaction prevents slip. As the load is increased, adhesion is lost and slip occurs, the ribs of a deformed bar restrain the movement by bearing against the concrete. In the case of plain bars, friction provides the resistance to slip once adhesion is destroyed.

Cyclic loads with a low number of stress reversals commonly represent seismic loading actions. The following section discusses slip in relation to this type of loading for deformed bars.

2.3.2 Bar Slip during Cyclic Loading

For deformed bars under cyclic loads, concrete strength, geometry and spacing of deformations, cover, bar spacing, and the amount of transverse reinforcement play a large role in the bond-slip behaviour .

For a specimen representing an interior beam-column joint, the bond stress-slip response of a bar loaded by low-cycle loads is shown in Figure 2.4. Initially the curve follows the envelope for behaviour under monotonic loading. If a bar is loaded beyond approximately one-half of its ultimate bond stress value, a significant permanent slip will remain after the bar is unloaded. Before load can be carried in the opposite direction the bar must move back to bear on concrete. As cycling proceeds, concrete in front of the ribs is progressively crushed and sheared. Hence increasingly larger slip occurs in each direction during cyclic loading before load and bond stress values increase. The values do not return, however, to previous levels of maximum stress [6].

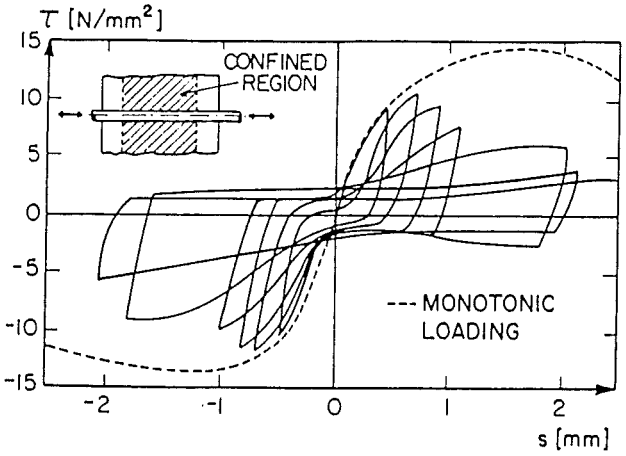

Figure 2.4 Bond Behaviour Under Low-Cycle Loads [6].

2.4 REVIEW OF EXISTING STRUCTURES

Research projects (36, 37) completed at the University of Canterbury Civil Engineering Laboratory have tested specimens representing existing members designed to earlier New Zealand concrete design codes. Bridge piers and columns each with plain round bars for longitudinal reinforcement have been tested with simulated seismic loading to examine their performance. These specimens lacked adequate bond between the plain longitudinal bars and the surrounding concrete. The column specimens (37) experienced significant softening of the lateral load-displacement relationship during the first cycle to three-quarters of the ideal lateral load capacity. The column units displayed a relatively low capacity to dissipate energy and a large reduction in strength by the end of testing. The available structural ductility measured for these specimens was between 2 and 2.5.

2.5 LAPPED SPLICES

2.5.1 General

The fundamentals of bond, anchorage and slip have been discussed in previous sections. They are crucial factors in the behaviour of lapped splices.

Two bars placed side by side forming a lapped splice are in effect two anchored bars. A transfer of force from one bar to the other is achieved with the development of bond stresses

in the surrounding concrete along the splice length. The bar forces being transferred generate shear stresses and splitting forces in the surrounding concrete. Adequate bond along the bar surfaces and the ability of the concrete to transfer shear without excess deformation is essential for a lapped splice to function satisfactorily.

Early testing of lapped splice performance was conducted under monotonic loading conditions. Since the late 1970's reversed cyclic loading conditions simulating seismic action has revealed significantly different lap splice behaviour. The Department of Structural Engineering at Cornell University appears to have been first to investigate this area [21]. They continued and have contributed much of the knowledge on this subject [13,15,16,18,23].

A number of parameters have been found to have significant influence on the behaviour of lapped splices. A survey of the literature is presented under these headings.

2.5.2 Longitudinal Reinforcement

The adverse effect of increasing bar diameter on bar anchorage has been known for some time [7]. Larger bond stress concentrations can be expected with larger bars as the ratio of cross-sectional area to bar surface area is directly proportional to bar diameter. Longer anchorage lengths for increasing bar diameters can offset this. The use of larger diameter bars results in an increase in the size of the cracks that can develop along the bar length. These cracks act as points of weakness which tend to initiate any eventual splitting failure. Tests have shown that it is almost impossible to avoid a splitting anchorage failure for bar sizes greater than 50mm [9].

In evaluating the performance of splices the actual reinforcement strengths that need to be developed during severe loading conditions should be considered. Yield stresses appreciably above the nominal design value and enhanced strength through strain hardening have been found to prevent a ductile response in members containing lap splices because of splice bond failure occurring before the bar reached yield [10]. Applying a safety factor to the lap length using a steel stress 25% above reinforcing nominal yield strength was found to be inadequate [11].

2.5.3 Concrete Strength

Cracks are formed in concrete when tensile stresses, induced by bond action, exceed the tensile strength of the concrete. It has been shown that these cracks develop further with increase in steel stress, causing bond deterioration and ultimately preventing force transfer between concrete and steel [12]. The tensile strength of concrete is usually considered to be a function of the compressive strength f'_c, and is generally less than $0.2f'_c$ [1]. On this basis, bond strength will improve with increasing concrete compressive strength.

Results from monotonic load tests show diminishing increases in splice strength with increasing concrete strength until a compressive cube strength of concrete around 70 MPa [8]. Concrete strengths beyond this had a negative effect on splice strength. Shrinkage of the concrete accounts for some of this, as shrinkage increases with increasing quantities of cement. Restraint of the shrinkage in the vicinity of the bar results in tensile stresses in the surrounding concrete. These tensile stresses are superimposed on bond stresses around the reinforcing bars [8].

Another reason for the reduction in splice strength is the greater stiffness of higher strength concrete. This leads to poor bond performance when high localised bond stresses are unable to be redistributed effectively [8].

The ability of concrete to redistribute stress is reflected in recommendations for the seismic design of lap splices. For higher strength concretes, shorter splice lengths were preferred with small stirrup spacings to encourage an even redistribution of bond stress near failure [13]. Concrete strength is considered to have a relatively minor role in the behaviour of lapped splices under simulated seismic conditions. Its influence over the onset of concrete splitting in monotonic loading is reduced in seismic conditions where considerable concrete damage may occur before failure [24].

2.5.4 Splice length

Research into splice performance under monotonic loading conditions has shown increasing splice strength and reduced average bond stress with increasing splice length [7]. For splices without transverse steel an upper limit on splice length was found beyond which there was no increase in strength [14]. Later study found the use of transverse steel allowed further increases in strength with increases in the splice length [8].

Orangun et al [5] developed an expression for the bond strength of embedded and spliced bars using regression analysis of published data. Development and splice lengths were found to be equal and provisions were given for their reduction with enhanced confinement from increased concrete cover and larger quantities of transverse steel. The data base for this study, however, was limited to specimens that were tested under monotonic loading and that failed prior to yielding of the main reinforcement.

The relevance of equal development and splice lengths for cyclic loading conditions was discussed by Gergely et al [15]. Tests at Cornell University had shown that this was valid for splices with relatively little confinement. These splices failed when one spliced bar began to lose its anchorage as stirrups yielded at the splice ends. Splices with sufficient confinement, particularly during repeated loading situations, experienced a redistribution of forces well before failure. Yielding of the spliced bars led to splitting of the surrounding concrete. Progressive yield penetration during the repeated loading reduced the length over which one spliced bar could transfer forces to the other. Bond forces became almost uniform in both spliced bars, superimposing the radial bursting forces and requiring a splice length greater than the development length. A minimum splice length of 30 bar diameters was suggested for splices designed to resist a limited number of cycles beyond yield.

Finite element analyses completed at Cornell University verified the assertion that spliced bars require greater bond lengths than single anchored bars with equal amounts of confinement [16]. The authors considered shorter splices (30-40 bar diameters) demonstrated superior performance because they displayed more favourable redistribution properties.

Research conducted at Canterbury University [24] concluded that long splice lengths did not prevent splices "unzipping" due to gradual yield penetration during cyclic loading.

2.5.5 Cover and Splitting Patterns

Increases in splice strength have been reported with increases in concrete cover or beam width for monotonic loading conditions [7]. Similar effects on splice strength have been found when the spacing between two splices is increased [14]. Tepfers [8] agreed, reporting that for monotonic loads the cover splitting pattern at failure is a function of bar size, cover and bar spacing. Based on test observations a set of cover splitting patterns were selected and used to develop equations of splice strength.

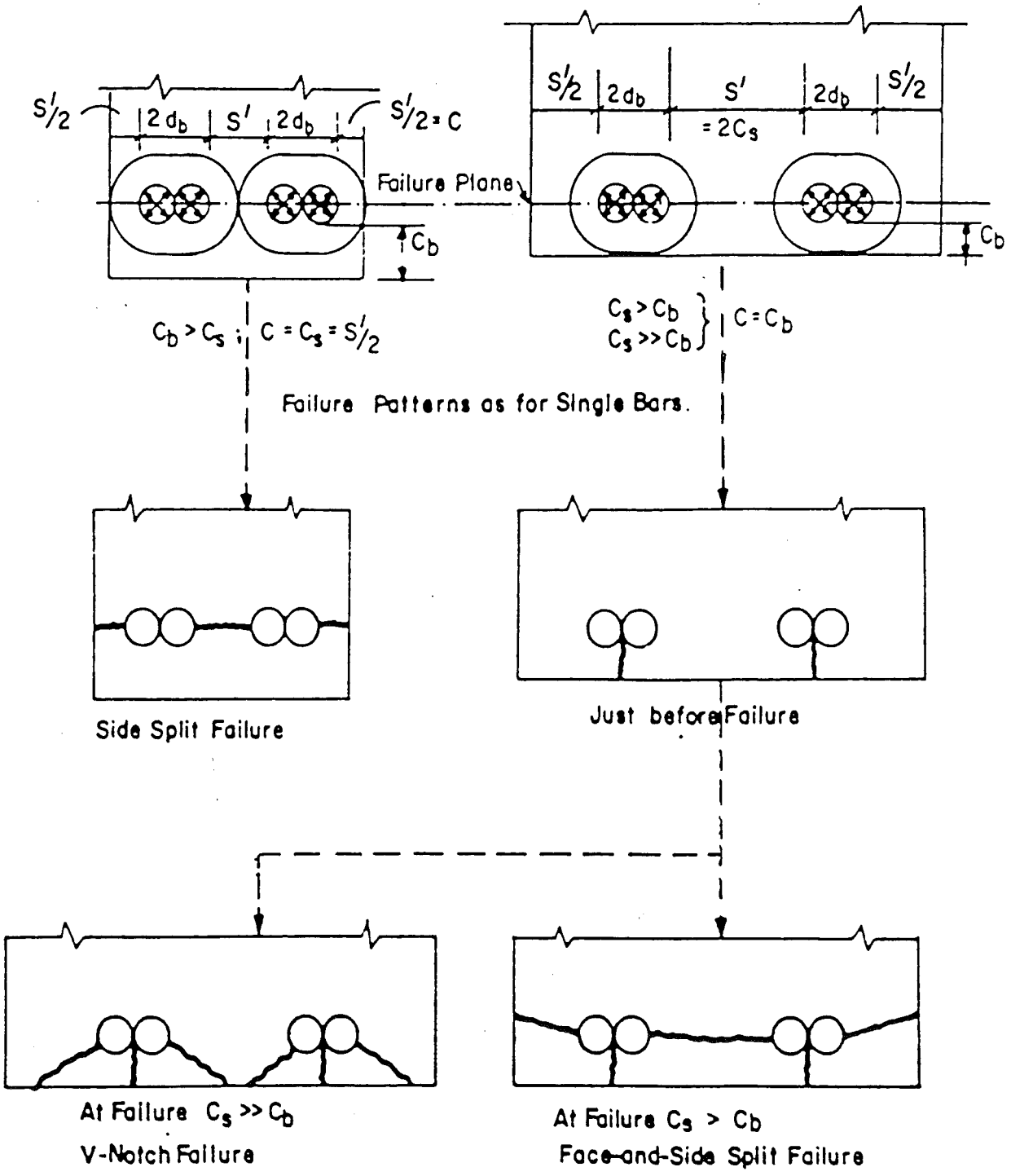

Figure 2.5 Failure Patterns in Lapped Splices [5].

Figure 2.5 shows the failure patterns for spliced bars and the effects of the amount of clear spacing c_s and bottom cover c_b. Increases in the value of c_s or c_b delays the onset of splitting of the concrete cover that occurs due to the radial and circumferential tensile stresses that arise from the transfer of forces between the spliced bars.

Analysis of results from monotonically loaded spliced bars led Orangun et al [5] to conclude that the limit between pullout and splitting failure is a cover distance to bar diameter ratio c/d_b of about 2.5 [5].

Concrete cover plays a less significant confinement role for splices subjected to cyclic loading compared to those loaded monotonically [16,18,24]. The considerable cover cracking before failure led the Cornell University researchers to believe that cover resistance was an unreliable factor. Provided that the cover did not suppress a longitudinal splitting mode of failure, it was not a consideration when developing a model predicting splice strength. A minimum clear cover of $1.5d_b$ was found to be sufficient for load transfer requirements. All beams subjected to cyclic loading with splices located in a constant moment region experienced longitudinal bond splitting failures. Typically, side and bottom cover cracking lead to a corner cover spalling mechanism and the loss of force transfer between spliced bars [16].

2.5.6 Loading History

The application of many cycles of repeated loads, with loading applied only in one direction are reported to have little effect on the performance of anchored and spliced bars when the load level is below 70% of the ideal strength [8,19]. A few cycles of repeated load above 90% of the bar yield forces, however, rapidly increased the rate of bond deterioration in a splice [18].

The effects of stress reversals (loading cycles applied in both directions) with load levels beyond the ideal strength of lapped splice members was first investigated by Cornell University [15]. Beams containing lap splices were subjected to reversed loading and compared with specimens subjected to repeated or monotonic loading. The rates of cracking, damage penetration and strain increase were greater for the specimens with reversed loading. The number of cycles before failure was always significantly greater for repeated loading [15].

Further research concluded that the greater severity of reversed loading was partially due to the alternating directions of bond stress and associated cracking during each cycle. Other effects included cover damage due to reversing curvatures of the primary bars and localised concrete failure at the deformations and at the bar ends. In these respects larger diameter bars were considered more damaging [16].

At Cornell University, researchers using reversed cyclic loading were unable to prevent longitudinal bond splitting failures for spliced bars located in constant moment zones [16]. Suggestions for design were based on splices sustaining a specified number of cycles in the inelastic range. A minimum of 15 to 20 reversed load cycles beyond the yield of the bar and a maximum steel strain (one-off) in the splice of at least 2.5 times the yield strain were considered as indicative of satisfactory performance. It was recommended that splices should not be used close to ground level in the first storey columns due to the high demands of plastic hinges in those columns [13].

The behaviour of compression lap splices under inelastic repeated loading was examined in beam and column specimens detailed to satisfy the above design suggestions [23]. Most of the specimens failed with crushing of the concrete outside the splice region after meeting previous criteria for satisfactory performance. A small number of changes to the original guidelines [13] were proposed. It was concluded that the design recommendations may be used for tension and compression lap splices subjected to inelastic cyclic loads [23].

2.5.7 Transverse Reinforcement

Investigations by Tepfers [8] under monotonic loading conditions revealed increases in splice strength and changes in the modes of failure when stirrups or spiral transverse reinforcement was present. Whereas splices without transverse reinforcement burst in a brittle manner with little warning, the presence of confining steel resulted in a gradual method of failure. Stirrups spaced uniformly along the splice were found to be less effective than a number of stirrups concentrated at each end of the splice where bond stresses were largest.

Tests under repeated and reversed cyclic loading showed the importance of stirrups spaced uniformly along the splice length [15]. As stresses at the splice ends reached yield, damage spread along the splice. With relatively short splice lengths (30 to 35 bar diameters) larger stirrups at greater spacing were considered inferior to smaller stirrups at closer spacing [15].

According to the ACI Committee 408 (1979) provisions for development and splice lengths [20] the maximum effective amount of transverse reinforcement of area A_{tr} required for monotonic loading is

$$\frac{A_{tr}}{s} = \frac{10.5 d_b}{f_y} \; mm \tag{2.1}$$

where s = stirrup spacing, f_y = the yield strength of the longitudinal reinforcement and d_b = the nominal diameter of the longitudinal reinforcement.

A lapped splice in a beam provided with transverse steel satisfying Eq. 2.1 failed in flexure when tested under monotonic loading [21].

Further investigations involving reversed cyclic loading have concluded that the presence of transverse reinforcement reduces the propagation of longitudinal splitting, bar slip and to some degree yield penetration along the splice length. The presence of transverse reinforcement was also recognised as an important factor in bond-shear interaction. Specimens were detailed with up to twice the amount of transverse reinforcement required by Eq. 2.1. Generally stirrup strains did not reach yield in the most heavily confined splices and failure of the splice was delayed until damage of the cover concrete induced failure. An equation giving the recommended spacing of stirrups along a splice was suggested [16].

Research at Canterbury University during the early 1980s investigated the performance of lapped splices in column and bridge pier specimens under reversing cyclic loads [25]. Large amounts of transverse reinforcement were found to improve bond performance by limiting yield penetration into the splice region. Progressive longitudinal bond failure was sometimes prevented, and in those cases main bar fracture occurred during large inelastic displacements. The study indicated that lapped splices could be used in columns designed to resist severe seismic loads provided that the splices were not located in regions where there was significant yielding of longitudinal reinforcement [25].

2.5.8 The Effect of Shear Force on Splice Placement

When lap splices are located in zones of constant moment, both bars are equally stressed. When shear is present, a moment gradient exists and the maximum force in one of the bars is less than in the other.

Monotonic load tests indicate that a moment gradient has little influence on splice strength if the shear force is moderate. However, splices located in regions of high varying shear may not perform as well [5].

Investigations at Cornell University [16] into splice behaviour during inelastic cyclic loading included an examination of the influence of moderate levels of shear. Figures 2.6(b) and 2.6(c) show the details used for splices placed in regions of constant moment and regions of shear. When shear was present, damage and yield penetration was found to be confined to one end of the splices resulting in superior splice performance. Bond failure had not occurred when the loading was discontinued for some of these specimens. The amount of transverse steel provided for confining the splice was at least four times greater than the amount required to resist levels of nominal shear stress up to 1.73 MPa. To counter the effects of dowel action on the anchorage capacity of the spliced reinforcement it was recommended that the close spacing of the stirrups should be continued for a distance d beyond the high moment splice end, where d = the effective depth of the beam.

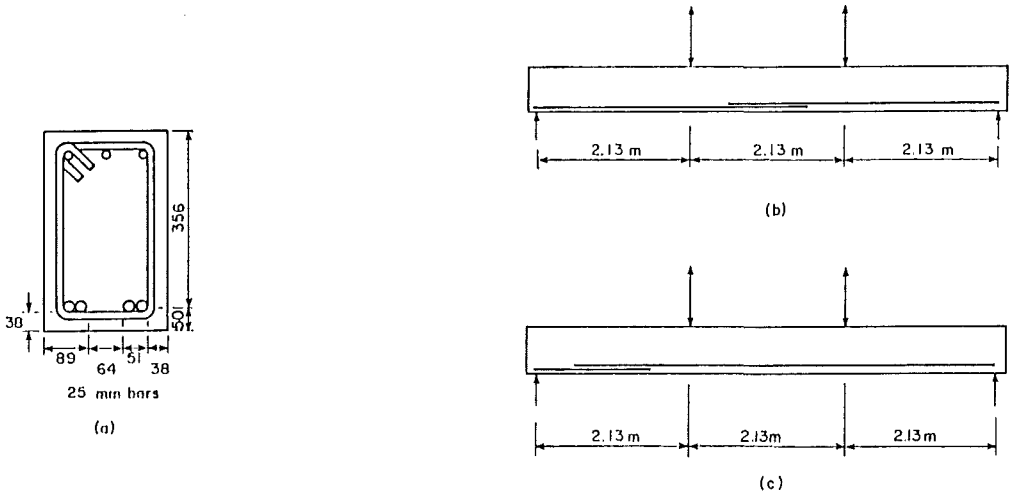

Figure 2.6 Beam Specimen Details (a) Typical Cross-Section (b) Splice in Constant Moment Region (c) Splices in Shear Region [16].

Comparison of tests indicate no significant difference in the overall behaviour of specimens with splices lapped side by side (as shown in Figure 2.6 (a)) and those lapped one above the other. Earlier side cover splitting and increased strains in vertical stirrup legs was noted in the latter case [18].

The depth of cast concrete has an effect on the bond strength of splices in the top layer of bars in horizontally cast members. These splices were found to experience more cover splitting than those with less concrete cast underneath the bars. The weaker concrete matrix surrounding the top bars and water gain in the top in easily workable mixes were recognised as contributing factors [18].

2.5.9 Summary

The performance of lap spliced reinforcing bars has been investigated in a number of research programmes. The literature review in this Chapter considers factors affecting the behaviour of splices under a variety of loading conditions. Reversed inelastic cyclic loading simulating intense seismic action, however, is of particular interest. The following conclusions have been drawn from the literature review:

1. Increase in bar diameter leads to a decrease in anchorage capacity for a given splice length, and is detrimental to splice performance during reversed cyclic loading.
2. Concrete strength has relatively little effect on the performance of lap splices confined by significant quantities of transverse reinforcement during simulated seismic loading, because of the considerable concrete damage before failure.
3. The development length for single anchored bars, determined from monotonic testing, is insufficient for spliced bars designed to resist a limited number of load cycles with the bars in the inelastic range. Additional splice length may improve the splice performance during cyclic loading. However, it will not prevent a longitudinal splitting failure if progressive bond deterioration occurs.
4. When large amounts of transverse steel are used to provide splice confinement in reversed cyclic loading conditions the role of the concrete cover in providing confinement is less important.
5. The amount and distribution of transverse reinforcement in a spliced region is an important factor for all loading conditions. Sufficient confinement will limit the propagation of longitudinal splitting along the splice.
6. The loading history governs the anchorage behaviour of spliced bars when cyclic loading exceeds 70% of the ideal strength of the splice. Reversed cyclic loading causes more bond deterioration along splices than repeated (single direction) loading and the number of cycles to failure is significantly less. It is impossible to prevent progressive

bond deterioration along splices located in constant moment regions under inelastic reversing loads.

7. When shear and moment are present in a spliced region the damage and yield penetration occurs only at the end of the splice where the moment is maximum.

CHAPTER THREE
LAP SPLICE CODE REQUIREMENTS

3.1 INTRODUCTION

This chapter reviews some of the previous code requirements that relate to the placement and detailing of lap splices, particularly those from NZS 3101:1982 [2] to which Specimen One was designed.

Bond and anchorage provisions in the current code of practice NZS 3101:1995 [30] are briefly discussed to highlight the changes between the codes.

3.2 CODE REQUIREMENTS FOR SPLICE LENGTH AND LOCATION

3.2.1 General

Anchorage requirements in the previous New Zealand concrete design code NZS 3101:1982 [2] closely followed ACI Committee 408 recommendations [20] for development and lap splice lengths. Orangun et al [5] completed an analytical review of development length and lap splice data from monotonic test conditions and gave equations for predicting anchorage strength. These were simplified by ACI Committee 408 to facilitate design usage and after minor alterations were adopted for the New Zealand code.

The New Zealand code NZS 3101:1982 [2] specified that the minimum lengths for lap splices in tension and compression were the development lengths for tension and compression, respectively. The development length of deformed bars was a product of the basic development length and any applicable modification factors.

3.2.2 Development Length for Deformed Bars in Tension

For deformed bars in tension the basic development length was

$$l_{db} = \frac{380 A_b}{c\sqrt{f'_c}} \qquad (3.1)$$

where A_b = area of bar being developed, mm^2

c = the smaller of cover parameters c_s and c_c, as shown in Figure 3.1, mm

f'_c = specified compressive cylinder concrete strength, MPa.

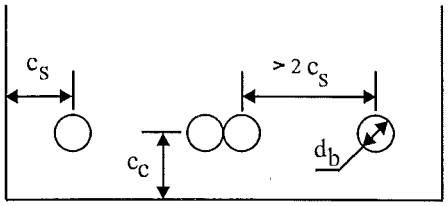

c_s- The smaller value of either the horizontal cover plus $0.5d_b$ or half the horizontal centre - to - centre distance between bars (ignoring lap splice pairs).

c_c- The vertical cover plus $0.5d_b$.

Figure 3.1 Definition of Distances c_c and c_s.

Other basic development length equations allowed simpler calculations when greater bar spacing and cover was available and any reduction in development length due to transverse reinforcement was ignored.

The final development length l_d for a bar was the resultant of the basic development length l_{db} multiplied by modification factor or factors as follows:

(i) With reinforcement having a lower characteristic yield strength (f_y) other than 300 MPa

$$\frac{f_y}{300}$$

(ii) For top horizontal reinforcement with reduced bond quality due to more than 300mm of fresh concrete cast below the bar .

1.3

(iii) In members not resisting seismic load with reinforcement in excess of that for flexure, shrinkage and temperature requirements.

$$\frac{A_{sr}}{A_{sp}}$$

(iv) Where at least three transverse reinforcing bars crossed a potential crack over the development length

$$\frac{c}{c+k_{tr}} \qquad \text{where} \qquad k_{tr} = \frac{A_{tr} f_{yt}}{10s} \leq d_b \qquad (3.2)$$

However the development length for deformed bars in tension was to be not less than 300mm.

The symbols used in the equations are also defined in the list of symbols at the beginning of the thesis.

3.2.3 Development Length for Deformed Bars in Compression

For compression splices the basic development length was

$$l_{db} = \frac{0.22 d_b f_y}{\sqrt{f_c'}} \qquad \text{[Amendment No.1, December 1989]} \qquad (3.3)$$

but not less than $0.040 d_b f_y$ where d_b was the nominal bar diameter.

Modification factors could reduce this development length by a factor of 0.75 if sufficient transverse steel existed, and in proportion to reinforcement in excess of that required by analysis provided it was not a detail required to resist seismic loading.

The length of a lap splice in compression was not to be less than $0.067 f_y d_b$ for steel with a f_y of 430 MPa or less, $(0.12 f_y - 22) d_b$ for a f_y greater than 430 MPa, nor 300mm [Amendment, No. 1, 1989]. When the specified concrete strength was less than 20 MPa the splice length was to be increased by one-third.

3.2.4 Splice Placement and the Development Length for Plain Bars

The use of plain bars for longitudinal reinforcement in structures has been restricted since the issue of the draft New Zealand code DZ 3101:1978 [27]. NZS 3101:1982 did not permit their use in structures designed to resist seismic loading as their bond performance was considered unsatisfactory under inelastic reversed loading conditions. Plain bars were only acceptable as flexural reinforcement under other loading conditions when special reasons existed; for example, they could be considered when fatigue criteria governed [28]. In such cases the

development length for a plain bar was twice that of a similar sized deformed bar and not less than 24 bar diameters for a plain bar in tension.

Earlier New Zealand codes of practice [27,29] recognised that lap splices should be located away from points of maximum tensile stress. This was encouraged by specifying increased lap lengths when large percentages of the tensile reinforcement were spliced or in conditions of high steel stress. NZS 3101:1982 [2] set restrictions on lap splice placement in members designed for seismic loading. To ensure reliable anchorage for longitudinal beam bars, no portion of a lap splice could be located within a beam/column joint region, or within one effective depth of the member from a potential plastic hinge region.

Bundled bars were able to be lap spliced with increases in lap length of 20% for a three bar bundle and 33% for a four bar bundle. The increases allowed for reductions in the exposed perimeters of the bars. Bars larger than 35 mm in diameter could not be lap spliced.

3.3 TRANSVERSE STEEL CODE REQUIREMENTS FOR LAP SPLICES

Transverse reinforcement in potential plastic hinge regions of beams serve three purposes:

(i) Prevent the buckling of longitudinal bars in compression.
(ii) Provide confinement for the concrete in the compression zone.
(iii) Act as shear reinforcement.

The New Zealand code, NZS 3101:1982 [2], had the following transverse steel requirement for lap splices in beams and columns. Tensile reinforcement was not to be spliced in a region of tensile or reversing stress unless each spliced bar was confined by a stirrup-tie so that

$$\frac{A_{tr}}{s} \rangle \frac{d_b f_y}{48 f_{yt}} \qquad \text{[Amendment No.1, December 1989]} \qquad (3.4)$$

where A_{tr} was the area of transverse reinforcement with a specified yield strength f_{yt} and at a spacing s.

Lap spliced column specimens tested in accordance with the above equation were found to support at least 85% of the ideal column strength in at least 20 cycles of reversed loading. These splices were found to sustain a few limited cycles beyond yield [28].

3.4 REVIEW OF NZS 3101:1995

NZS 3101:1995 [30] contains refinements and design simplifications which have been developed since NZS 3101:1982 was released. Changes relevant to the requirements discussed previously in this chapter are revisions to the clauses for bond and anchorage. Some of these revisions are discussed here. In Appendix I both the previous and present equations are used to calculate the length of the lap splice of Specimen One.

Deformed reinforcing bar is to be used for all non-prestressed longitudinal reinforcement unless there is a special reason for using plain bars.

The equation for the development length of deformed bars in tension is based on a combination of the recommendations of ACI 318:1989 [33] and recent research into the bond strength of deformed bars [32]. This equation includes a factor for the depth of fresh concrete cast beneath the bar. A lower value for the development length may be obtained if a further three factors are considered. These factors account for: any additional concrete cover or clear distance between bars, transverse reinforcement perpendicular to the bar, and excess reinforcement provided in a flexural member not subjected to seismic forces.

Within specified limits the relevant development lengths remain the minimum length for lap spliced deformed bars in compression or tension. The amount of transverse reinforcement required for a reduction in the lap length in spirally reinforced compression members is redefined.

For a deformed bar in compression the basic development length is unchanged from the previous ACI 318 based requirements released in an amendment in 1989. NZS 3101:1995 includes the area of non-prestressed tension reinforcement in an equation determining the amount of transverse steel required for a reduction in the basic development length.

The anchorage requirements for plain bars in tension are revised with hooks specified for their development. Lap splices for plain bars require the hooks to be located at right angles to the concrete surface when the concrete cover thickness does not exceed 50mm.

Lap splices are not to be used for any transverse reinforcement placed in potential plastic hinge regions.

3.5 SUMMARY

To ensure satisfactory performance from lap splices during seismic loading the current and previous New Zealand concrete design codes prevent splice placement in positions that are unable to provide dependable anchorage conditions.

NZS 3101:1995 provides revised development length equations in a simplified format.

CHAPTER FOUR
EXPERIMENTAL PROGRAMME

4.1 INTRODUCTION

The two specimens tested were beam-column joint subassemblages. The longitudinal beam bars of each specimen were lap spliced in the potential plastic hinge region on one side of the column. The overall dimensions of the two specimens are shown in Fig. 4.1.

Specimen One was designed to meet NZS 3101 (1982) with the exception of the position of the lap splices.

Specimen Two was constructed to test beam reinforcement details from a building designed in the late 1950's (see Fig. 4.2). Beam cross-section dimensions and the longitudinal reinforcement (plain bars) were identical to those of the existing building. To prevent possible shear failure in the beams additional transverse steel was used. The column dimensions were kept close to the original size to model similar bond conditions for the beam bars through the joint. The beam longitudinal steel areas and cross-section dimensions of Specimens One and Two were identical.

4.2 SPECIMEN DESIGN

4.2.1 General

New Zealand Standard Code of Practice, NZS 3101 (1982) with amendment No.1, and capacity design methods were used in the calculations.

4.2.2 Specimen One

Deformed bars were used for longitudinal beam reinforcement. Four D24 Grade 300 steel bars (ρ= 1.37%) were used as top flexural beam reinforcement and two D24 Grade 300 bars (ρ'= 0.69%) were used as bottom beam reinforcement.

The calculations revealed that the area of transverse steel needed to meet shear requirements was 30% greater than that required for splice confinement needs. The spacing of the transverse steel was governed by anti-buckling requirements (see Table 4.1 below).

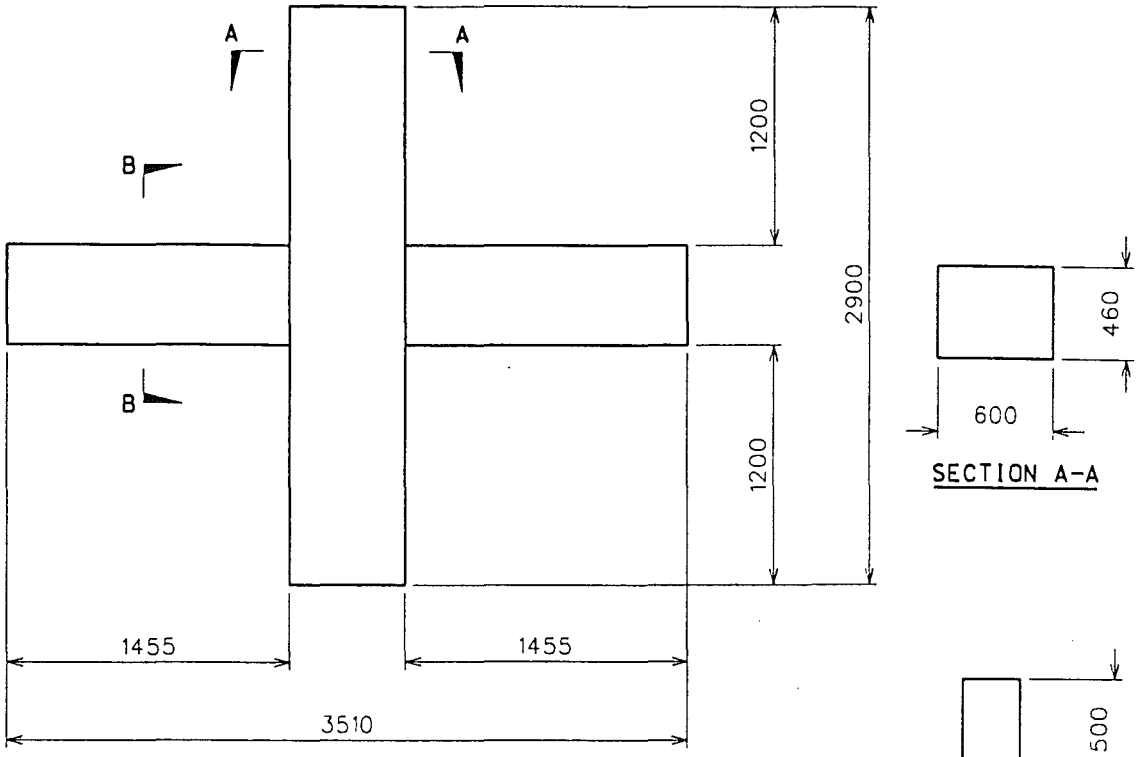

SPECIMEN ONE

SECTION A-A

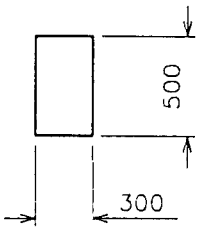

SECTION B-B

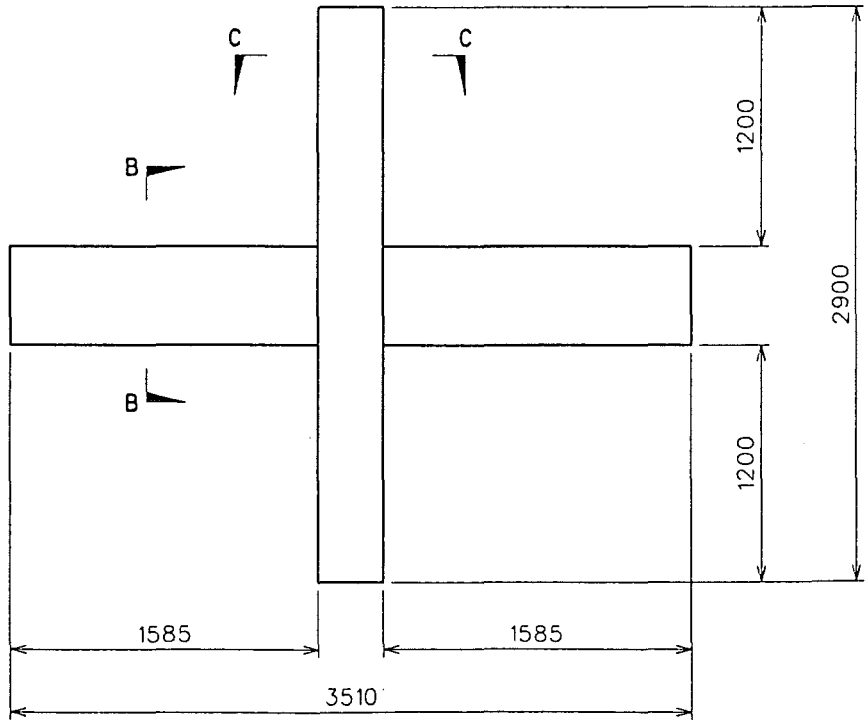

SPECIMEN TWO

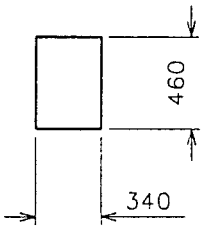

SECTION C-C

Fig. 4.1 Dimension of the Specimens

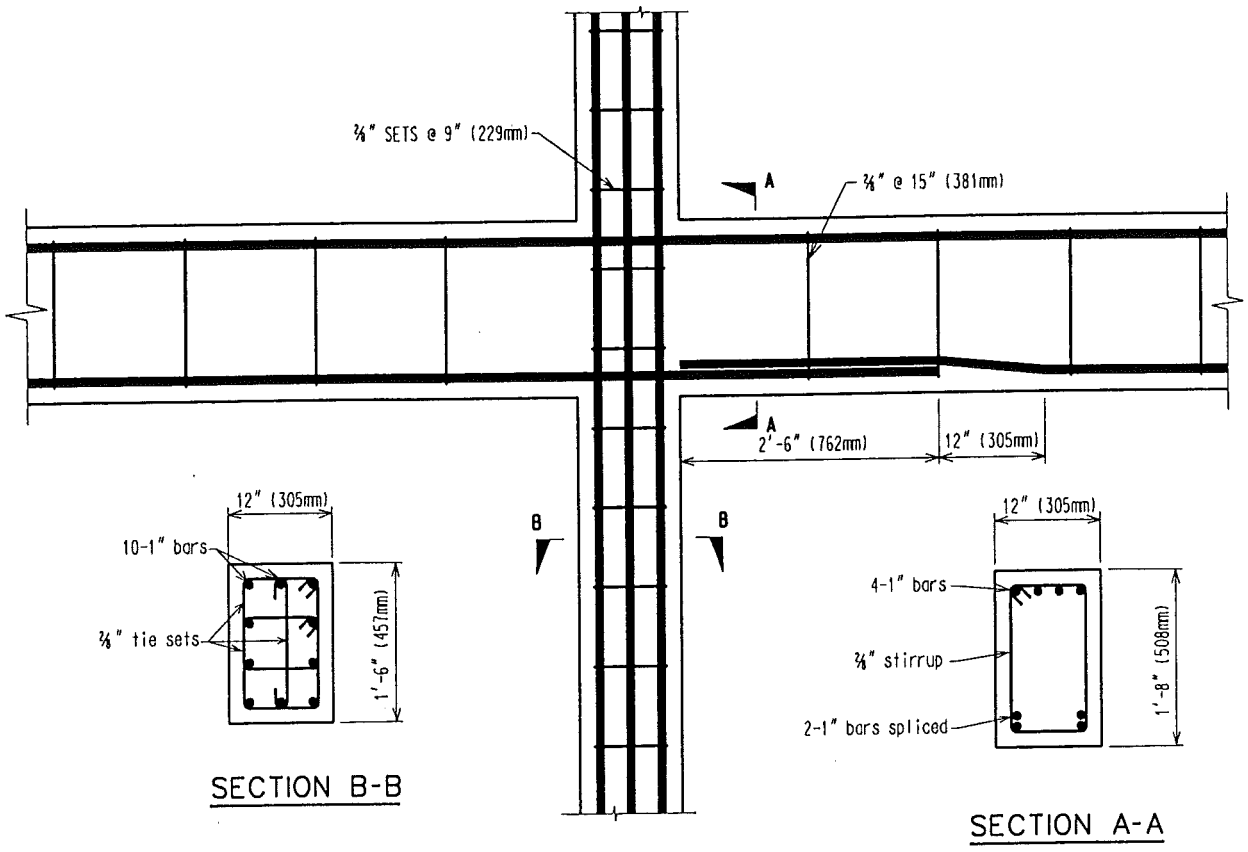

Fig. 4.2 Beam-Column Detail of an Exterior Frame from an Existing Building

Anti-buckling areas are based on the area of a single stirrup leg. The value should be doubled (in brackets) to enable a comparison with the other requirements.

The transverse steel used in the specimen met the required steel areas, while the anti-buckling spacing requirement was eased by 10 mm. This provided an area of transverse reinforcement which just met the shear reinforcement requirements, and minimised any addtional confinement. Double stirrup ties were placed at each bend of the cranked beam bars to restrain any buckling.

The beneficial effect of transverse steel recognised by NZS 3101 in Cl.5.3.7.3. (d) was used to reduce the lap length from the basic development length for a D24 bar. Minimum requirements for the length of lap splices in compression (Cl.5.3.20.1, Amendment No. 1, 1989) determined the lap length. This reduction in lap length led to spacers being placed below the cranked D24 bar at each splice (see steel reinforcement drawing, Fig. 4.3). The calculations determining the length of the lap splice are presented in the Appendix.

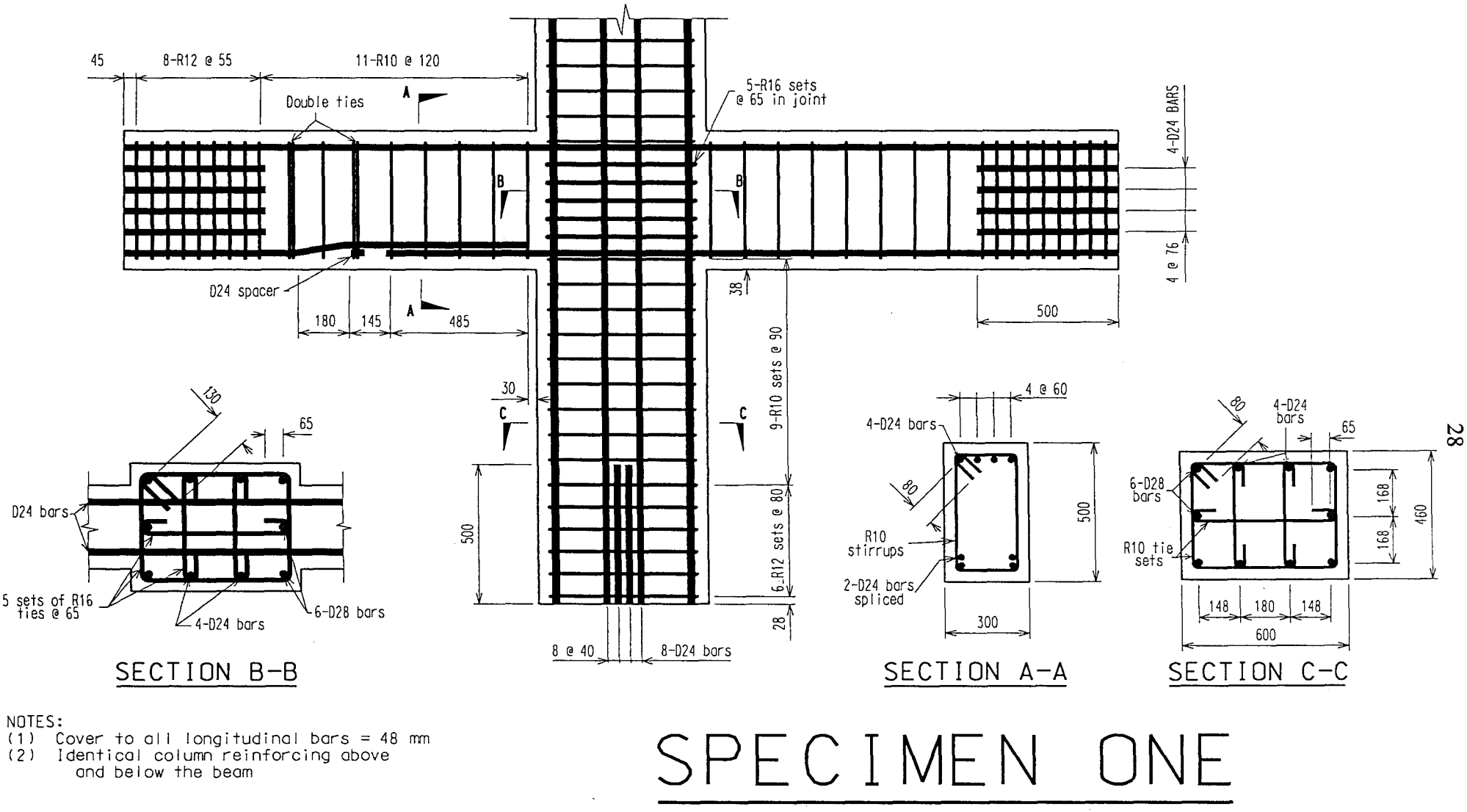

Fig. 4.3 Reinforcing Details for Specimen One

Code requirements for the maximum diameter of longitudinal beam bars passing through interior joints (Cl.5.5.2.5 (b)) set a minimum column width which was used in the design. Six D28 and four D24 (Grade 300) bars were used as column flexural reinforcement. This provided an ideal moment capacity 97% greater than the beam overstrength moment demand.

Large amounts of horizontal joint shear steel (R16 tie sets) led to considerable congestion in the joint. The lack of an axial compression load contributed to this.

Table 4.1 Summary of the Transverse Steel Requirements for Specimens One and Two

Requirement	**Area required/spacing**		**Spacing required**
Shear	A_v/s =	1.30mm²/mm	≤ 220 mm
Anti-buckling	A_{te}/s = 0.57 mm²/mm	(1.14 mm²/mm)	≤ 110 mm
Splice confinement	A_{tr}/s =	1.00 mm²/mm	
Steel used in S1		1.31 mm²/mm	120 mm
Steel used in S2		0.71 mm²/mm	220 mm

4.2.3 Specimen Two

The construction drawings of the existing building (see Fig. 4.2) were examined and Specimen Two was designed to match the beam details as closely as possible. Only the amount and spacing of the transverse steel was changed. Plain round bars were used for longitudinal beam reinforcement. Lengths of the laps and crank, and the number and type (Grade 300, R24) of longitudinal bars remained the same.

To avoid a shear failure in the beam, additional transverse steel was provided. To minimise the confinement provided to the spliced bars by the additional transverse steel the ideal concrete shear stress assumed in the calculations differed from that specified by NZS 3101 (1982). The ideal shear stress in the potential plastic hinge regions was assumed to be one

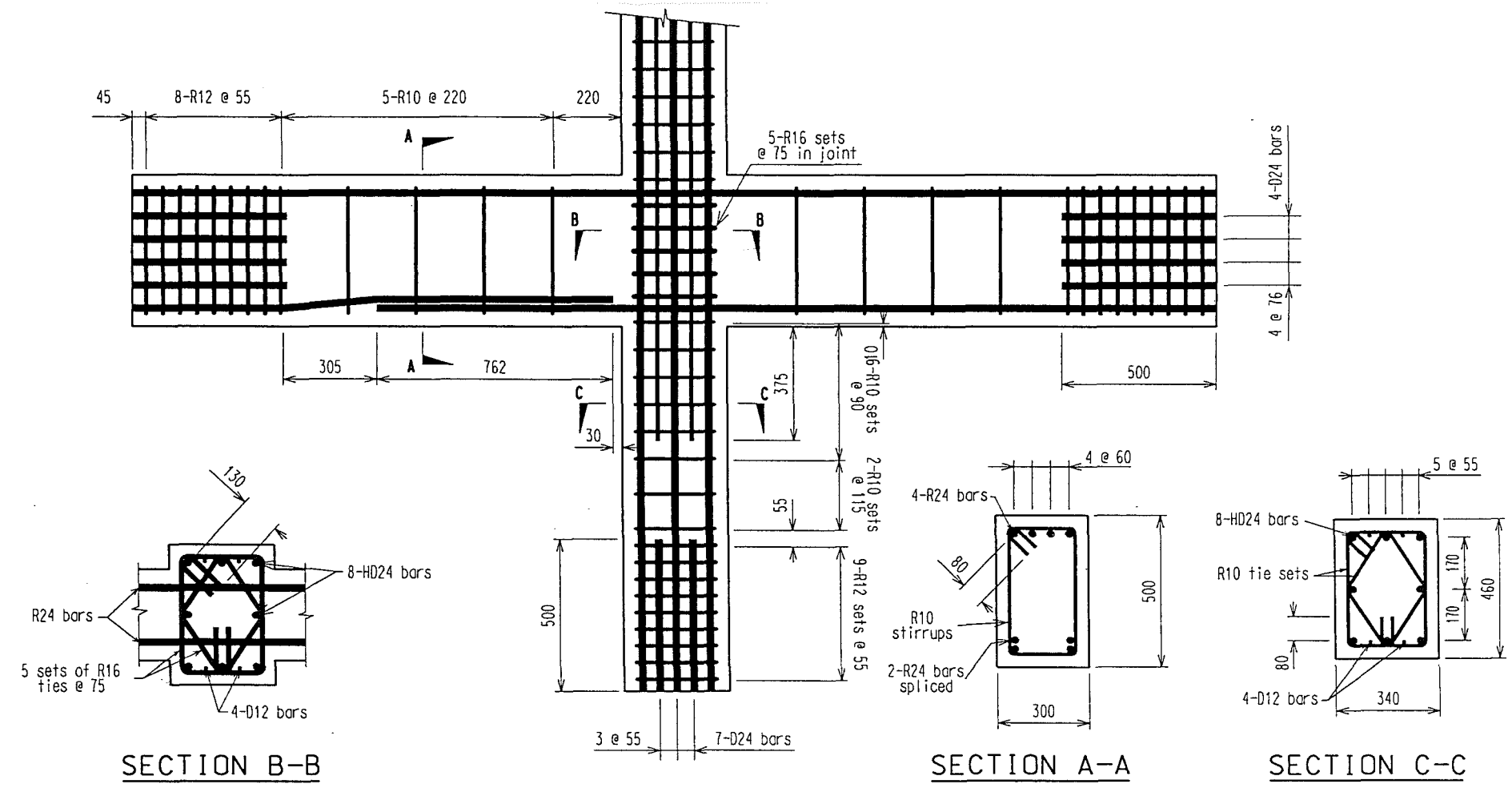

Fig. 4.4 Reinforcement Details for Specimen Two

half of the code allowance for gravity loading conditions. The maximum spacing permitted by shear requirements was chosen for the transverse steel. An arrangement that met none of the steel area requirements and exceeded the anti-buckling spacing conditions (as shown in Table 4.1) resulted. The first stirrup was placed the full spacing from the column face as in the existing building.

Bond conditions for the beam bars passing through the joint needed to be similar to those in the existing building. Eight HD-24 bars as column flexural reinforcement limited the column width to 340 mm (305 mm in the existing building).

Tie sets of R16 bar were used for horizontal joint steel and four D12 bars were required as vertical joint shear steel. Reinforcement details for Specimen Two are shown in Figure 4.4.

4.3 SPECIMEN FABRICATION

All longitudinal reinforcing bars were supplied cut to length and threaded or bent as required. The majority of the transverse reinforcement was supplied bent, some additional reinforcement was prepared in the laboratory.

Templates of the member cross-sections were used to construct the reinforcement cages. Wire ties were placed at every practical position to improve the cage rigidity during lifting.

The plywood formwork was oiled before casting to help strip the specimens. Spacers were placed in the bottom of the mould to ensure the correct cover thickness and the cage was lowered into the mould. Inserts were placed to allow lifting brackets to be attached. Figure 4.5 shows Specimen One ready for concrete placement. Concrete was supplied from a ready mix plant, it was placed with a skip and compacted by an electrical vibrator. Hessian was laid over the specimen and kept moist for seven days to allow the specimen to cure in damp conditions. The formwork was then stripped and the specimen was lifted to prepare for testing.

Once in the test rig the specimens were instrumented, painted white to improve crack visibility and a grid was marked to help identify deformations.

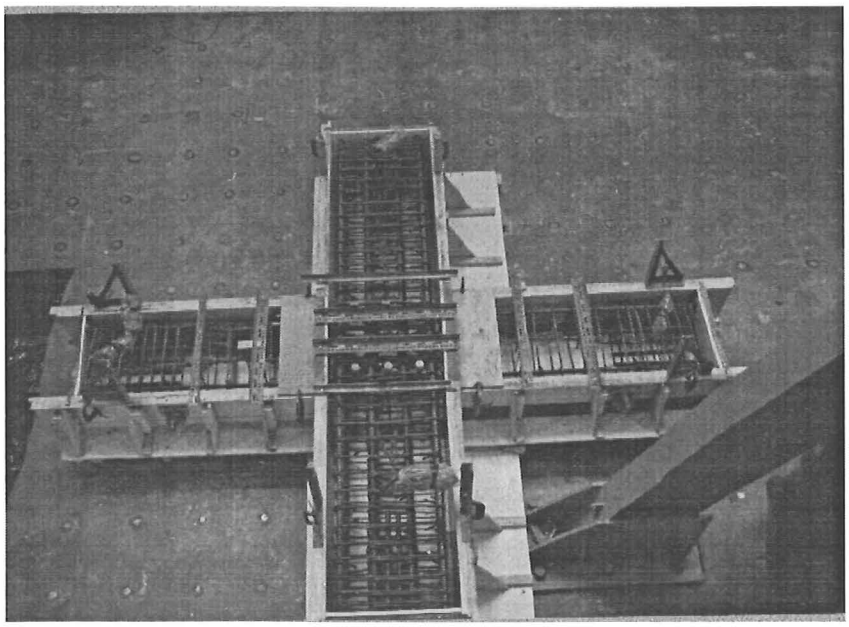

Fig. 4.5 Specimen One Ready for Concrete Pour

4.4 MATERIALS

4.4.1 Concrete

The concrete for Specimen One had a specified twenty-eight day compressive cylinder strength of 30 MPa and a slump of 100 mm. A compressive strength of 25 MPa (at twenty-eight days) and a slump of 100 mm was specified for Specimen Two. Twelve 100 mm diameter x 200 mm test cylinders and three 120 mm x 120 mm x 360 mm test beams (for flexural testing) were cast with each specimen. These were cured at 100% humidity and a temperature of 20^0 C. The actual concrete properties are shown in Table 4.2

Table 4.2 Concrete Properties

Specimen	**One**	**Two**
Slump (mm)	80	90
Age at test of specimen (days)	24	30
f'_c at test of specimen (MPa)	32.0	31.8
f'_t (MPa), at age (days)	3.8, 60	4.8, 36

4.4.2 Reinforcing Steel

Reinforcing steel test samples were either cut from the delivered lengths of bar or supplied cut to a suitable testing size.

Three samples of each bar size were tensile tested with increasing monotonic load in an Avery Universal Testing Machine. An extensometer was placed on the bars for strain measurements over a 51 mm gauge length. Values of load, displacement and extension were automatically recorded during the tests on a computer.

The steel properties are shown in Table 4.3.

TABLE 4.3 Reinforcing Steel Properties

Specimen	**One**				**Two**				
Bar	D24	D28	R16	R10	R24	HD24	D12	R16	R10
Measured f_y (MPa)	313	318	325	325	318	434	365	325	340
Measured f_u (MPa)	471	481	479	474	469	581	513	471	491

(1) Also used as transverse beam steel in Specimen Two.

4.5 TEST EQUIPMENT

Figure 4.6 shows an elevation of the test rig and a specimen. Each specimen was positioned with end-plates over each beam and column end. Nuts tightened over each longitudinal bar held the end-plates in place. All the connections between the end-plates and the rig were steel pins which allowed free rotation at the member ends. Apart from the column base all member ends were free to move horizontally in the direction of loading.

A jack loaded the top of the column horizontally and was supported by a reaction frame placed to one side. The load was applied to the column via the steel pin through the end-plate. The restraining action provided by the supports at each beam end applied vertical reaction forces to the beams.

Earthquake loading was simulated by alternating the direction of the statically applied jack load.

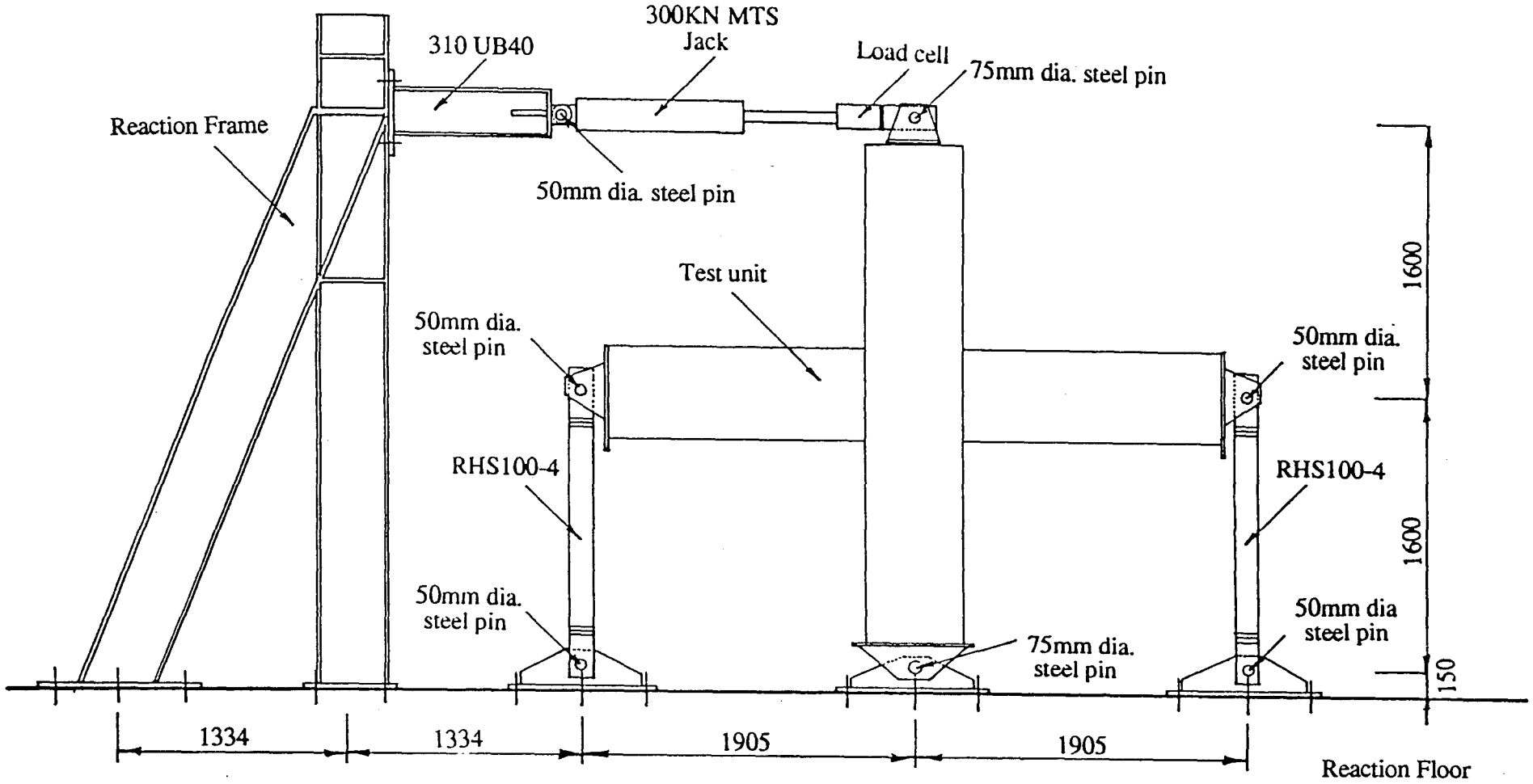

Fig. 4.6 Elevation of the Test Rig

Each beam end support consisted of two steel RHS sections attached via steel pins to the beam end-place and to an end-plate on the laboratory floor. Four electrical resistance strain gauges placed on a steel section enabled it to be used as a load cell.

Jack movements could be load or displacement controlled as values for both were available. A load cell at the end of the jack was connected to a Budd Strain Indicator. The column top horizontal displacement was registered by a linear potentiometer and displayed by a digital voltmeter. Calibration charts converted the microstrains and millivolts into kilonewtons and millimetres respectively.

4.6 INSTRUMENTATION

4.6.1 General

All load cells, linear potentiometers, electrical resistance strain gauges and clip gauges were connected to a 256 channel data logger computer.

Between increments of applied load or displacement (during a test) a scan was taken by the data-logger recording information from each of the channels.

Five load cells provided the values of forces applied during testing. One load cell was placed at the end of the jack, the remainder were on the support legs at each end of the beam. The latter four load cells consisted of four electrical resistance strain gauges on each leg wired as a bridge circuit connection.

Before testing commenced data and calibration equations were obtained for the five load cells. These had been generated by calibration tests using a Budd Strain Indicator, a data-logger and a 1000 kN Avery Universal Testing Machine.

A progressive plot of load versus inter-storey displacement was obtained during the tests. Supplying the load axis of the plotter was a circuit from the jack load cell. Displacement values from a linear potentiometer connected to the top of the column drove the displacement axis.

4.6.3 Measurement of Displacements

Linear potentiometers measured member distortion or travel and the movement of reinforcing bars. Steel bars (10 mm diameter) internally threaded at each end, were placed through the reinforcing cage between the sides of the formwork. Other small lengths of internally threaded bar were welded to reinforcing steel. The bars projected outwards so the threaded ends became flush with the concrete face. Lengths of 5 mm threaded rod were screwed into the 10 mm bars and used to mount the linear potentiometers onto the specimen. Before the concrete was cast short pieces of timber, polystyrene or plastic hosing were placed around the 10 mm bars. When removed they left space to prevent concrete bearing on the 10 mm bar (and altering the readings) during testing.

Fig. 4.7 shows the arrangement of potentiometers recording slip in the lap-splice. An estimation of the amount of slip possible was made and spacers were placed around the 10 mm bars to allow it.

A potentiometer with a maximum travel of 500 mm registered the displacements at the top of the column. It was connected to a digital voltmeter which provided readings allowing loading to be based on displacements.

Each potentiometer was calibrated before testing of a specimen began. Metal spacers of specified thicknesses placed between the target and the potentiometer gave readings on the datalogger to provide a calibration equation.

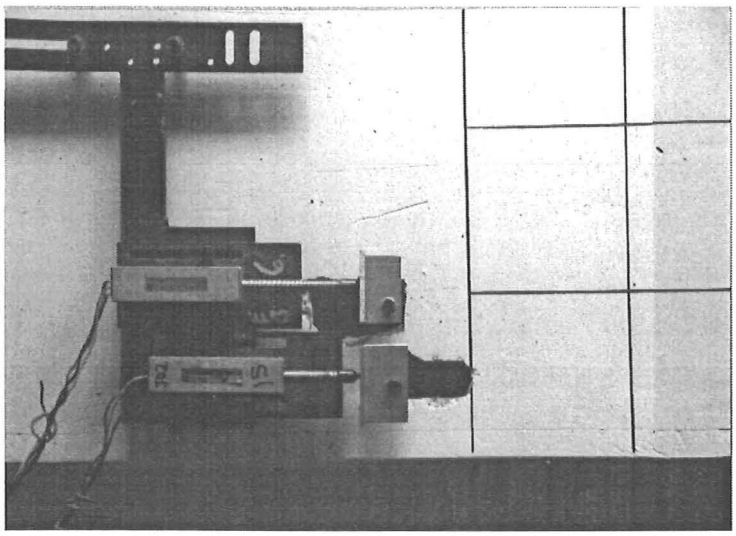

Fig. 4.7 Potentiometers Recording Bar Slip in the Lap Splice

4.6.4 Measurement of Strains

Electrical resistance strain gauges were placed on longitudinal and transverse reinforcing to enable strains to be monitored.

The placement of strain gauges was similar for both specimens. Both sets of lapped bottom beam bars in a specimen were strain-gauged so as to minimise the effect of losing any before or early in the test. One of the four top beam bars was strain-gauged. A set of beam stirrups on each side of the column were strain gauged. Half of the longitudinal column bars were strain gauged to provide strain information at the beam faces. A selection of the joint shear steel and column transverse steel (near the joint) were also gauged. Positions of the strain gauges placed on Specimen One reinforcing steel are shown in Figure 4.8.

Gauges were placed on the transverse steel in such a manner that bending strains due to bowing of hoops and stirrups were not recorded. The gauges used were Showa 120 ohm foil strain gauges with a 5 mm gauge length.

Reinforcing steel was filed, polished and swabbed clean before strain gauges were attached with cement. Five or six coats of a waterproofing compound were applied before a small piece of mastic tape was added for further waterproofing and extra protection during casting.

Slip of the beam bars was considered likely. To prevent the strain gauge leads to gauges on the bottom beam bars for both specimens from being pulled from the gauge the leads were folded twice just beyond the mastic tape. The folds were covered with shrinkwrap which was heated. It was hoped the lead would gradually pull out of the sleeve as the bar slipped.

As the Specimen One longitudinal bars were deformed it was thought the deformations may protect the gauge (by removing concrete ahead of the gauge) as the bar slipped. The plain bars of Specimen Two gave the strain gauges no protection. Instead a small amount of a flexible water sealer was placed in front of each gauge allowing a small area without concrete to exist for the gauge to slide into.

Values for the amount of longitudinal beam bar area lost with the placement of the strain gauges and polystyrene (to allow potentiometer rod slip) vary for each specimen in the joint and the lap splice. The bottom beam bar in the joint of Specimen One with the three

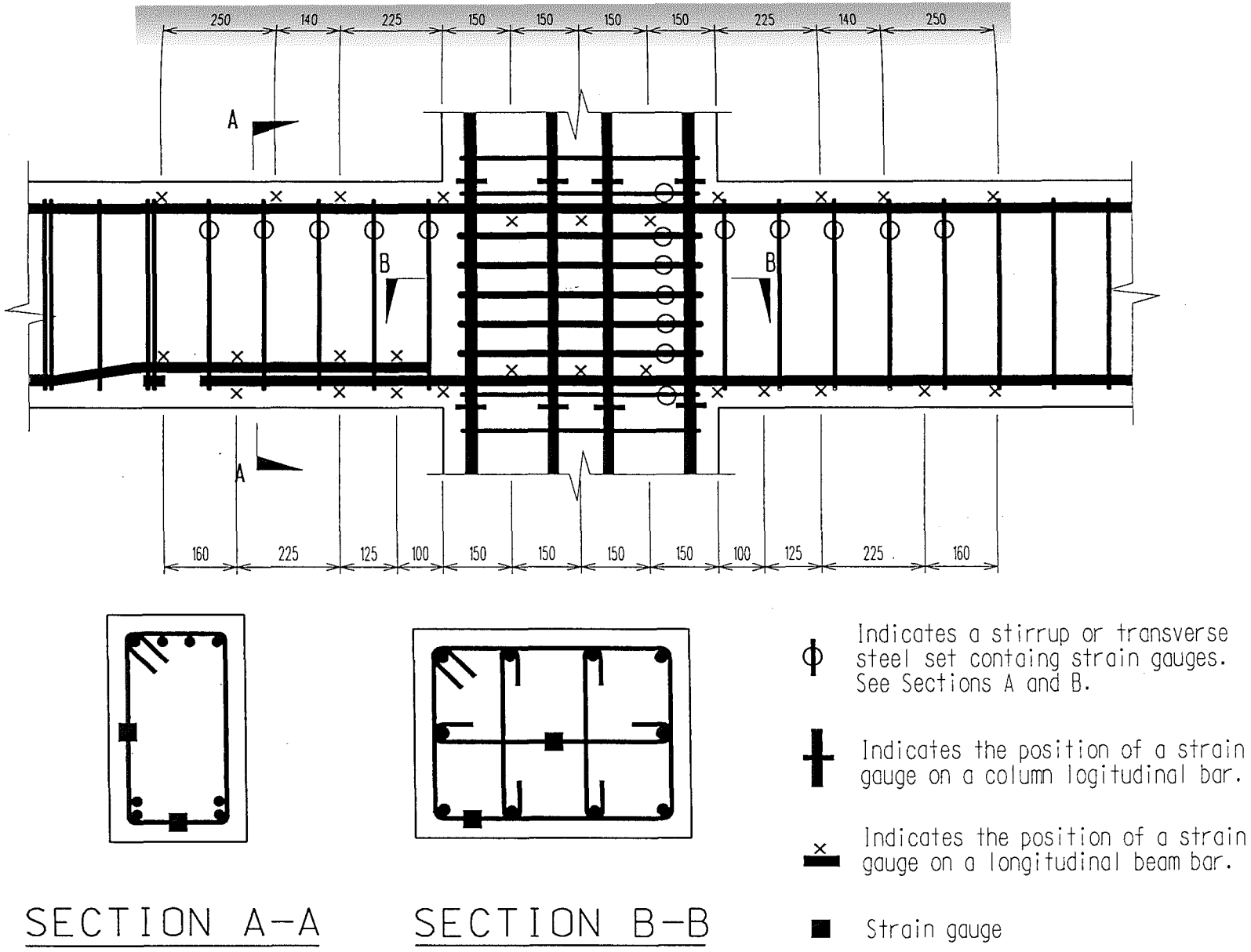

Fig. 4.8 Position of Strain Gauges on the Reinforcing Steel of Specimen One

potentiometer rods lost 8% of the available bar area. In the lap splice region each bar of Specimen One lost 7% of the bar area. The maximum area lost from a beam bar in the joint of Specimen Two was 10 % and 4% was lost from the area of the bars in the lap splice region.

Leads from the strain gauges were gathered together in bundles for protection during casting, and directed along the member to emerge around 600 mm from the faces of the joint core.

The strain gauges were not expected to last the entire test on Specimen Two. Six clip gauges were placed to reveal longitudinal beam bar strains in the joint and near the pinned end of both beams. One top and two bottom beam bars were instrumented. Gauges were connected between two internally threaded 10 mm bars welded to a longitudinal beam bar. A polystyrene spacer was placed around both before concrete was cast.

4.7 TESTING OF SPECIMENS

4.7.1 Loading Pattern

The specimens were tested in the cyclic loading pattern shown in Fig. 4.9. The pattern has been used in previous tests completed at the University of Canterbury for determining the performance of specimens in simulated seismic loading. The first two cycles of the tests were load controlled and the remainder were displacement controlled.

In the first cycle of loading the beams were taken to one-half of their theoretical ultimate load. The load was calculated on the basis of actual material strengths. The second cycle of loading was to three-quarters of the ultimate load and the corresponding column top displacement in each direction, Δ^+ and Δ^- was noted. The column top displacement for each direction at first yield was taken as

$$\Delta_y = \frac{4}{3}\Delta^- \text{ and } \qquad \Delta_y = \frac{4}{3}\Delta^+$$

Displacement ductility factors in each direction were defined as

$$\mu = \Delta/\Delta_y$$

where Δ was the maximum displacement at the column top.

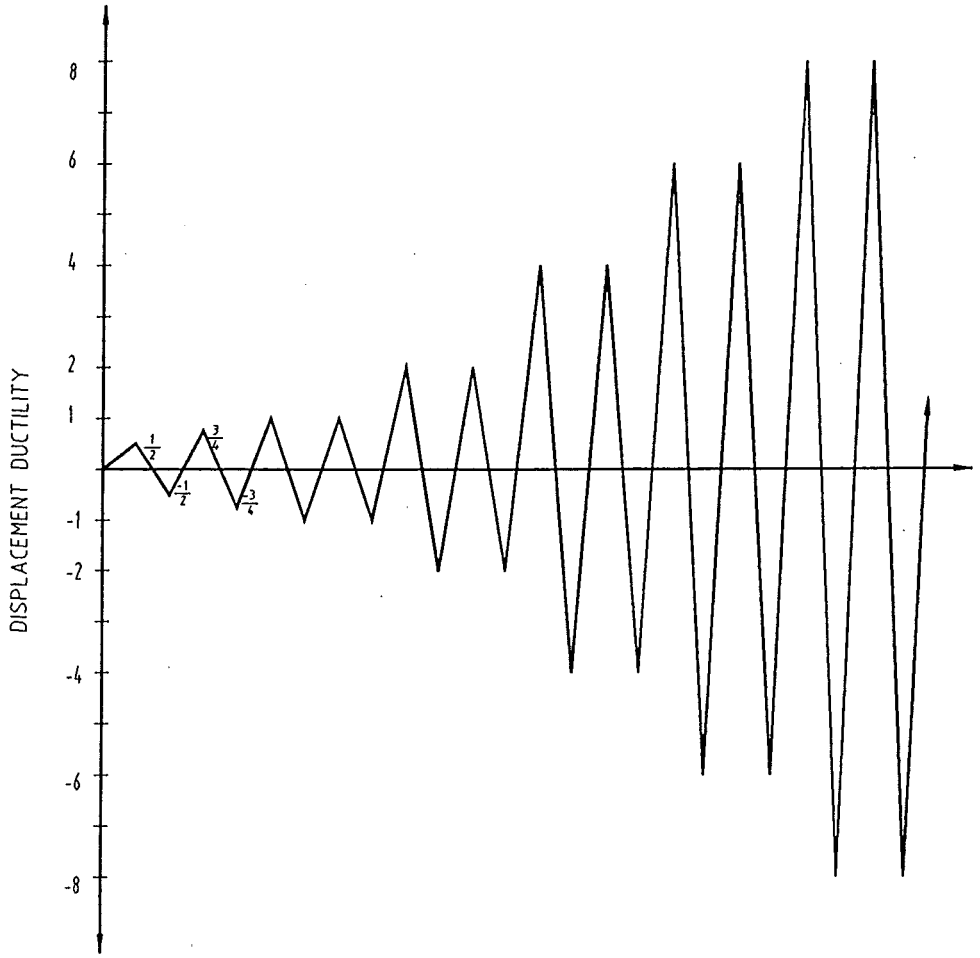

Fig. 4.9 The Loading Pattern

4.7.2 Testing Procedure

Two scans were taken by the data-logger before a test began, a scan was recorded at every increment during a test.

All cracks on the white painted surface were marked with felt-tip pens when they became visible. Crack widths at the beam-column boundaries and in the lap splice region were measured using an Ultra-Lomara crack microscope. Photographs were taken at the peak of each loading run and at other stages as desired.

CHAPTER FIVE

TEST RESULTS AND OBSERVATIONS

5.1 INTRODUCTION

This chapter describes the response of the two specimens to testing. Test observations, charts and photographs illustrate each specimen's performance.

Data is presented and the progress of tests are discussed relative to the ideal horizontal load V_i for the load controlled cycles, and the displacement ductility factor μ for the remaining displacement controlled cycles. These were defined in the description of the test procedure in section 4.7.1.

All photographs or charts in this chapter displaying a representation of a specimen will have the lap splice located in the left beam which may also be described as the west beam.

The performance of the datalogger during testing restricted the amount of strain gauge data that could be presented for each specimen. Several ambiguities were noticed in data recorded by the data logger.

If strain gauge readings for a datalogger channel were discontinued during a test (this was assumed to be the result of a strain gauge damaged by specimen deterioration) the remaining channels on the same datalogger section recorded unaccountable data readings. For the data scans in which the strain gauges were damaged, losses in tension strain or gains in compression strain were registered, often in unrelated sections of the specimen. As the true data readings for the scan were unrecorded, the remaining test data was unable to be corrected and had to be ignored.

Another irregularity affecting some banks of the datalogger was a gradual change in the zero reference for each channel. This problem had occurred during previous testing with the datalogger and no suitable methods for correcting it had been found. Data produced on these banks was disregarded once the 'zero shift' had appeared.

The results from the strain gauges are considered to give an indication of the distribution of strain in the bars rather than an accurate value of strain at the gauge locations. The general impression is the strains are higher than expected but the reason for this is unclear.

5.2 TEST RESULTS OF SPECIMEN ONE

5.2.1 General

Specimen One complied with NZS 3101:1982 except for the presence of lap splices in the bottom bars in the potential plastic hinge region of a beam.

The voltage setting for a power supply led to a discrepancy between the load and the displacement controlled cycles of the test. The voltage at which all calibration equations for the datalogger were generated (and at which the test was completed) was not consistent with the voltage used to generate the calibration equation for the column top displacement which governed the displacement controlled loading. This led to displacements 24% larger than anticipated during the displacement controlled loading cycles. Several cycles of these were completed before the inconsistency was noticed, but loading was continued to preserve the sequence of displacement ductility factors.

After two cycles at a displacement ductility factor $\mu = 8$ were completed, it was considered that sufficient reserve remained in the specimen to continue to a ductility factor $\mu = 10$. Several potentiometers were reaching the end of their available travel so it was decided the remaining cycles would be completed for the horizontal load - deflection relationship only. To prevent the column top potentiometer running out of range the displacement values for the ductility factors of $\mu = \pm 10$ were averaged and used in each direction.

5.2.2 Observed Behaviour

The loading cycle to $\pm 0.5V_i$ developed three or four equally spaced flexural cracks in the top and the bottom of both beams over a distance of 700 mm from the column faces. When the splice went into tension during negative (upward) loading, flexural cracking occurred in the beam at the column face, within the splice length and beyond the splice near the location of the crank in the top spliced bar. In the corners of the joint short cracks appeared at the location of the longitudinal beam bars.

During loading to - $0.75V_i$ the flexural crack beyond the splice extended to three quarters of the beam depth and several horizontal cracks developed from it following the section of cranked bar and the spacer bar beside the splice. Other changes during the loading cycle were the formation of flexural cracks in the column and diagonal tension cracks across corners of the joint.

Figure 5.1a shows the horizontal cracking between two spliced bars after the two displacement runs to $\mu = -1$. The largest crack in the splice had a width of 0.4 mm, starting from the column face and continuing 70 mm over the splice length. Another crack extended 30 mm horizontally from a flexural crack which had crossed the splice earlier. Diagonal tension cracks crossed the centre of the joint during the cycle to $\mu = \pm 1/1$.

Further damage to the splice occurred during the displacements at $\mu = -2$ with cracking extending three quarters of the splice length in Fig. 5.1b. The maximum crack width in the splice was 0.9 mm at 50 mm from the column face. It was noted that the cracking at the column faces no longer closed upon returning to zero displacement. The maximum width of these was 3.5 mm in both beams at peak displacements. Very little additional cracking occurred in the column and joint after $\mu = 2$.

During displacements to $\mu = -4/1$ the concrete around the splice was split apart and the splice failed as shown in Fig. 5.1c. Before the $\mu = -4/1$ peak displacement was reached cracking developed along the entire splice and the depth of the beam increased by 7 mm. Most of this increase in depth was due to the crack width along the splice. The width of the flexural cracks through the splice increased and the main crack in the beam was 150 mm from the column face. Visible in the cavities for the potentiometer studs was concrete that had been turned to powder between the spliced bars. At $\mu = -4/2$ the concrete cover along the splice fell from beneath the beam exposing the bottom bars of each splice.

Large amounts of yielding occurred in the longitudinal beam bars at $\mu = \pm 4$. The cracks in the beams at the column faces no longer closed during the peak loads in the opposite direction. Figure 5.2a shows both beams had well defined flexural cracks in the plastic hinge regions. Some concrete crushing was observed at the bottom of the east beam during the negative displacement cycles.

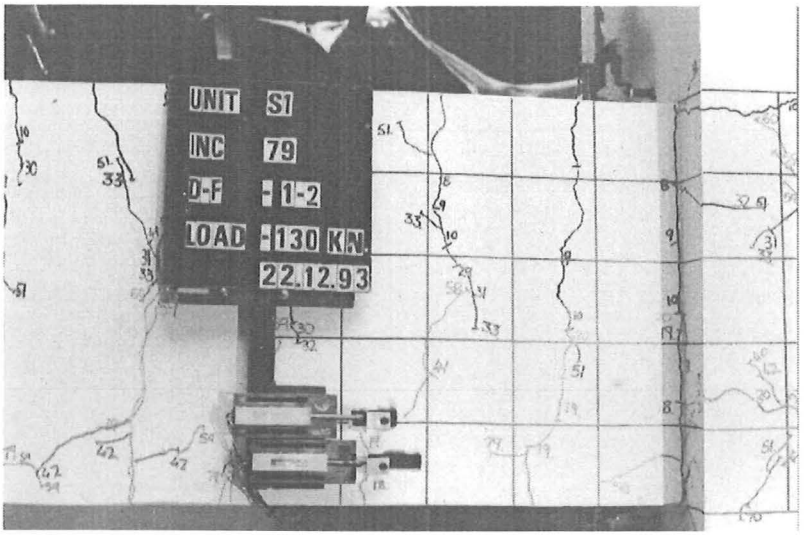

Fig. 5.1a Cracking in the Splice Region at $\mu = -1/2$.

Fig. 5.1b Cracking in the Splice Region at $\mu = -2/2$.

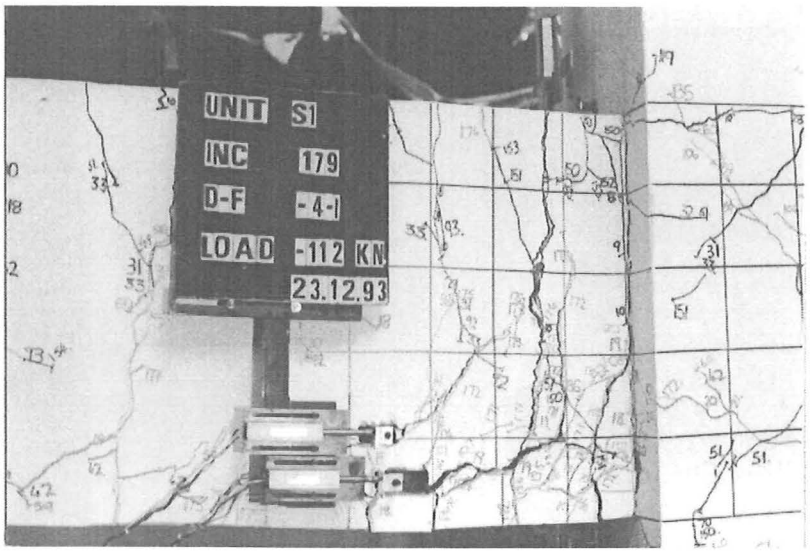

Fig. 5.1c Cracking in the Splice Region at $\mu = -4/1$.

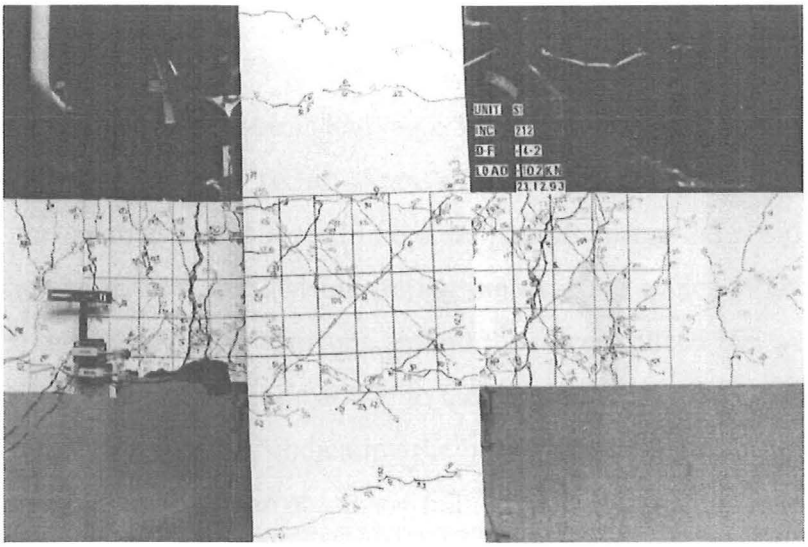

Fig. 5.2a Condition of the Specimen at μ = -4/2.

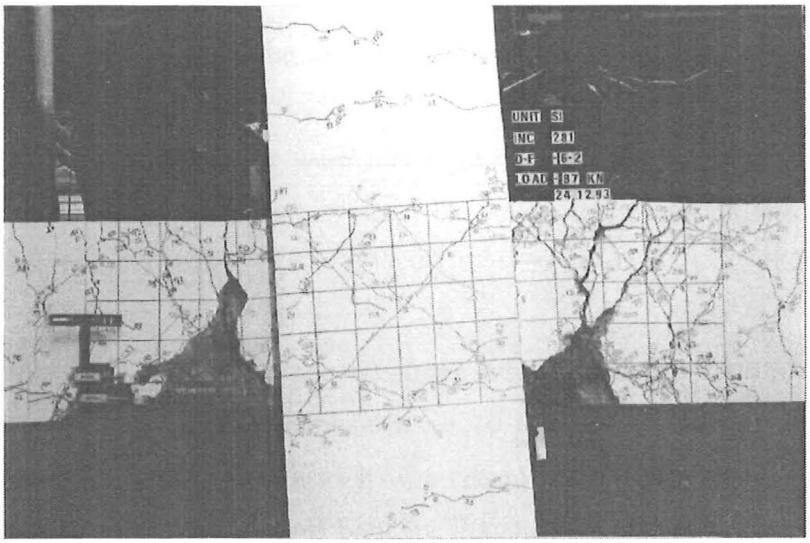

Fig. 5.2b Condition of the Specimen at μ = -6/2.

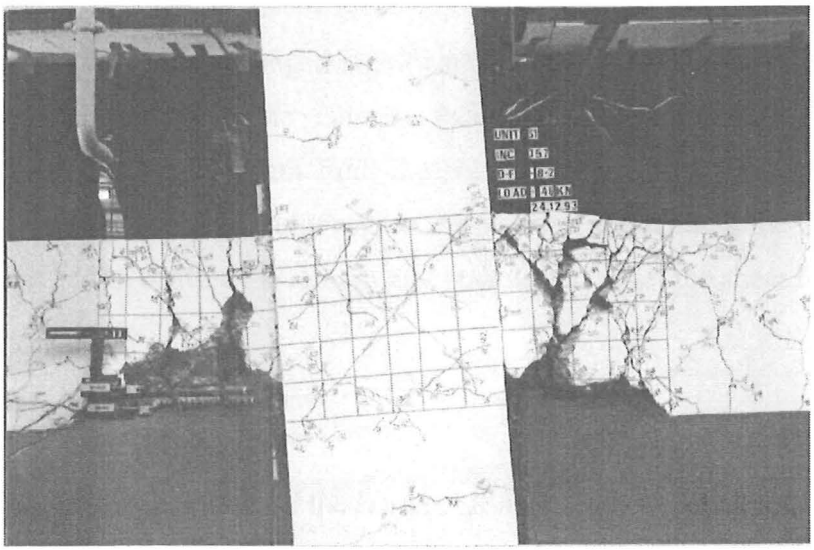

Fig. 5.2c Condition of the Specimen at μ = -8/2.

The plastic hinge regions of both beams had large flexural cracks at $\mu = \pm 6$, Fig. 5.2b shows the result of testing at this ductility factor. Areas of cover concrete above the splice expanded from the side of the beam as it was forced into compression during the positive displacement cycles. When the splice went into tension during the negative cycles large amounts of slip occurred between the spliced bars. Stirrups around the lower spliced bar were pulled out of plane during displacements. Cracking parallel to the bottom of the east beam occurred in the compression region during $\mu = -6/1$ indicating the bars were starting to buckle. The concrete cover fell from beneath the east beam at $\mu = +6/2$.

Displacements to $\mu = +8/1$ caused further concrete cover to fall from beneath the east beam leaving 400 mm of the two longitudinal beam bars exposed. From Fig. 5.2c these bars experienced large amounts of buckling during the negative displacement cycles at $\mu = 8$ and shear displacements of 20 mm occurred between the grid lines in the hinge region. The bars from the west beam in the lap splice were forced to bear against concrete on the side of the joint during the positive displacement cycles. However, there was no sign of buckling in either of the spliced bars.

The test was continued to $\mu = 10$ as the specimen was performing well during the positive displacements. At the peak displacement of $\mu = +10/1$ the cover concrete sitting loosely on the top of the east beam was removed as it was taking no compression load. The four top longitudinal bars in the east beam were bent by the shear displacements resulting from the wide cracks in the beam. A maximum vertical displacement of 45 mm occurred between the grid lines on the concrete on each side of the break in the beam.

The behaviour of the east beam changed significantly in the latter stages of the test. All the longitudinal bars were bent at the column face as the beam completed large shear displacements through a gap 150 mm from the column face. Load resistance in the beam relied on the concrete in the plastic hinge region interlocking and holding the longitudinal bars apart. The stirrups had to confine the remaining concrete and resist the shear load.

5.2.3 Load-Displacement Response

Figure 5.3 plots the shear force versus the horizontal displacement relationship at the column top for Specimen One. Also displayed are the ideal horizontal load V_i for the specimen and

the drift angles. Figure 5.4 provides two plots to illustrate the effect of each beam on the response of the specimen. One plot shows the load resistance from the west (spliced) beam for the test, the plot of total beam load represents the additional load from the east beam.

The $0.75V_i$ loading cycle showed less stiffness existed in the specimen for the negative loading direction. The displacements reached were 10.4 mm and 14.2 mm for the positive and negative loading runs. These were factored to provide the displacements used for the remainder of the test.

The lateral load resisted by the specimen during displacements to $\mu = +1$ reached a maximum of $0.92V_i$. In the opposite direction the ideal load was achieved twice with a maximum of $1.10V_i$ for the first run. The values of interstorey drift at $\mu = 1$ in the positive and negative displacement directions were 0.44% and 0.60% respectively. After this the maximum lateral loads for each ductility factor were recorded during the positive displacement runs.

At $\mu = 2$ the maximum load reached was $1.06V_i$ at $\mu = +2/1$. The ideal lateral load was carried for both runs in the negative direction.

The specimen exceeded V_i in both runs to $\mu = +4$. However, during displacements to

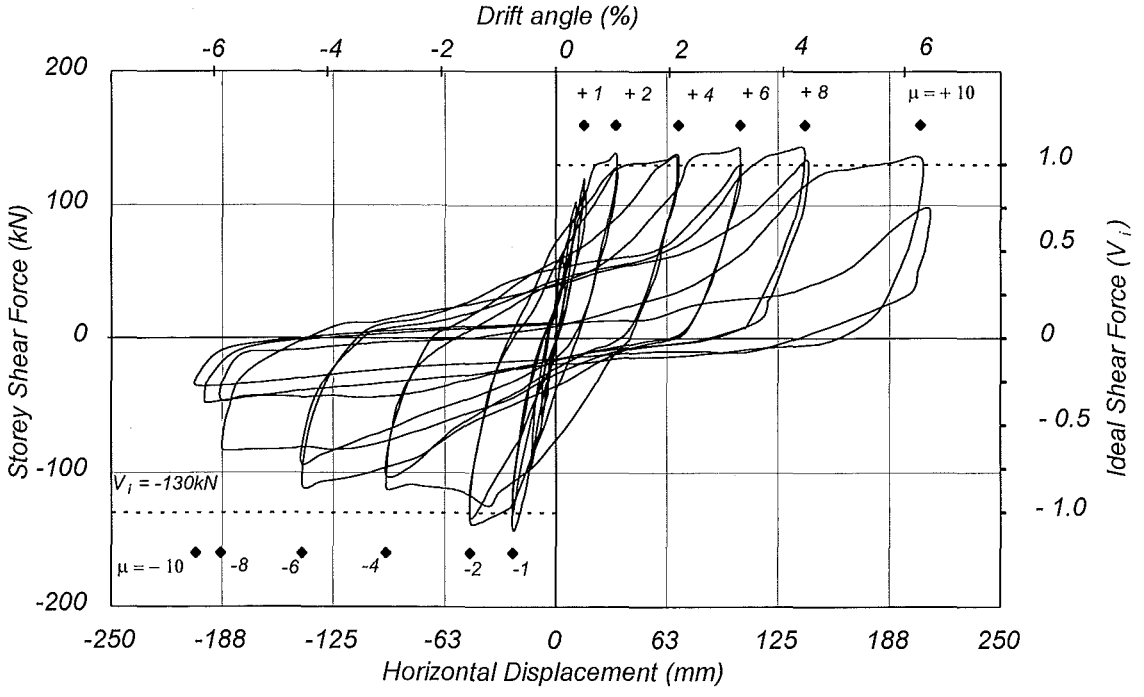

Fig. 5.3 Lateral Load-Deflection Response for Specimen One.

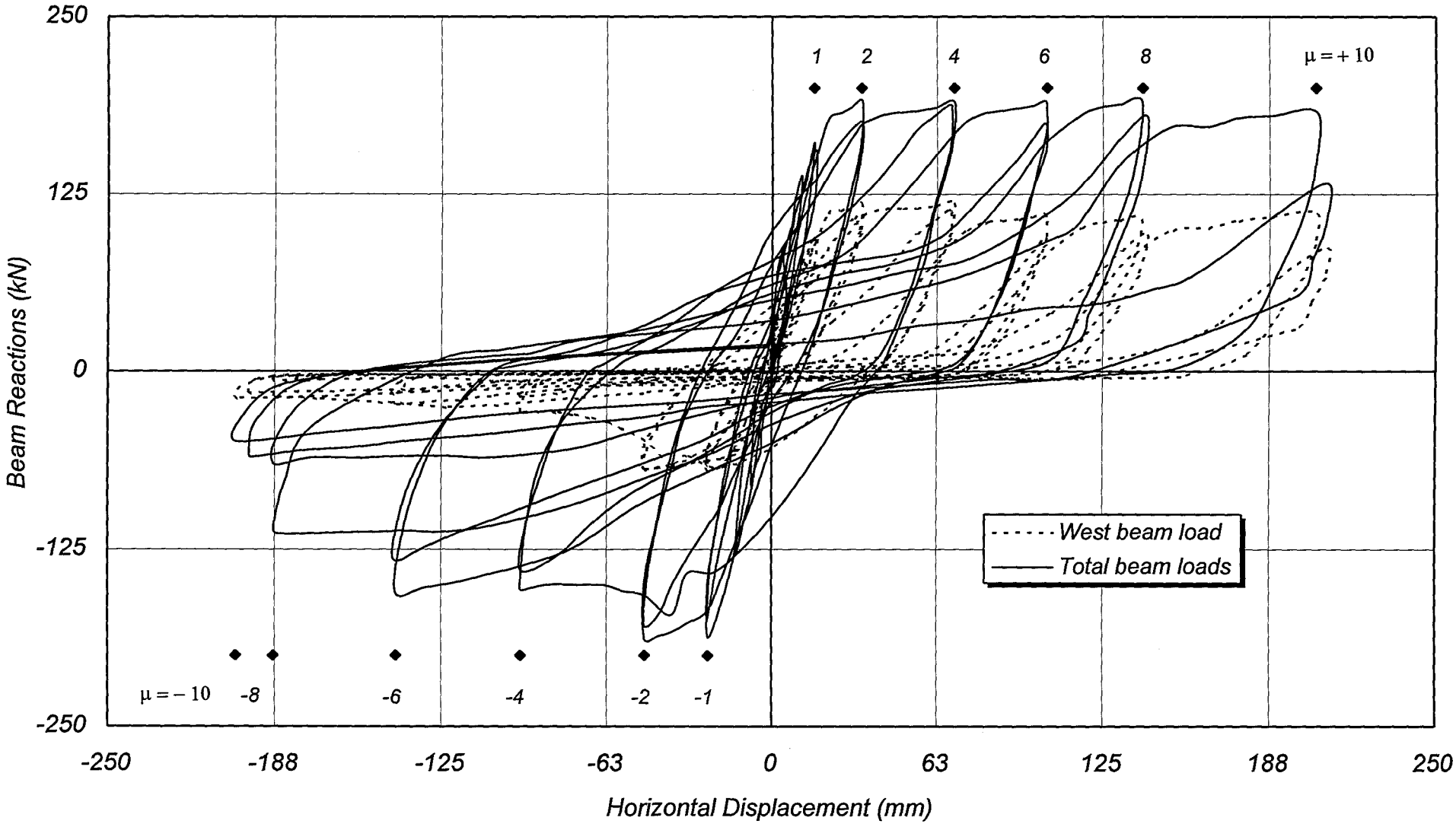

Fig. 5.4 West and Total Beam Loads Versus Column Top Displacement.

μ = - 4/1 the lateral load dropped as the splice came apart under tension load. At a level of displacement which had been exceeded twice previously during runs to μ = - 2, the west beam began to lose load capacity. It was reduced to 40% of its previous load capacity by μ = - 4/1. The specimen reached $0.87V_i$ and $0.78V_i$ at the peak of μ = - 4/1 and -4/2. The response of the east beam helped to offset the loss of load initially but the performance of the specimen deteriorated over the remaining negative displacement runs. The loss of the splice capacity caused pinching of the hysteresis loops and a reduction in the energy that could be dissipated during displacements in each direction. The lateral load resisted by the specimen in the negative direction for the first cycles at μ = 6 and 8 was $0.85V_i$ and $0.65V_i$ respectively. Figure 5.4 indicates the east beam carried 80-85% of the load during these runs.

The ideal horizontal load was reached at the peak of all the positive displacements to μ = 6 and 8, with the maximum specimen load $1.1V_i$ repeated at μ = +6/1. Figure 5.4 shows load resistance in the west beam was slow to return in these runs until it approached the preceding displacement in the positive direction. The lack of effective compression steel, a large crack above the splice and the loss of concrete around the splice region left little initial compression resistance for positive direction loading in the west beam.

The specimen responded to the increased positive displacements at μ = 10 by carrying $1.04V_i$ in the first run and $0.75V_i$ in the second. The large shear displacements in the hinge region of the east beam contributed to the serious pinching in these hysteresis loops.

5.2.4 Beam Behaviour

Curvatures and Shear Strains

The curvatures and shear strains in the beams were obtained from potentiometers located as shown in the detail between Figures 5.5 and 5.6. The vertical lines on the graphs represent the column faces and the potentiometer gauge lengths. As different values of displacement were used in each direction, only the curvature and shear strain trends can be compared between the beams.

Figure 5.5 shows the curvatures recorded in each beam. For the first two displacement cycles the middle gauge length of the west beam was slightly stiffer than the east beam. The

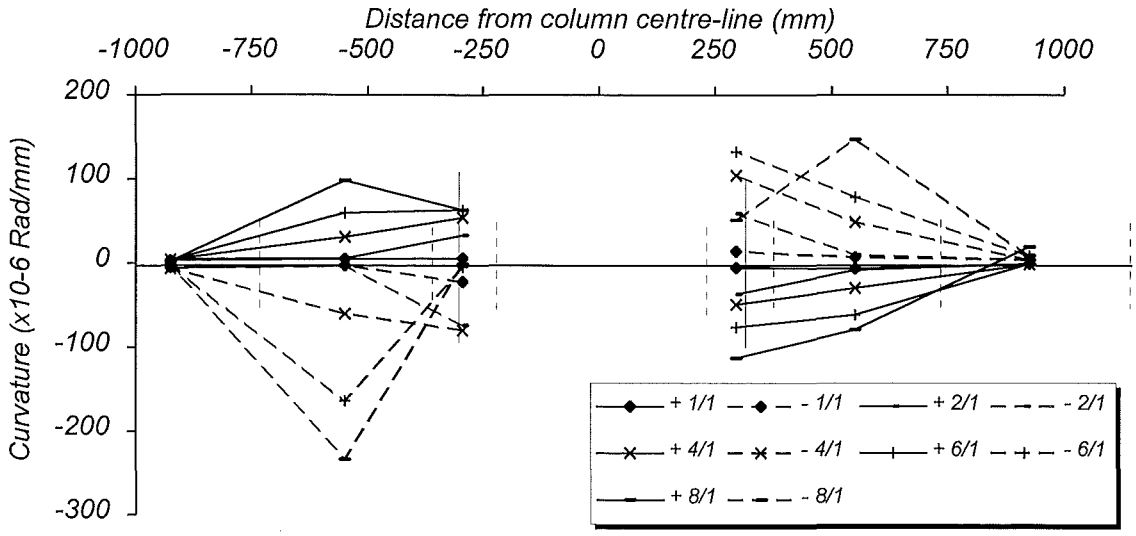

Fig. 5.5 Beam Curvatures.

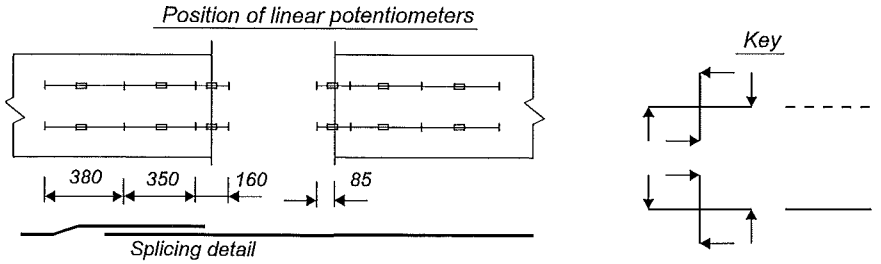

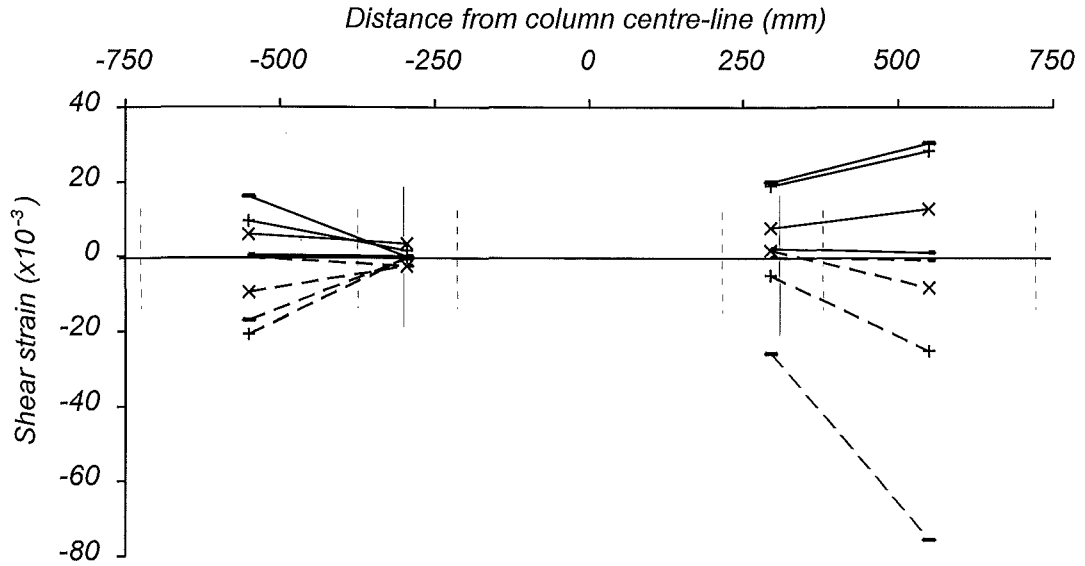

Fig.5.6 Beam Shear Strains.

increased stiffness of the west beam in the splice region generated larger curvatures beyond the splice at the column face. Once the splice let go at μ = - 4/1 the west beam curvature increased through the cracking in the splice region. At μ = - 6 and - 8 two large cracks through the splice led to the majority of the curvature in the beam occurring in this region. During the test the curvatures in the east beam increased steadily. At μ = - 8/1 the curvatures at the column face and in the second gauge length decreased and increased respectively as the large crack developed 150 mm from the column face.

Fig. 5.6 shows the shear strains which developed in the beams of Specimen One. Initially in the west beam the shear strains were greatest at the column face. Once the splice came apart at μ = - 4/1 the shear displacements developed at the flexural cracks in the middle of the splice region leaving very little displacement at the column face.

After μ = - 4 the east beam carried most of the load during the negative displacement cycles. The shear strains increased particularly over the second gauge length as large shear displacements occurred through several cracks. The shear forces transferred across the crack at the column face led to considerable strains and kinking of the longitudinal beam bars.

Longitudinal Beam Bar Strains

Figure 5.7 provides a profile of the strains in a top longitudinal beam bar. As previously mentioned the strains appear larger than those expected for the levels of testing shown. These results indicate the top bar yielded only in tension. The smaller steel area of the bottom bars was unable to develop sufficient tension load to yield the top steel in compression. Slightly higher tensile strains at the column face for the negative ductility factors may be a consequence of the larger displacements used for this direction. Displacements to $\mu = \pm 2$ led to inelastic tensile strains in the bar at the column faces. Plastic strains remained in the bar at the west column face for μ = - 2/1.

Figures 5.8 and 5.9 give the distribution of bar strains for the set of spliced bars cast in the top of the formwork. Figure 5.9 provides further detail of the strains in the splice. Several strain gauges were lost from the other pair of spliced bars before testing began and a less complete strain profile was available. Generally, the bar strains adjacent to each column face were slightly larger on the lower cast pair of bars. Superior bond conditions for bars placed lower in the formwork would have reduced any bar slip and led to higher strains.

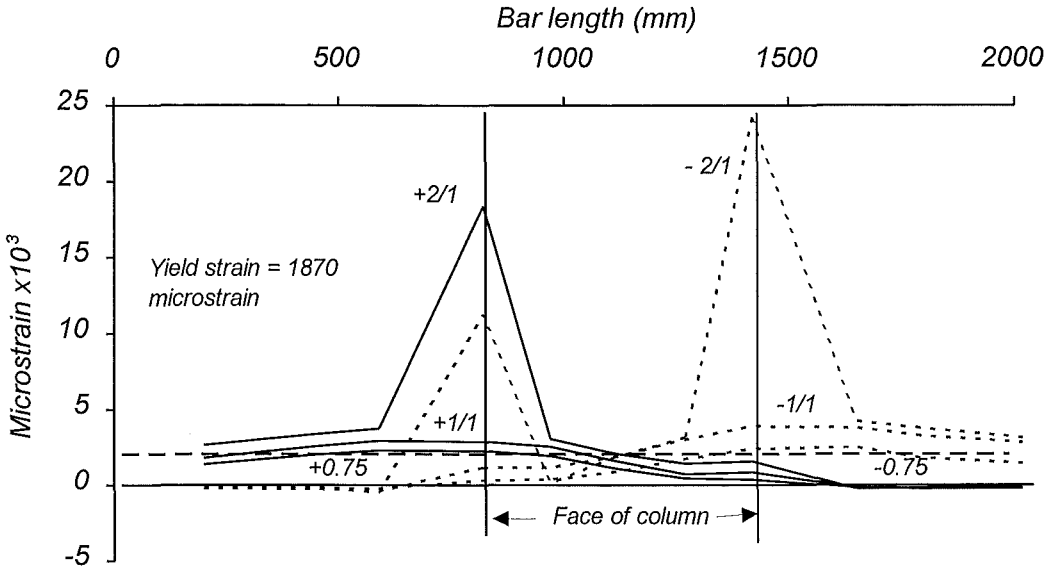

Fig. 5.7 Strains Recorded from a Top Longitudinal Beam Bar.

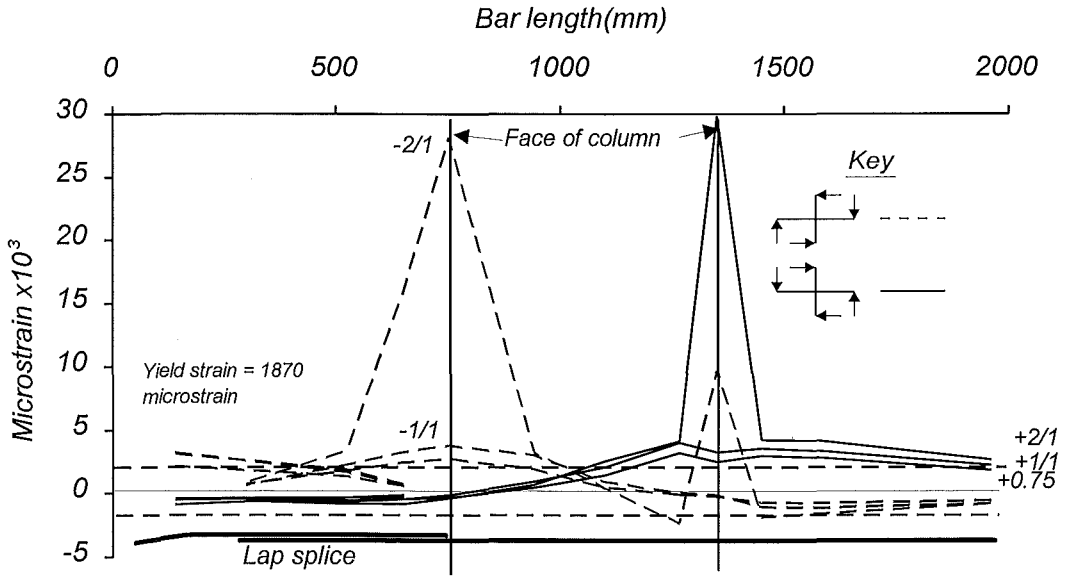

Fig. 5.8 Strains Recorded from a Pair of Bottom Bars.

The compressive bar strains which developed in the bottom bars were larger than those seen in the top longitudinal bars due to the difference in steel areas. They probably did not reach the yield strain in the cycles shown but later in the test the bars buckled at the column face in the east beam.

The yield strain was exceeded in tension in the longer spliced bar on each side of the column for displacements to $\mu = \pm 2/1$. The length of the lap splice was sufficient to allow the longer spliced bar to develop the large tensile strains in the west beam. The bond conditions in the splice deteriorated as the test proceeded with the spliced bars coming apart before $\mu = -4/1$.

Figure 5.9 gives the distribution of strain in the spliced bars for the transfer of forces. The largest strains occurred at each end of the splice with the length of the splice used to transfer the bar forces. During most of the ductility factors shown the rate of change of strain along the splice was relatively constant. This changed at $\mu = -2/1$ generating large bond stresses at the end of the splice by the joint. A review of the strain gauge data indicated that only the two displacements to $\mu = -2$ and the displacements to $\mu = -4/1$ developed large inelastic strains in the splice before it failed.

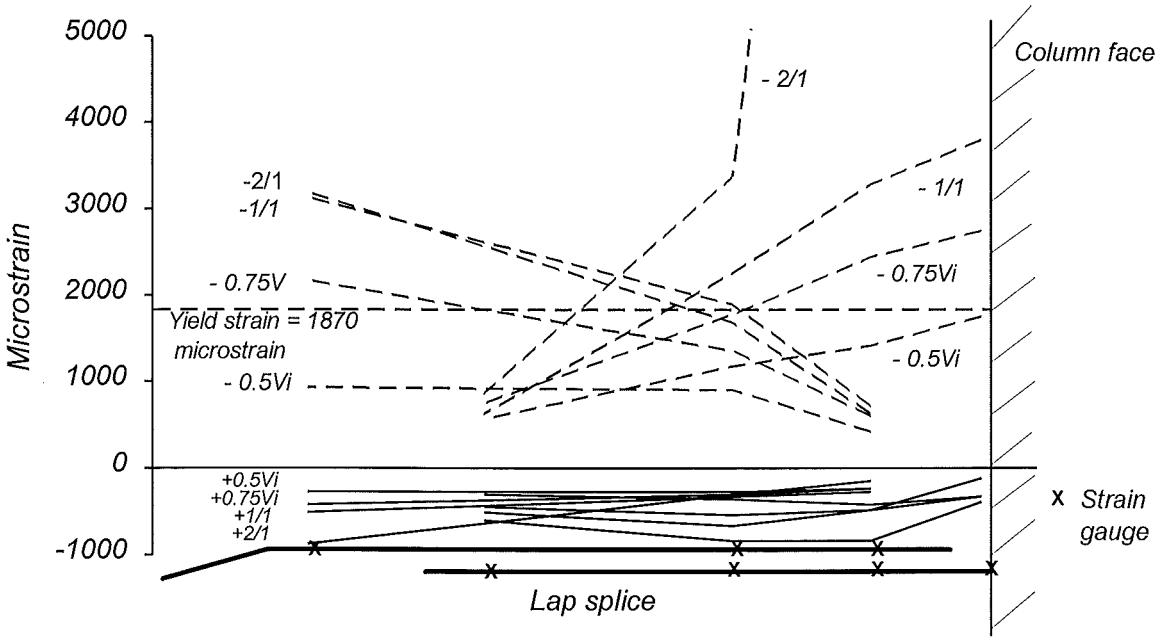

Fig. 5.9 Bar Strains Recorded Within a Splice.

Transverse Beam Reinforcement

Four graphs provide the strain data from the legs of the five stirrups strain gauged in each beam. Unfortunately the amount of data available from the gauges was limited by the loss of some of the gauges during displacements to $\mu = +4/1$, leaving the remaining gauges with invalid results. Figures 5.10 and 5.11 present strains from the side and bottom legs of stirrups in the west and east beam respectively.

Figure 5.10a displays the strains recorded on the sides of the stirrups in the west beam. The difference in strain for each direction of loading indicates the stirrups were working to contain the splice during the early negative cycles. The strains recorded by the five stirrups were greater when the splice was in tension at μ = - 1/1 than at μ = + 2/1 when the west beam was carrying a greater load at a larger displacement.

The sides of stirrups 7 and 8 in the middle of the splice developed the largest strains particularly during the negative displacement cycles. Stirrup legs 6S and 10S at each end of the splice began to resist load as cracking increased.

Compression strains were recorded by the gauge on one side of stirrup 7 during the positive displacement cycles. Once some side cover was lost, this stirrup was observed being held by the lower spliced bar and being pulled out of plane during displacements. Possibly in the early stages of testing the splice slip was sufficient to drag the stirrup leg and develop compression strains in the gauge on the side of the stirrup.

The crack widths in the beam were still small at $\mu = \pm 2/1$ and the stirrups were not required to resist large shear loads until later in the test.

The values of strain recorded by the gauges on the bottom section of the west beam stirrups are shown in Fig. 5.10b. Gauges 7B and 10B produced inexplicable results from the start of testing which varied little as the loads in the beam increased. Other strains recorded for the bottom section of the stirrups show slight increases in strain for the period of results shown. The vertical legs of the stirrups were not highly stressed for the early stages of the test so the demands on the bottom sections were minor.

The strains recorded by the five gauged stirrups in the east beam are presented in Figures 5.11a and 5.11b. The strains for the vertical stirrup legs in Fig. 5.11a developed more consistently than those in Fig. 5.10a for the west beam. The maximum strain recorded in the east beam was less than in the west beam with the three middle stirrups sharing the largest strains in each cycle.

Figure 5.11b displays the strains from the gauges on the bottom legs of the five stirrups in the east beam. Generally the strains increased slowly following the trends of the vertical stirrup legs. Gauge 2B differed from this, recording tensile strains during the negative displacement factors which were greater than those in the vertical stirrup leg. The reason for the compression strain in 5B at μ = - 2/1 and the behaviour of 2B is unknown.

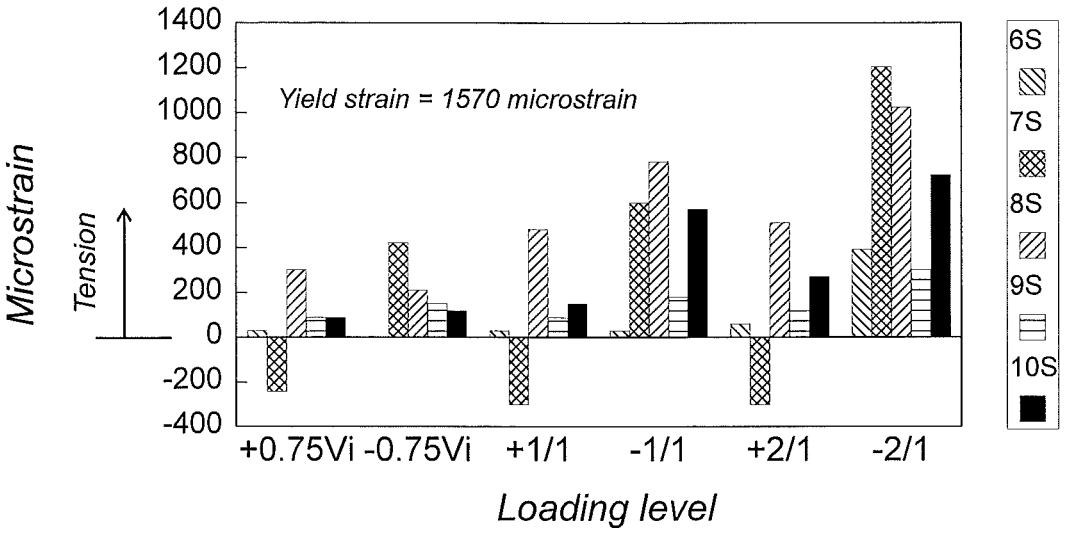

Fig. 5.10a Strains Recorded From the Side of the Stirrups in the West Beam.

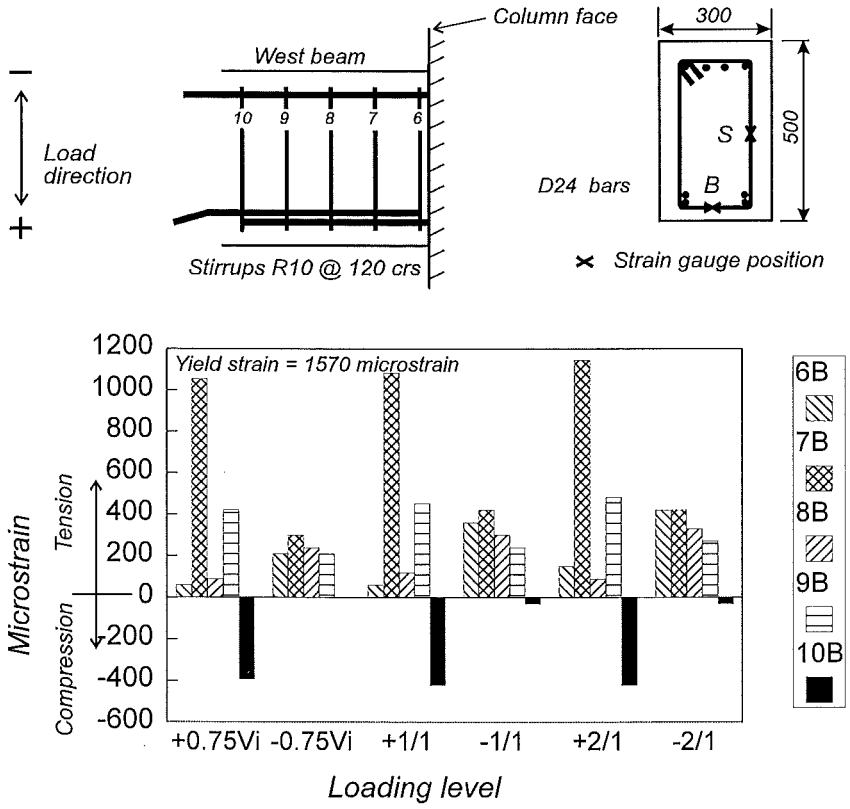

Fig. 5.10b Strains Recorded From the Bottom of the Stirrups of the West Beam.

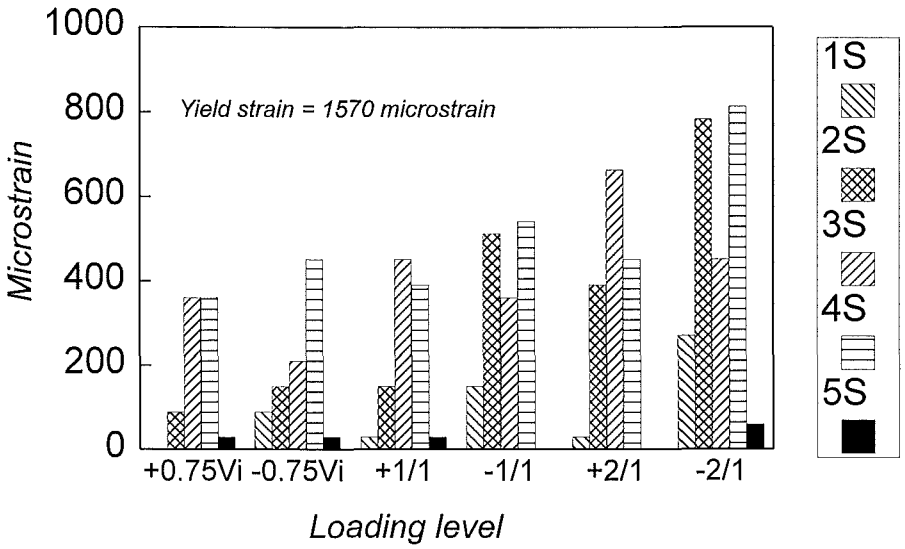

Fig. 5.11a Strains Recorded From the Sides of the Stirrups in the East Beam

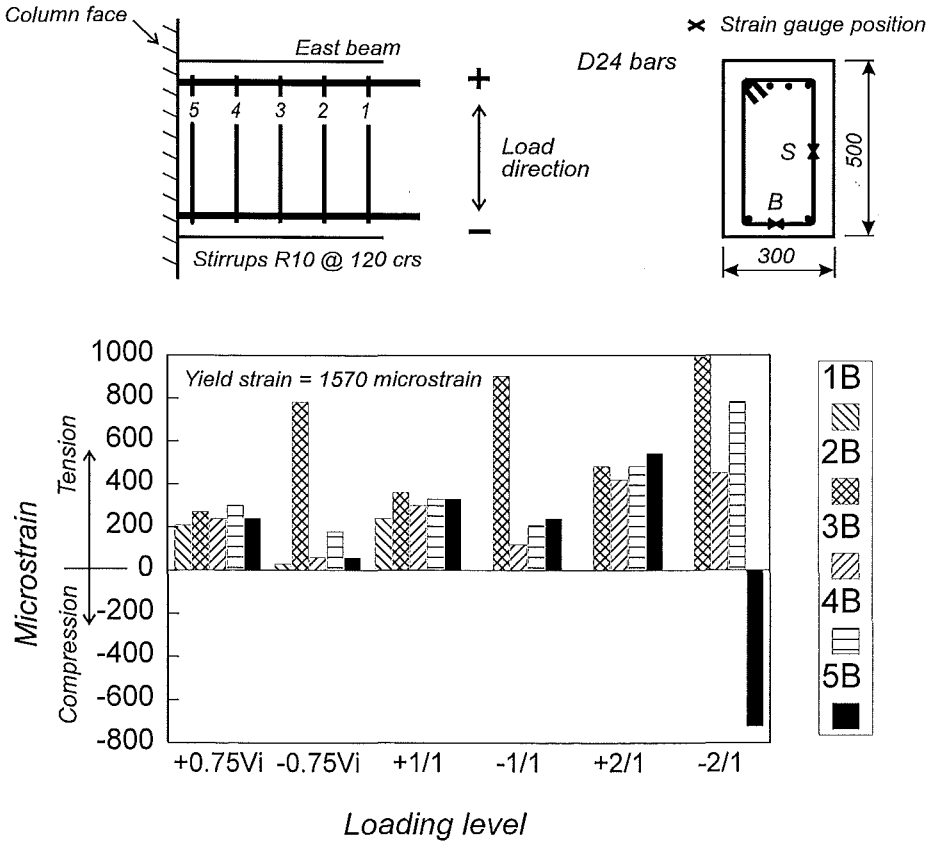

Fig. 5.11b Strains Recorded From the Bottom of the Stirrups in the East Beam.

Lap splice slip

The potentiometers recording the slip of the lap splice bars were supported from steel rods embedded at the mid-depth of the beam to provide stable anchorage. Consequently, the effect of beam curvature is included in the readings. No satisfactory method was found for removing the component of curvature from each potentiometer reading. Results illustrating splice slip give the difference in slip between the bars. Only the differences in curvature between the bar positions (approximately 50 mm) in the splice remain.

Figures 5.12, 5.13 and 5.14 plot the load carried by the west beam against the slip between a pair of spliced bars. Figures 5.12 and 5.13 focus on movement in the splices early in the test, Fig. 5.14 displays the extend of slip once a splice had come apart.

Comparison of Figures 5.12 and 5.13 shows that different amounts of slip occurred between each set of spliced bars in the initial stages of testing. The relative position of each splice as it was cast is presented with each figure.

The top cast splice provided the poorer bond performance from the beginning of the test. Figure 5.12 shows the slip between the spliced bars cast in the bottom of the formwork was 0.15 mm for μ = -1/1 and 0.28 mm for μ = -2/1. The corresponding values of slip for the splice cast higher in the formwork are given in Fig. 5.13 as 0.35 mm and 0.54 mm respectively.

The cycles to μ = -1 and -2 provided several indications the concrete surrounding the splices was stressed beyond the elastic capacity causing non-recoverable slip. Figures 5.12 and 5.13 show moderate increases in negative load for the west beam until the slip in the splice approached previous limits. Both splices experienced further bar slip during the second cycle of displacements to μ = -2 than in the first, however, Fig. 5.3 shows there was no difference in the values of column top displacement for these two cycles.

During the displacements to μ = -4/1 the cracking in the concrete surrounding the lapped bars reached the length of the splices and both lap splices came apart. Figure 5.3 shows the loss of load began before the previous displacement peak of μ = -2 had been reached. Figures 5.12 and 5.13 show considerable additional slip occurred before the beam lost load.

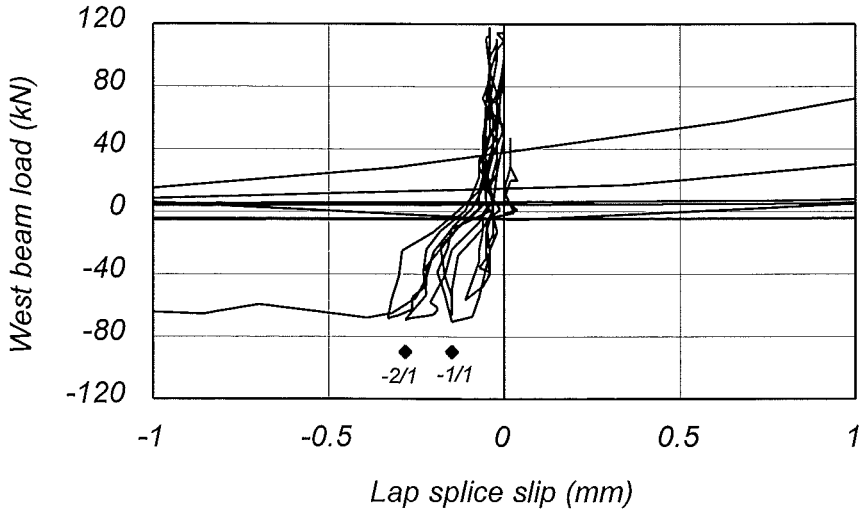

Fig. 5.12 Relative Slip of the Splice Cast in the Bottom of the Beam Formwork.

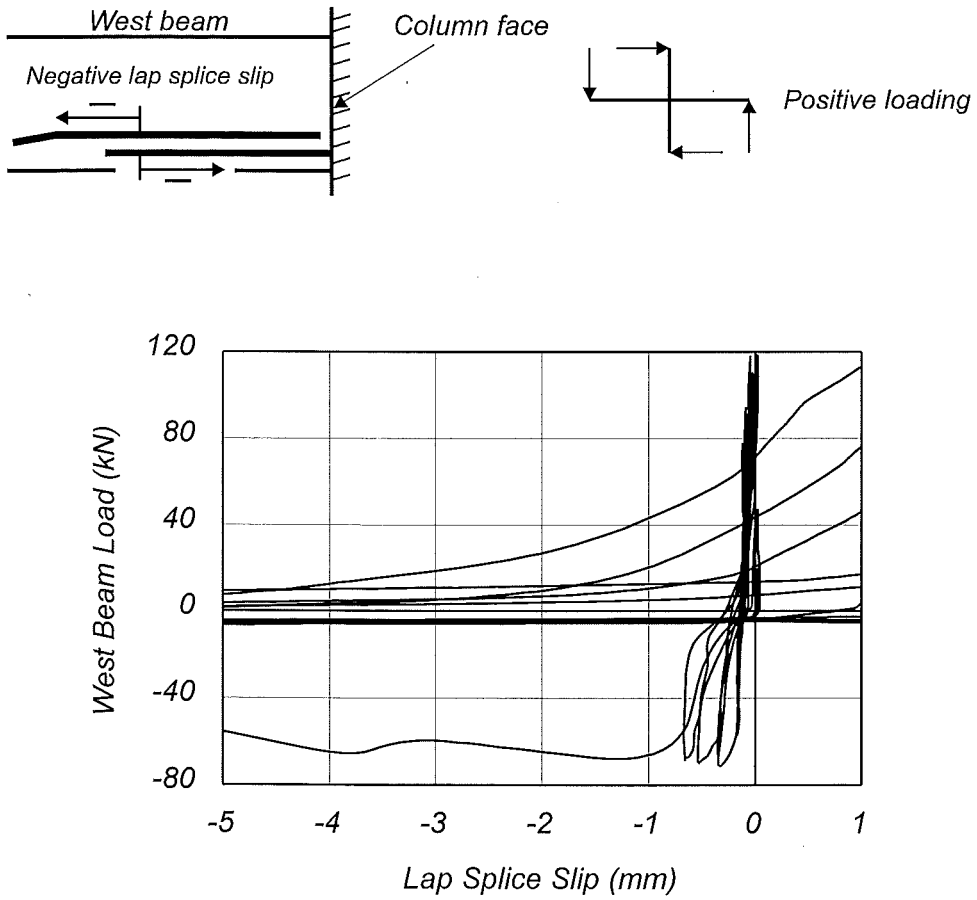

Fig. 5.13 Relative Slip of the Splice Cast in the Top of the Beam Formwork.

Figures 5.12 and 5.13 present the slip in each splice to the point when load was temporarily regained in the west beam before μ = - 4/1. For the splice cast in the top of the formwork this was at a splice slip of 3.86 mm and for the bottom cast splice the load was regained at a slip of 0.86 mm. Data from the strain gauges which remained active on the spliced bars was reviewed to located the cause of the load increase. No increase in tension strain was recorded on the reinforcing bars of the upper cast splice once the initial loss of load occurred. Strain gauges on both bars of the splice cast lower in the formwork recorded an increase in tension strain for the scan in which load was temporarily regained in the west beam. The remaining load-slip profiles in Figures 5.12 and 5.13 were recorded between later ductilty factors.

Figure 5.14 shows the slip that occurred during the remainder of the test for the splice cast lowest in the formwork. The results were very similar to those of the other splice.

As the splices came apart during displacements to μ = -4/1 the loss of load in the west beam was gradual. The capacity of the west beam during negative loading was unable to return once the splices had separated. The increased displacements of subsequent negative ductility factors are reflected in the slip of the splice.

Positive lap splice slip occurred after μ = -4/1 indicating the spliced bars slid together. Loosening of the splices allowed them to close further when they went into compression. This slip increased as more concrete was lost from the splice regions. There was no significant change in the positive load carried by the west beam for the rest of the test.

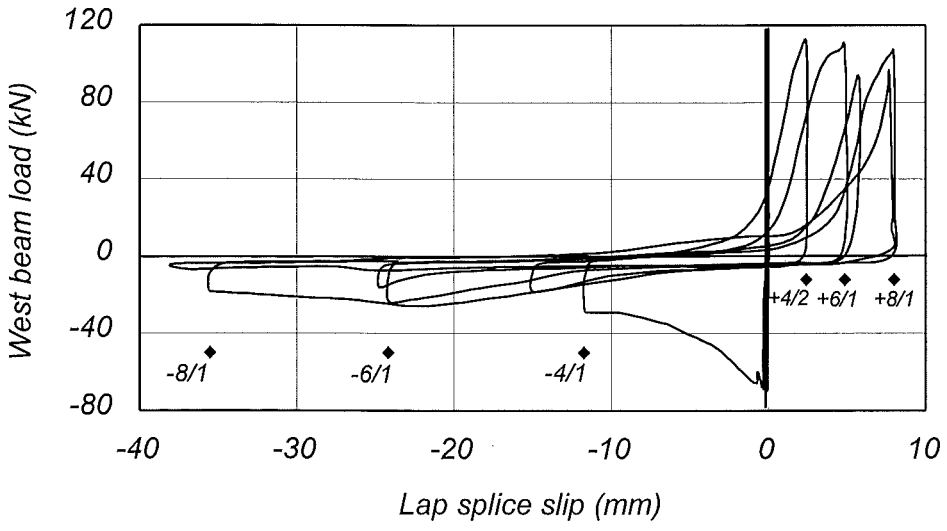

Fig. 5.14 Total Slip of the Splice Cast in the Bottom of the Beam Formwork.

5.2.5 Column and Joint Behaviour

Joint Bar Slip

Potentiometers were used to monitor the slip of a top and a bottom longitudinal beam bar through the centre of the joint. The maximum slip recorded for the top and bottom bars was 0.20 mm and 0.68 mm respectively during positive ductility factors at $\mu = 8$ and 10. The slip occurred cyclically and gradually increased as yielding in the bars penetrated further into the joint.

Column longitudinal steel

The bar strains from strain gauges on four longitudinal column bars in Specimen One are presented in Figures 5.15a and 5.15b. The gauges were located above and below the joint at the beam faces. All the strain gauges on the column longitudinal bars remained functional for the test. The peak bar strains for ductility factors $\mu = \pm 6$ and beyond were gradually reduced from the values at $\mu = \pm 4$.

The values of strain recorded above the joint in Fig. 5.15a gradually increase with the ductility factors. Crack sizes in the column remained small and the bars were not required to resist large compression loads. Small demands were made upon the interior column bars which recorded strains one half the size of those on the outer bars. The loss of the load capacity in the splice before $\mu = -4/1$ had a slight effect with the strains falling below those for $\mu = -2/1$.

In Fig. 5.15b the maximum strains recorded below the joint for the negative ductility factors were consistently less than those for the positive factors. As the splice failed the strains in the bars reduced until at $\mu = -4/1$ they were below the values recorded for $-0.75V_i$. The loss of load in the west beam led to a direct reduction in the demands made upon the longitudinal steel adjacent in the column. The reason for the reversal in the strain profile for the two intermediate longitudinal bars during $\mu = 2/1$ and 4/1 is not clear. These gauges were on bars placed in the bottom of the formwork and tentative vibration through the joint to avoid damaging gauges during concrete placement may have lead to less than ideal bond conditions.

The column longitudinal bars did not experience large strains into the inelastic region due to the placement of column steel which exceeded the requirements for capacity design.

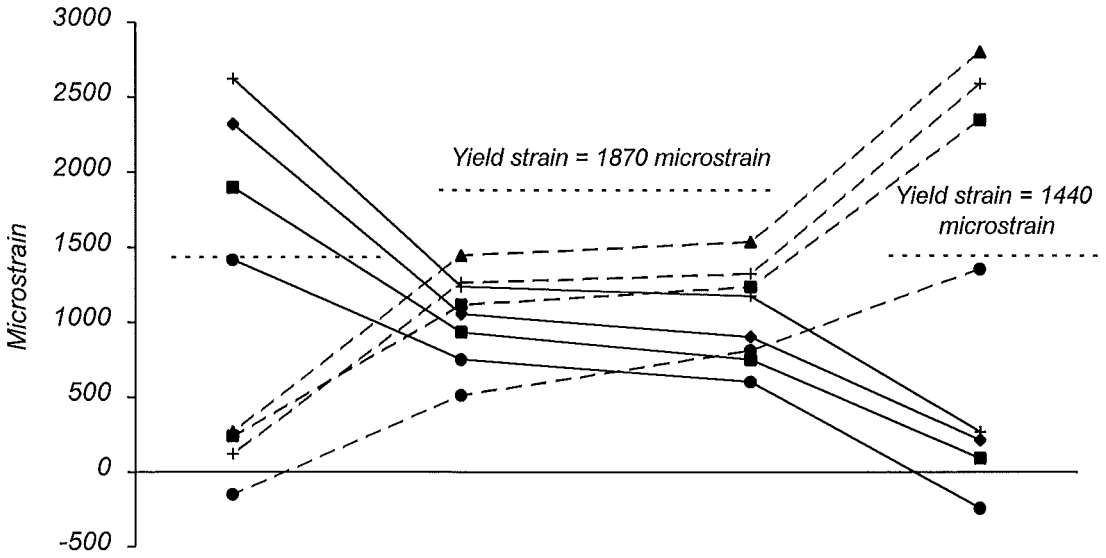

Fig. 5.15a Strains Recorded Above the Joint in the Column Longitudinal Bars.

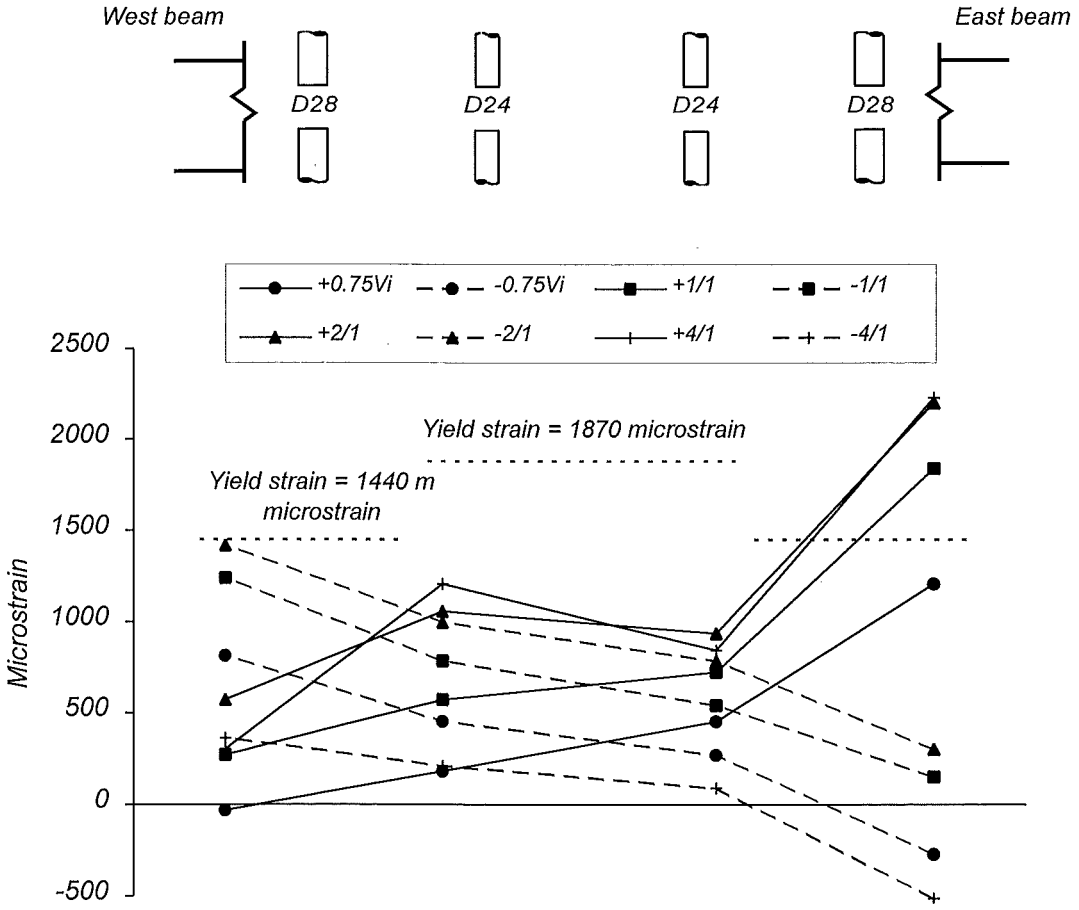

Fig. 5.15b Strains Recorded Below the Joint in the Column Longitudinal Bars.

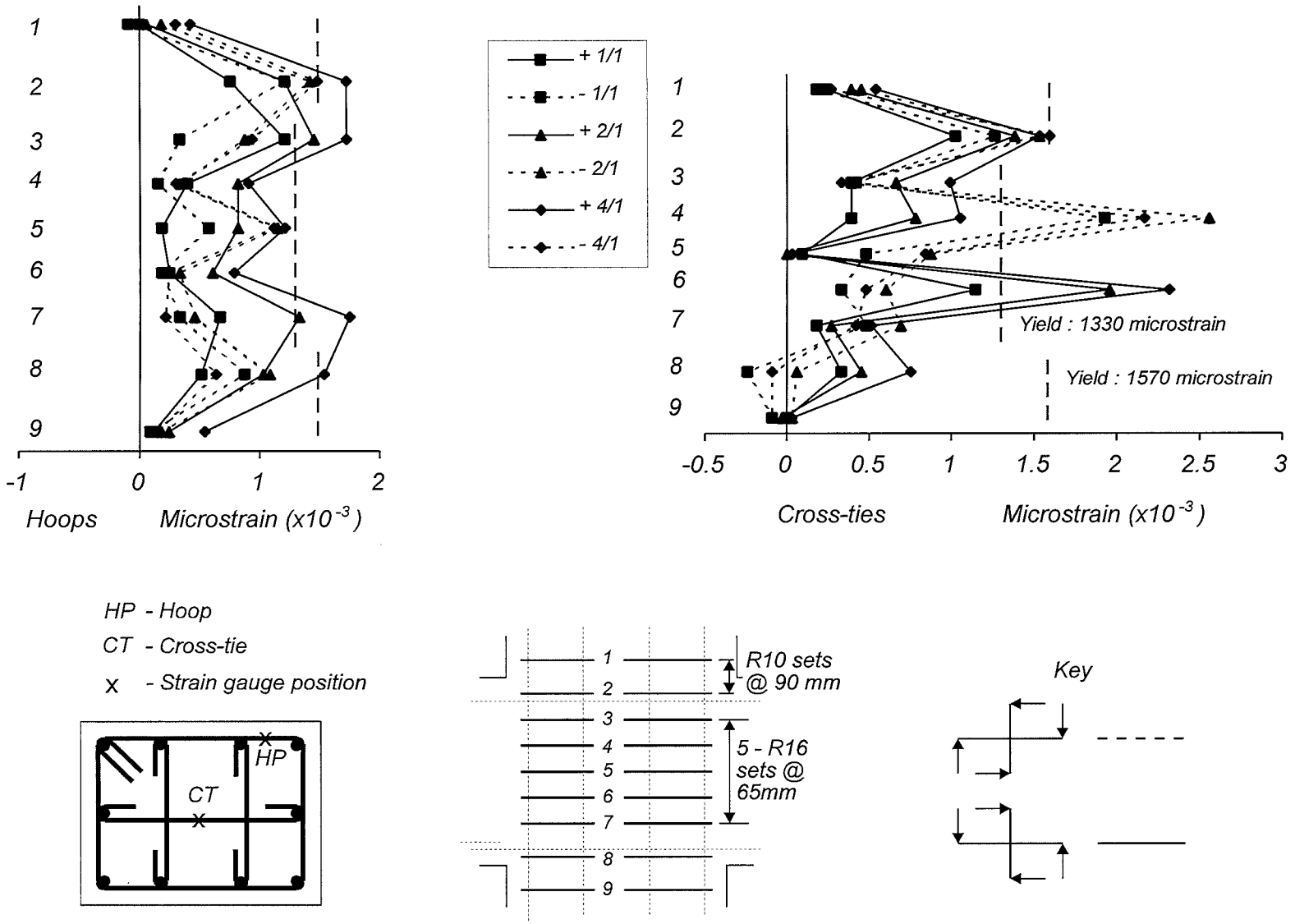

Fig. 5.16 Strains Recorded by the Column and Joint Transverse Reinforcement.

Column and Joint Transverse Reinforcement

The results from the strain gauges on the joint and column transverse steel are plotted in Fig. 5.16. One cross-tie and one hoop of each transverse steel set were strain gauged. The results are separated into the data from the cross-ties and the hoops. All the strain gauges on the column and joint transverse steel completed the test. Results are provided to $\mu = \pm 4/1$. The peak strains which followed remained at a similar level or decreased as deformations in the column and joint reduced.

The yield strains for the transverse steel are displayed. However, the accuracy of the data from the gauges remains in doubt. Strains recorded for the transverse steel were low as a result of the low stresses in the column bars and the lack of significant cracks. The largest strains were recorded in the joint cross-ties when the hoop of the same set carried considerably less. This may be due to a difference in fit for the hoops and ties around the column bars.

The strains recorded by the cross-ties and hoops below the middle of the joint for the negative ductility factors were noticeably less than those for the positive ductility factors. The cross-ties below the joint recorded slight compression strains for the first two negative ductility factors shown. The demands made by the spliced bars in the west beam upon the column led to transverse steel requirements which could be met by the hoops below the joint.

5.3 TEST RESULTS OF SPECIMEN TWO

5.3.1 Observed Behaviour

Specimen Two had beam details (including plain round bars, splice length and placement) of a Christchurch building constructed in the early 1960s', however the beam-column joint and column complied with NZS 3101:1982.

The loading cycle to $\pm 0.5V_i$ generated a large amount of cracking in the column and joint of the specimen. Several long fine diagonal tension cracks appeared in the joint during the loading cycles in each direction. Five or six equally spaced flexural cracks developed on both sides of the column above and below the joint over a distance of one metre from the beam faces. The longest of these crossed two-thirds of the column depth.

Three or four flexural cracks were generated from the top and bottom of each beam, including cracks on either side of the splice. At the column face cracking extended 80% of the beam depth, elsewhere within the potential plastic hinge regions the cracks reached the mid-depth of each beam.

The column top displacements at the positive and negative peaks of $0.75V_i$ were 49 mm and 42 mm respectively. These were three times greater than the equivalent values from Specimen One and indicate a dramatic lack of stiffness in the specimen. The maximum crack width at a column face was 3 mm at the top of the east beam. The diagonal cracks in the joint region increased in length and number. In the beams and the column the crack lengths increased slightly. One crack crossed the splice during - $0.75V_i$ extending 40% of the depth of the beam.

During $\mu = \pm 1$ the concrete in the top and the bottom of each beam at the column faces began to be crushed, as shown in Fig. 5.17a. The first displacement cycle saw small extensions added to the cracks in the joint, but little further damage was observed in the joint and column.

A maximum crack width of 15 mm was recorded at the column faces during displacements to $\mu = \pm 2$. Fig. 5.17b indicates crushing continued in the beams but other damage appeared to be minimal. Movement between the spliced bars was apparent from the positions of the potentiometers on the splice.

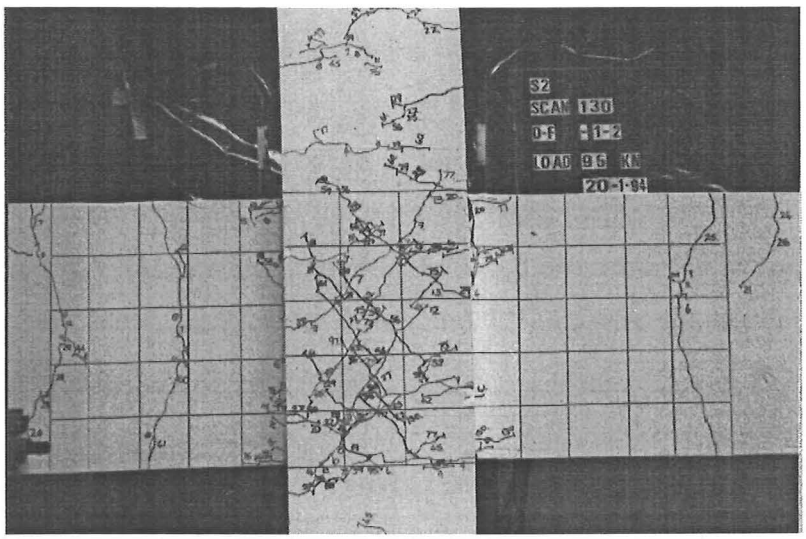

Fig. 5.17a Condition of the Specimen at $\mu = -1/2$.

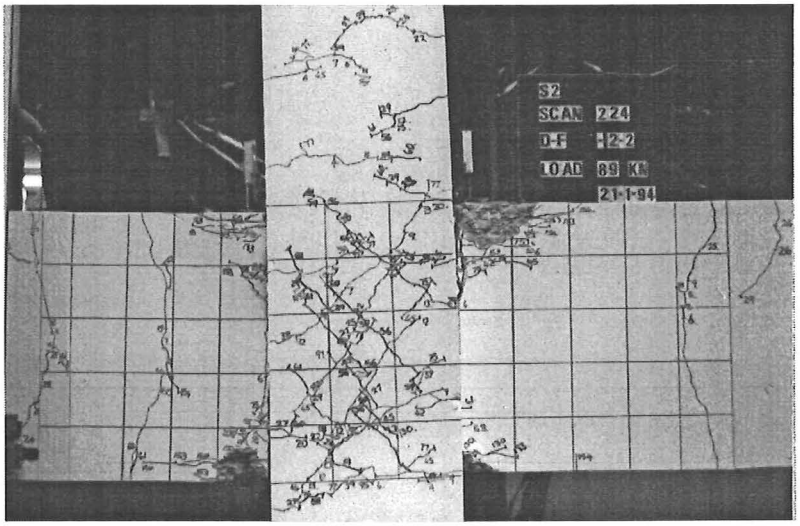

Fig. 5.17b Condition of the Specimen at $\mu = -2/2$.

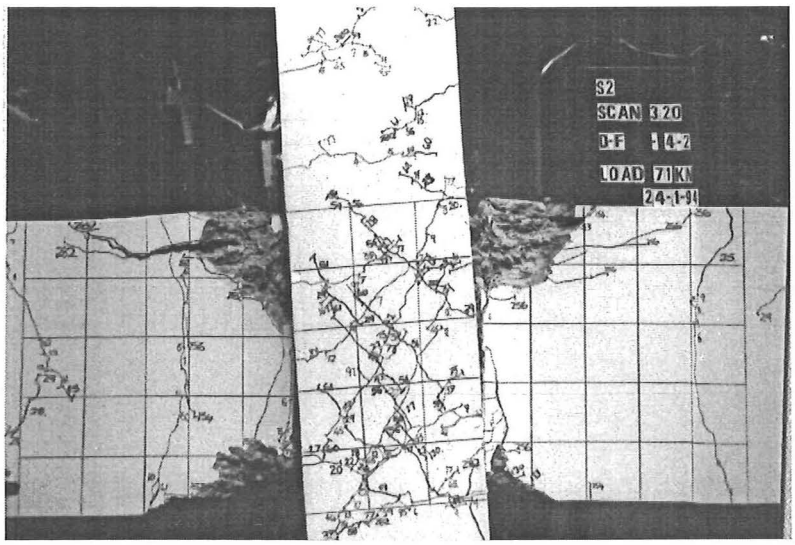

Fig. 5.17c Condition of the Specimen at $\mu = -4/2$

Fig. 5.17c shows the condition of the specimen after the two displacement cycles at $\mu = 4$. Concrete crushing and dowel forces from the top bars had lifted the top concrete cover from the beams. The concrete beneath the beams at the column faces did not experience as much damage. However, more material was lost as it fell from the beams. Where cracking at the column faces could be measured, a maximum of 35 mm was recorded at peak displacements. At zero displacement these cracks were 8 mm and 12 mm over the depth of the beams on either side of the column.

By the end of the test the top and bottom cover for the beams had been eroded at the column faces where the cracking extended to the depth of each beam. The damage elsewhere in the specimen was limited to a large number of fine cracks. Nothing distinguished the splice region from other areas in the potential plastic hinge regions of the beams.

5.3.2 Load Displacement Response

Fig. 5.18 shows a plot of the horizontal load versus the horizontal displacement at the column top. Fig. 5.19 is a similar plot presenting the beam loads at the column top displacements.

The lack of stiffness in Specimen Two is apparent from the first cycle of loading. The interstorey drift angles at one-half of the theoretical lateral load V_i were 0.83% and 0.61% for the positive and negative load directions respectively. The specimen did not respond smoothly to the increasing displacements. From Fig. 5.19 the west beam developed no additional load during one negative loading increment. Some loss of stiffness can be seen in Fig. 5.18 after unloading in this cycle.

The second cycle of loading in the 'elastic range' to $0.75V_i$ produced drift angles of 1.53% in the positive load direction ($0.72V_i$) and 1.31% in the negative direction ($0.74V_i$). These were increases of 84% and 115% respectively whereas an elastically responding specimen would have recorded a 50% increase in displacement between $0.5V_i$ and $0.75V_i$. Also interesting in this cycle is a 1.3 mm increase in displacement which occurred when unloading began from $0.72V_i$.

The maximum load recorded by the specimen in the positive displacement direction occurred during the first cycle at $\mu = 1$. At a drift angle of 2.04% the specimen reached 0.75 V_i and in

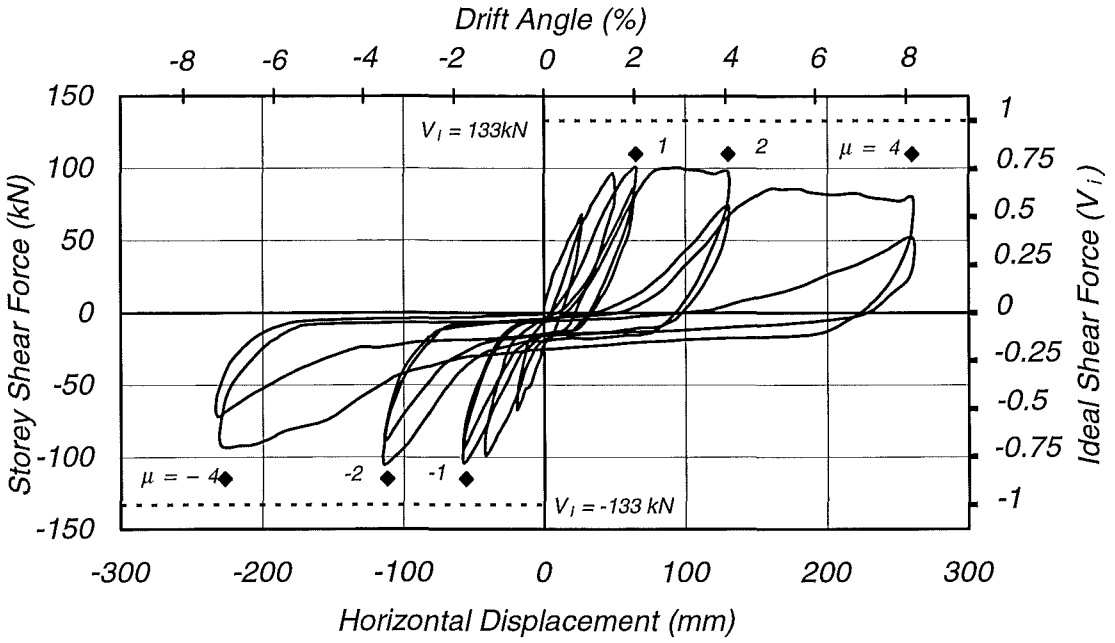

Fig. 5.18 Lateral Load-Displacement Response.

the second cycle $0.64V_i$. In the opposite direction $0.68V_i$ and $0.70V_i$ were reached in the first and second cycles respectively at a drift angle of 1.75%. At this stage the hysteresis loops had become very pinched as the slip of the beam bars through the joint increased.

Displacements to μ = + 2/1 pushed the specimen to the previous maximum load of $0.75V_i$ before it dropped to $0.73V_i$. The second run to μ = + 2 reached $0.56V_i$ and dissipated considerably less energy than the first. The maximum load held by the specimen for the test $0.79V_i$, was reached on the first run in the negative direction. For the second run in the negative direction $0.67V_i$ was held. Fig. 5.19 shows for the positive displacement direction in this and subsequent runs the west beam held approximately 80% of the total load. In the opposite direction the east beam took a similar percentage of the load instead of the 65% : 35% split expected from the moment capacities of each beam.

The reactions at the end of each beam during the first cycle at μ = 2 were the largest for the test. During the positive and negative displacement peaks the west and east beam reached 104% and 103% respectively of the ideal load capacity of the beam. These values are provided only as an indication of the beam loads. As considerable slip of the beam bars had occurred, the standard flexural theory equations are not applicable.

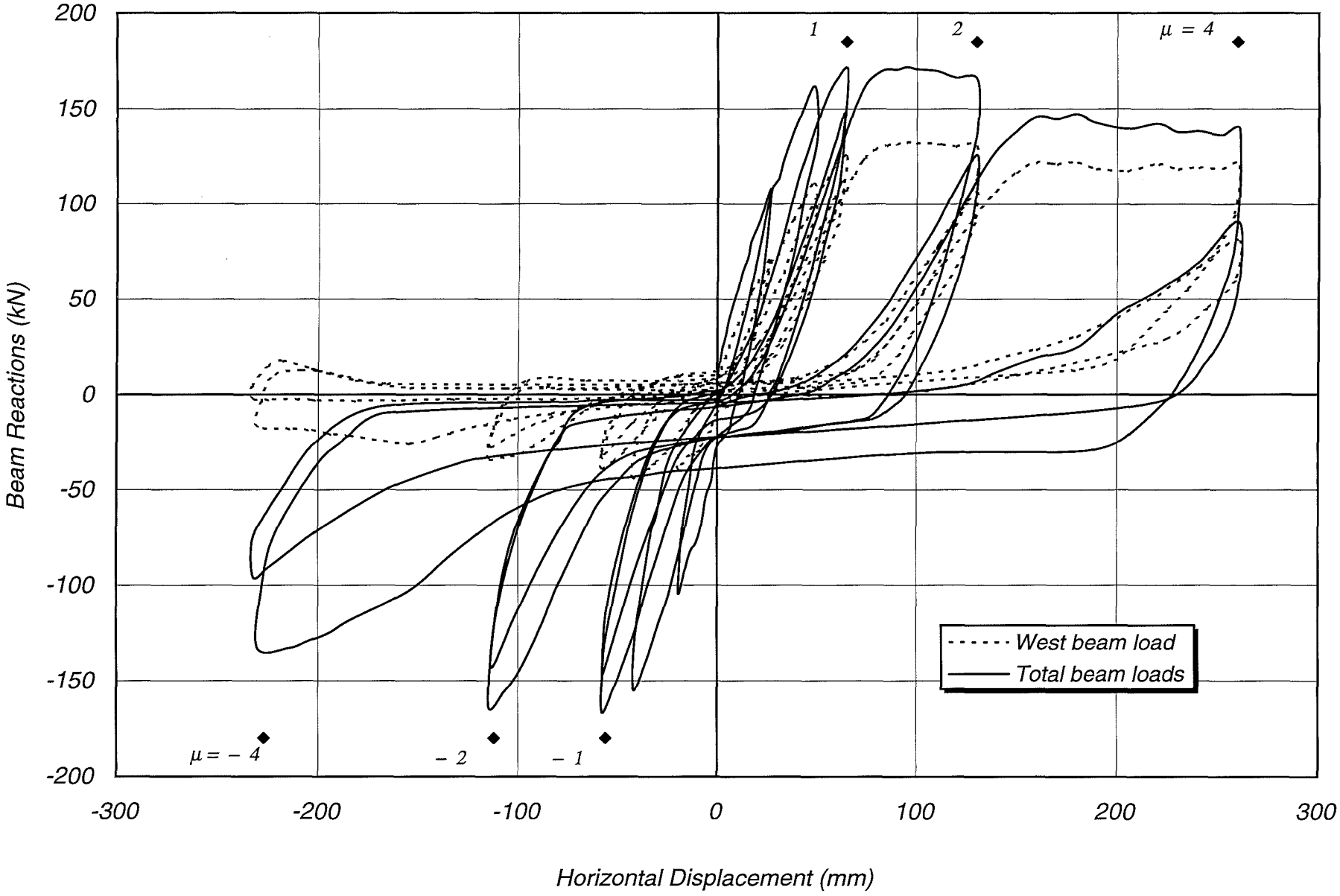

Fig. 5.19 West and Total Beam Loads Versus the Column Top Displacement

Slip had occurred between the plain longitudinal beam bars and the surrounding concrete. The bars could not gain sufficient bond from the concrete for the beams to resist the external shear forces with changing bending moments and tensile reinforcement strains. An alternative method for supporting lateral load evolved using the anchorage available from the test rig.

The beam carrying the greater proportion of load developed an inverted compression arch from the pinned end to the bottom of the beam at the column face. Anchored at the end of each beam, the top longitudinal bars provided the horizontal reaction required to balance the compression thrust. The vertical component of the inverted arch opposed the applied shear force. The opposite beam supported minor loads as the concrete cover above the tensioned top beam bars went into compression. As the specimen was gaining an advantage from the testing rig restraints the results are not a good indication of the seismic performance of the sub-assemblage in a building.

From Fig. 5.18 the hysteresis loops for the displacements to $\mu = +2/1$ and $\mu = +4/1$ were fuller than the loops for the other displacement runs at these ductility factors. As the subsequent displacements were resisted with the same mechanism the ability for the specimen to dissipate additional energy was reduced.

In Fig. 5.19 the difference between the total and west beam loads as the specimen returned from the positive ductility factors indicates a negative direction load developed in the east beam. The negative load in the beam after $\mu = 4/1$ was greater than the positive load recorded in the beam for displacements to $\mu = 4/1$. The negative load was a result of the longitudinal bar slip during the positive displacement loading. When the load was released after the displacement peak the slipped longitudinal beam bars and the gaps at the column faces remained. As the column top returned to zero displacement the offset bars were forced to recover some of the previous slip through the joint. Friction between the sliding bars and the surrounding concrete led to the negative load resistance in the east beam. A similar situation can be seen from Fig. 5.19 in the west beam load as the specimen returned from negative displacements.

The loads for the displacements at $\mu = 4$ decreased a little from the previous level of ductility. For displacements in the negative direction the column top loads were $0.69V_i$ and $0.54V_i$, exceeding $0.59V_i$ and $0.39V_i$ for the positive direction. Crushing in the bottom of the beams at the column faces had reduced the available compression zone and in the restraining beam the peak loads dropped.

5.3.3 Beam Behaviour

Lap splice slip

The slip recorded between a pair of spliced bars is plotted in Fig. 5.20 against the west beam load. The results were similar for each lap splice.

The lack of bond between the concrete and the spliced bars allowed bar slip to begin from the first cycle of loading. Slip occurred with each direction of loading as the crack on either side of the joint opened pulling the longitudinal bar from the splice. As the test progressed the increasing column top displacements led to the cracks widening at the column faces and greater amounts of bar slip occurred in the splice.

The displacements to $\mu = 2/1$ and $\mu = 4/1$ produced large values of slip to accommodate the strains in the top longitudinal beam bars. As very little cracking occurred in the beams beyond the column faces the slip in the lap splices represents the crack widths at the column faces.

During positive direction displacements the west beam was able to resist load as the bottom of the beam was in compression. This minimised the effect of the sliding splice bars. For the negative displacements the slip in the splice prevented a tension force developing in the bottom of the beam.

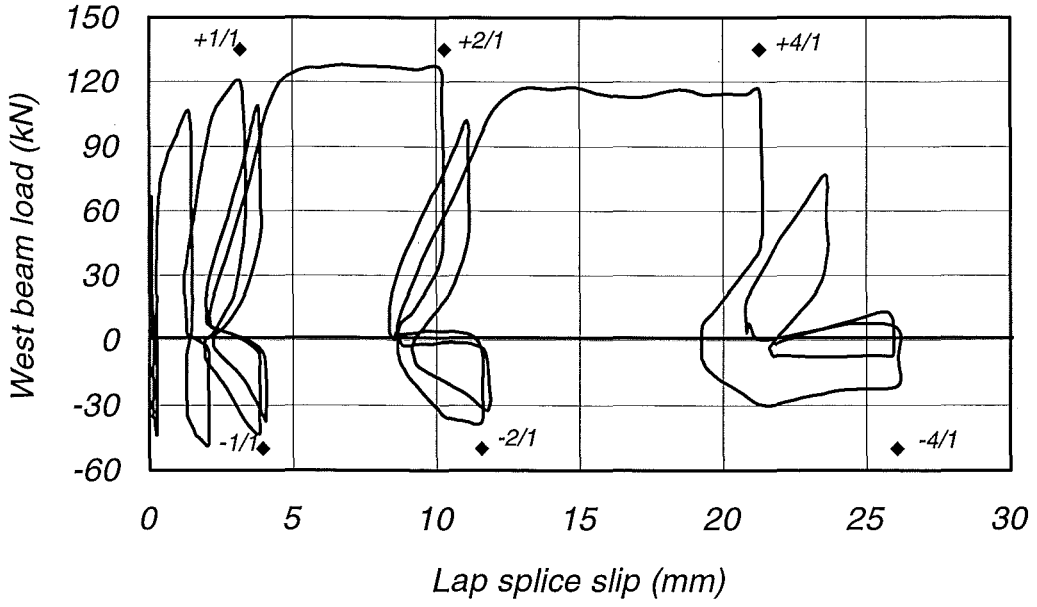

Fig. 5.20 Relative Slip in the Lap Splice Versus Load in the West Beam.

Curvatures and Shear Strains

The beam curvatures and shear strains for Specimen Two are shown in Figures 5.21 and 5.22. The vertical lines on the graphs represent the column faces and the potentiometer gauge lengths. As the values of displacement used in each direction were different, only the curvature and shear strain trends for the beams can be compared.

Fig. 5.21 shows the beam curvatures were concentrated at the column faces for the duration of the test. The large crack and the concrete crushing that occurred at each column face were theresult of fixed end rotations in the beams. The loss of bond for the longitudinal beam bars prevented the shear forces developing flexural bond stresses in the reinforcement. As a result the curvatures beyond the column faces were minimal. Figure 5.22 is a plot of the shear strains recorded in the beams. These strains were confined to the cracks at the column faces. In the beam supporting the greater proportion of load, the shear displacements were resisted by the vertical component of the compression arch and dowel forces from the longitudinal bars. In each beam the largest shear strain occurred while carrying minor loads without the influence of the compression strut at the column face. Positive shear strains were not generated in the west beam due to the slip of the longitudinal beam bars. The top and bottom bars slipped through the joint in opposite directions during the positive direction displacements and the beam rotated causing negative shear strains.

During the negative direction displacements the lower bars of the east beam experienced minimal slip through the joint and the beam maintained slight positive shear strains until $\mu = -4/1$. The beam did not reverse the negative displacements generated at $\mu = 4/1$ and was hindered by the loss of cover concrete from the bottom of the beam.

Longitudinal Beam Bar Strains

Longitudinal beam bar strains were recorded with strain gauges and clip gauges on Specimen Two. The clip gauges were valuable for providing data as the strain gauges did not continue to function once large bar slip developed. Some uncertainty remains over the accuracy of the strain gauge data. The same lower longitudinal beam bars were monitored with strain and clip gauges. Different top longitudinal beam bars were used to provide strain and clip gauge data.

The amount of slip between the longitudinal bars and the surrounding concrete limited the useful life of the strain gauges on the longitudinal bars. Figure 5.23 plots the strains recorded

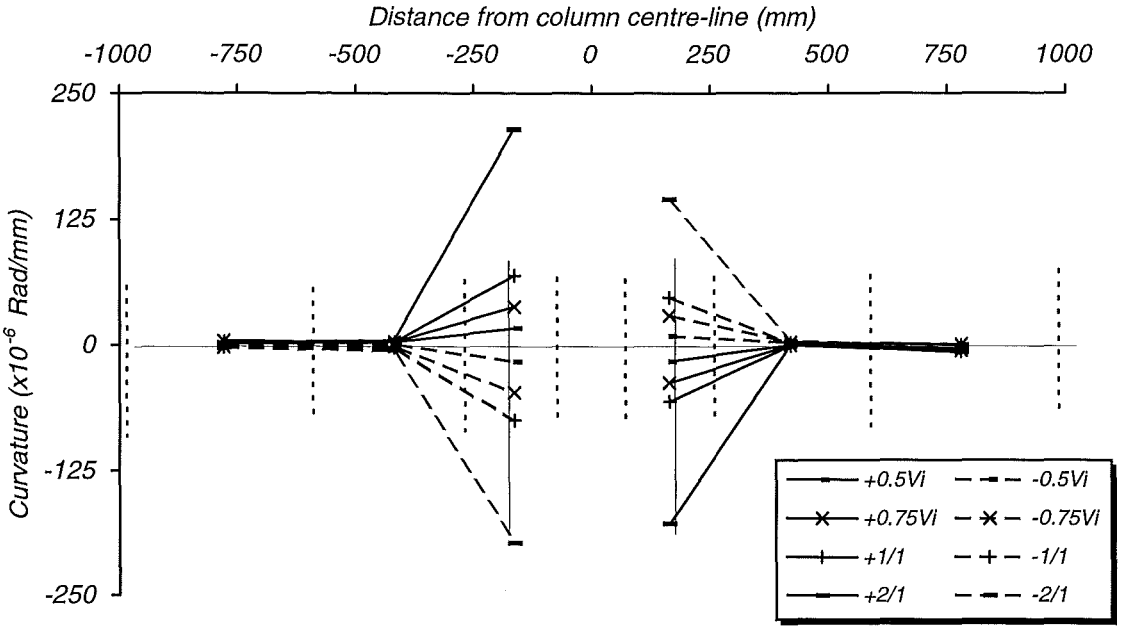

Fig. 5.21 Curvatures Recorded in Beams.

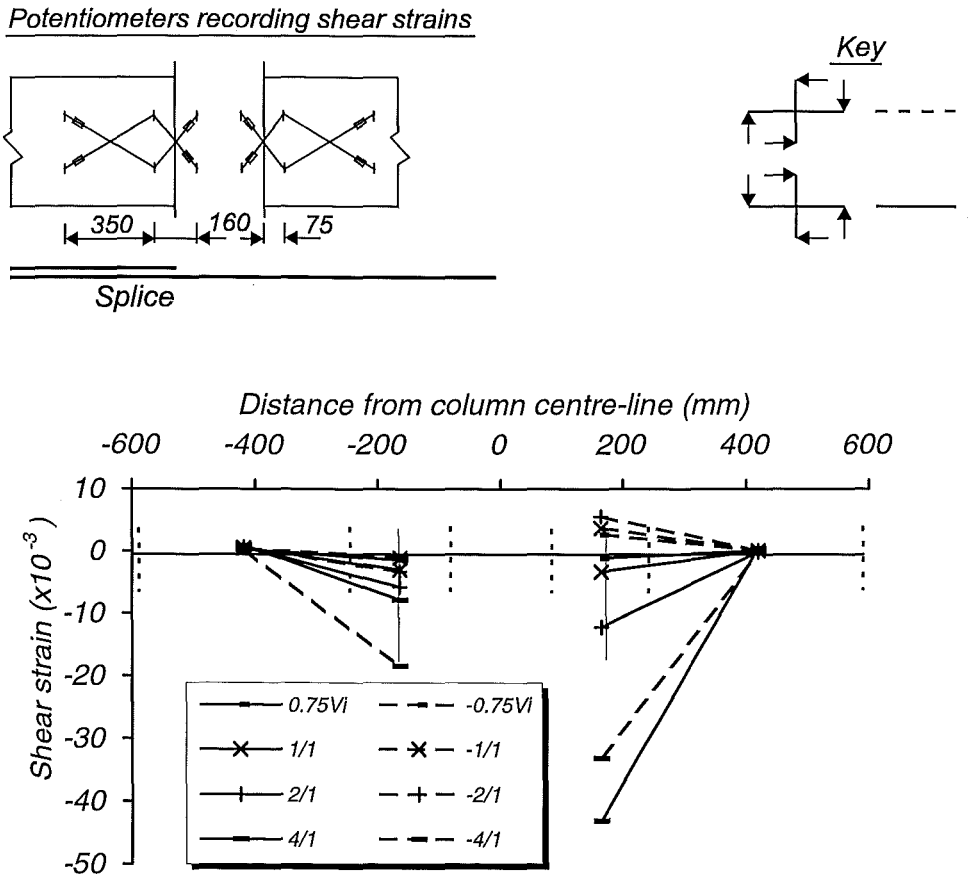

Fig. 5.22 Shear Strains Recorded in Beams

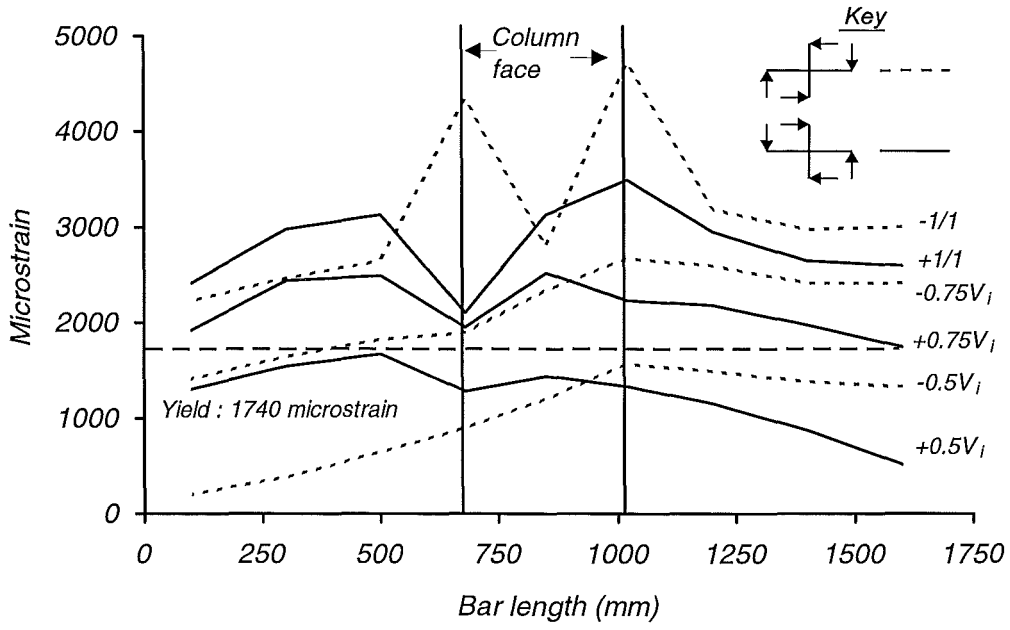

Fig. 5.23 Strains Recorded in a Top Longitudinal Beam Bar.

by the gauges on the top bar to $\mu = \pm$ 1/1. At this time a maximum slip of 2.3 mm was recorded for a top longitudinal bar through the joint.

The first loading cycle to $\pm$ 0.5V_i shows tension strains developed in the top longitudinal bar on both sides of the joint. As loading increased, the length of bar holding compression strain reduced as tension strains were recorded at additional gauge locations through and on the

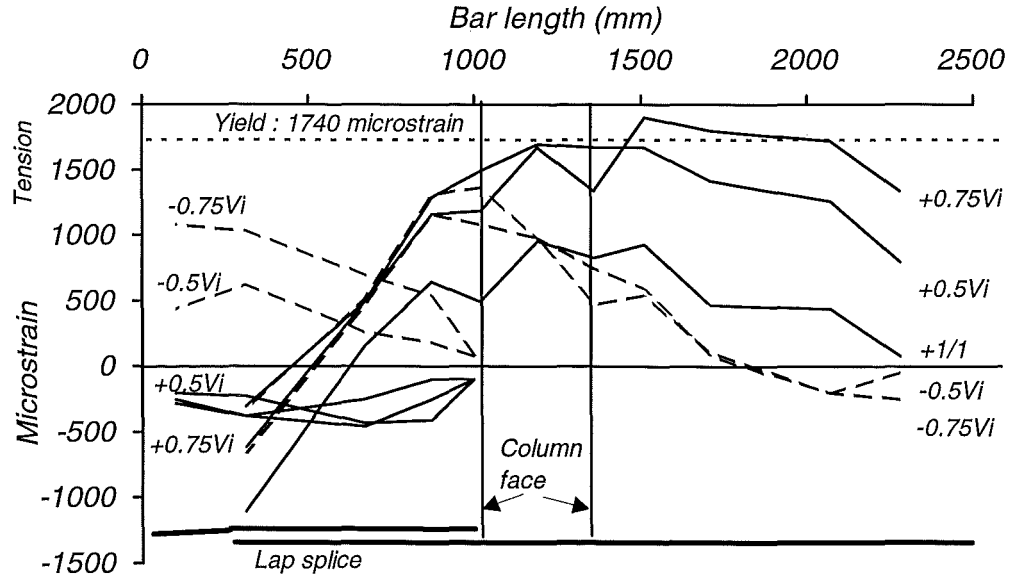

Fig. 5.24 Strains Recorded From Two Bottom Beam Bars.

other side of the joint. The tension strains in the bar increased with each cycle as the specimen developed an alternative method for resisting lateral load.

The strain profile from strain gauges on one set of spliced bottom bars is shown in Fig. 5.24. Results are shown for the first two load cycles before gauges were lost in bar slip. The shorter bar in the splice displayed compression and tension strains for the positive and negative displacements regardless of the strains in the other bar. Tension strains occurred in the longer spliced bar as it was pulled from the splice during the positive cycles. During the negative cycles the largest tension strains developed around the crack which opened at the column face in the west beam.

Figures 5.25 and 5.26 present the strains recorded by the clip gauges attached to one top and two bottom longitudinal beam bars. The gauges were mounted 300 mm from the end of each beam and in the middle of the column. They provided values of strain at three points and for display purposes a curve has been fitted. The continuous display for the bottom beam bars in figure 5.26 represents two separate bars on either side of a splice.

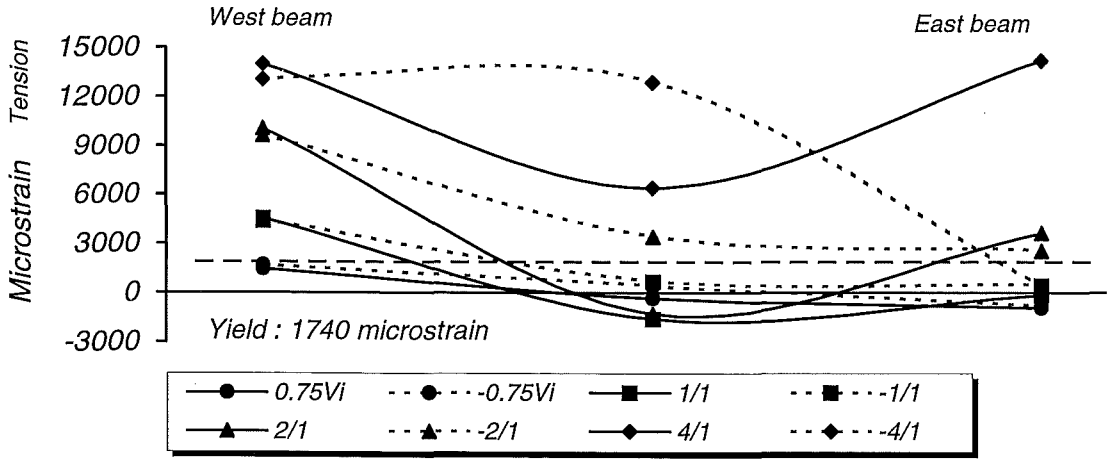

Fig. 5.25 Strains Recorded by Three Clip Gauges on a Top Longitudinal Beam Bar.

Figure 5.25 displays the strains recorded by three clip gauges on a top longitudinal beam bar. The data points for $\mu = \pm 0.75V_i$ indicate that the bond between the bar and the surrounding concrete had been lost at the location of the clip gauges. The tension and compression strains are not reversed for each direction of loading, with the bar in the west beam holding only tensile strains and in the east beam the bar recording only compression strains. The cycle to $\mu = \pm 1/1$ caused yielding between the gauge studs on the bar in the west beam. The second

half of this cycle saw tensile strains recorded at all three clip gauge locations. A comparison with Fig. 5.23 shows the strain gauged bar developed tensile strains through the joint from the first loading cycle. It appears the clip gauged bar attracted less of the initial tension load carried by the top beam bars and compression strains were recorded for the positive displacement factors to $\mu = 2$.

Strains exceeding the bar yield strain were recorded at the three gauges for the displacement to $\mu = -2/1$. Strains increased markedly into the inelastic range at the gauge in the east beam during displacements to $\mu = 4/1$. Seventy percent of this strain was recovered in the first scan after the displacement peak and this was repeated after $\mu = 4/2$. No satisfactory explanation for this result can be offered. The clip gauge at the joint recorded greater strain during $\mu = -4/1$ accommodating the loss of strain in the bar at the end of the east beam.

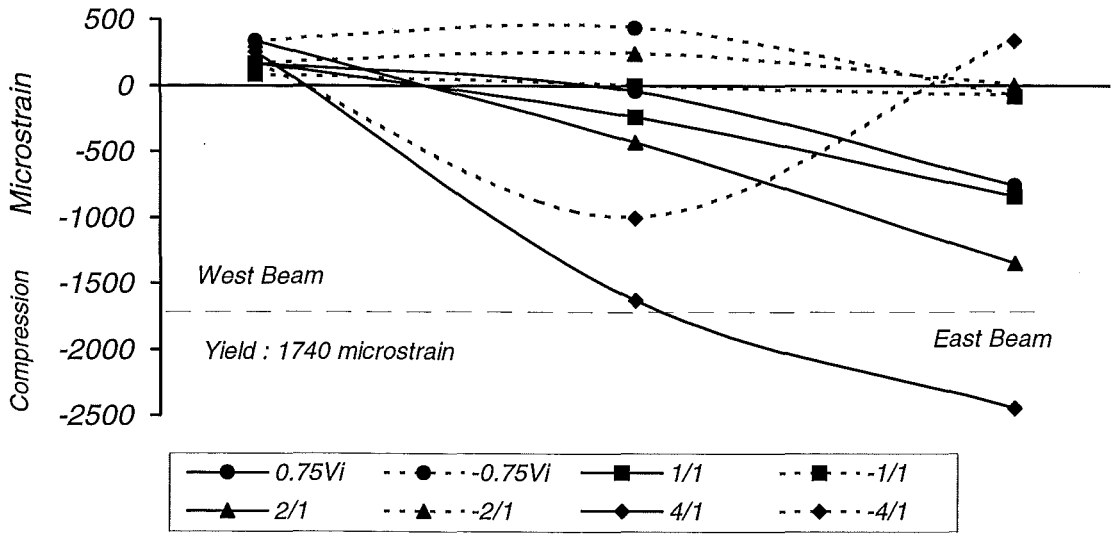

Fig. 5.26 Strains Recorded From Clip Gauges on Two Bottom Longitudinal Bars.

The strains recorded by the three clip gauges attached to one set of spliced beam bars are shown in Fig. 5.26. As the test proceeded the longitudinal bar from the east beam experienced increasing compression strains during the positive displacement cycles. The reason for the difference in results at $0.75V_i$ between the clip gauge in the joint and a similarly placed strain gauge (Fig. 5.24) is unknown. By $\mu = 4/1$ the compression strains had reached the yield strain at the end of the east beam and were approaching yield in the joint. This occurred while the east beam carried minimal load up to the positive displacement peak. From Figures 5.20 and 5.30 this bar slipped from the splice and through the joint during loading to the positive

displacement peaks. How the bar slipped and developed the compression strains is unclear, however, larger compression strains were recorded by the clip gauge in the joint upon unloading from $\mu = 4/1$. The compression strain in the bar increased as the negative load at the end of the east beam returned the bars through the joint.

The clip gauge for the bottom bar at the end of the west beam indicated little action occurred beyond the splice. It recorded low tensile strains for each of the displacement peaks with the lack of bond preventing the bar from operating effectively in the splice.

Transverse Beam Reinforcement

Strain gauge results from the transverse reinforcement in the two beams of Specimen Two are shown in Figures 5.27 and 5.28. One side leg and the bottom leg of the first three stirrups on each side of the joint were strain gauged. The lack of load in the stirrups seems to highlight some doubtful gauge behaviour. Any compression strains may be due to pressure on the stirrup leg out-of-plane. One gauge was placed at each location in a manner to avoid recording strains from bending in the plane of the stirrup.

Figure 5.27a plots the results from the strain gauges on the side of the stirrups in the east beam. The side legs carried little load and a disturbing trend is the slight gain of compression strain from the datalogger as the test proceeded. The large compression strains at $\mu = \pm 2/1$ from gauge 1S did not decrease with the removal of load and may reflect problems with the gauge.

The results from gauges on the bottom legs of the stirrups are shown in Figure 5.27b. They developed greater tension strains during the negative loading cycles than those on the side of the stirrups. Arch action developed during the negative displacements with compression loads carried by the concrete in the lower half of the east beam. The tension strains suggest some confinement was provided from the bottom longitudinal beam bars and the bottom stirrup legs to the concrete in compression. Recording the greatest tension strain for three of the four cycles shown is gauge 3B. This gauge was on the stirrup closest to the column face where the compression zone was lowest in the east beam and any confinement provided was greatest.

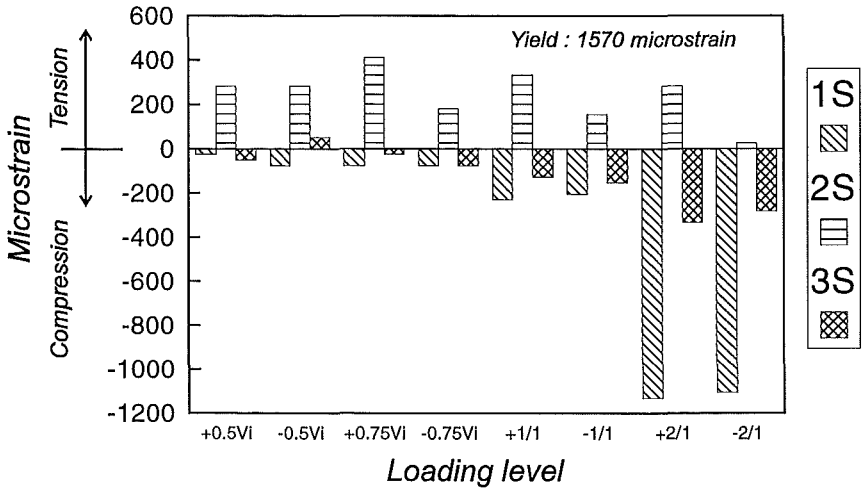

Fig. 5.27a Strains Recorded From the Side of the Stirrups in the East Beam.

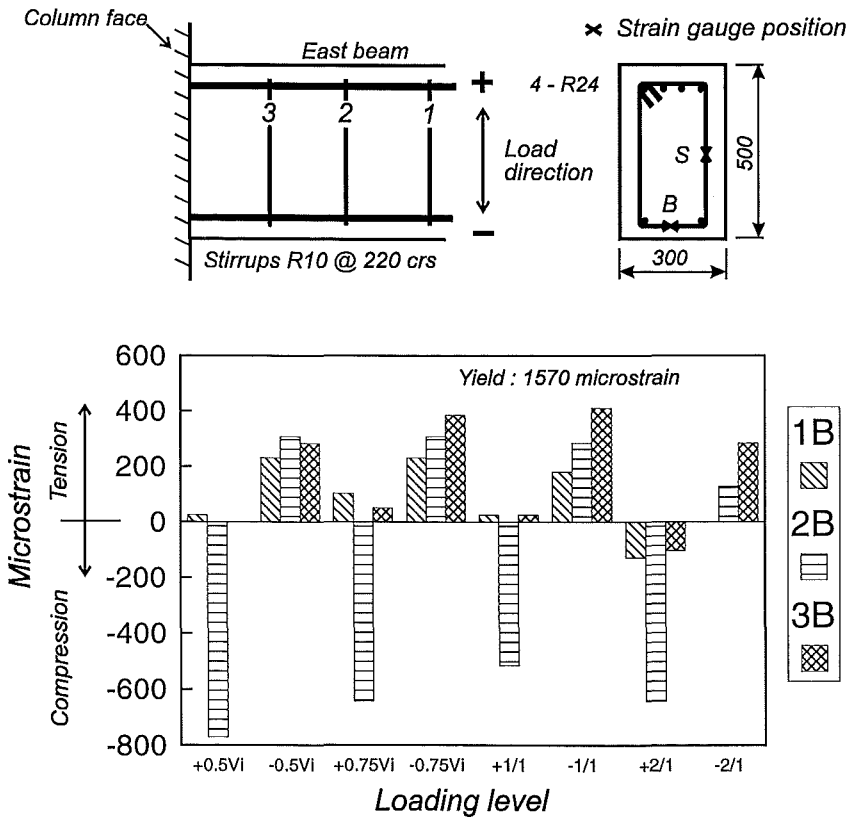

Fig. 5.27b Strains Recorded From the Bottom of the Stirrups in the East Beam

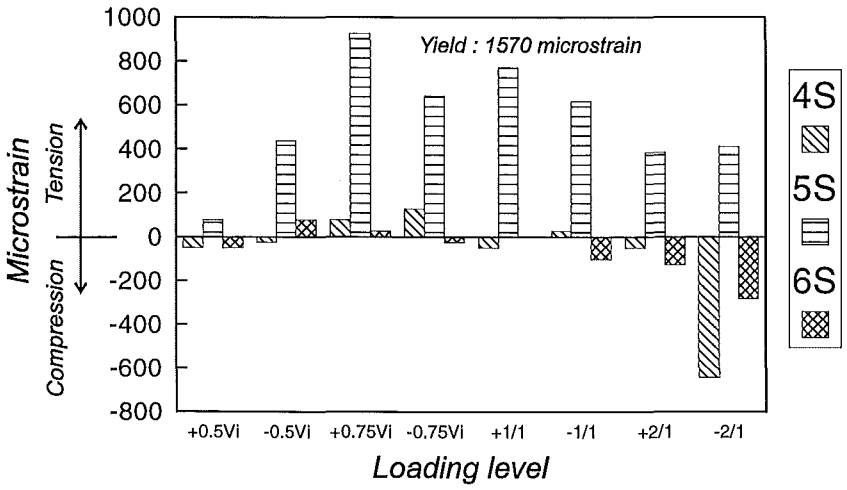

Fig. 5.28a Strains Recorded from the Sides of the Stirrups in the West Beam

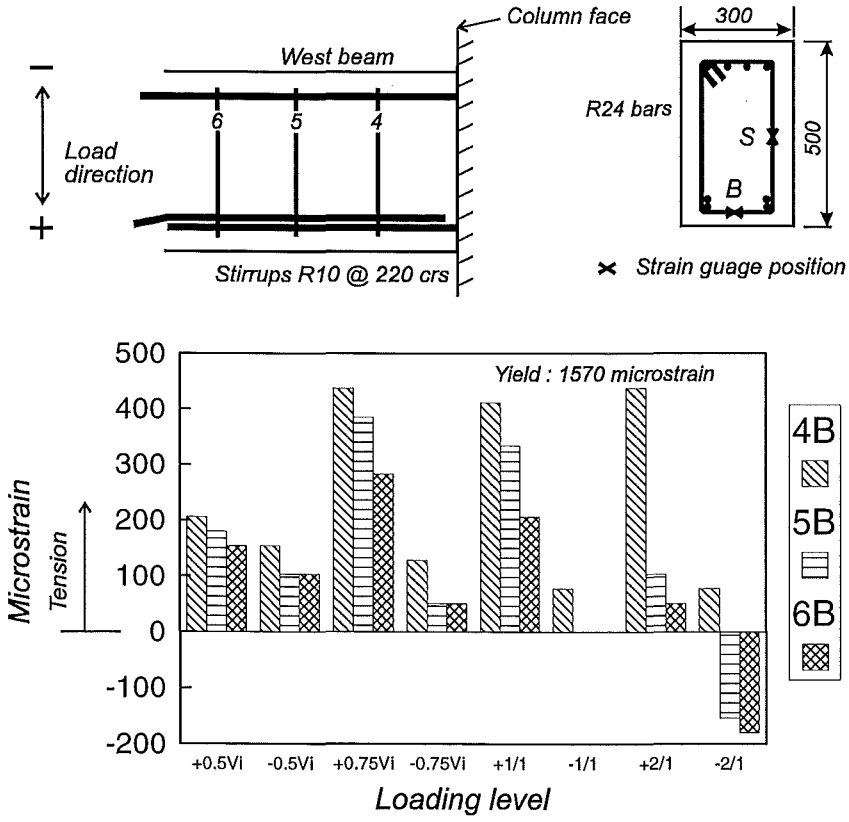

Fig. 5.28b Strains Recorded by the Bottom of the Stirrups in the West Beam.

The results from strain gauges on the side and bottom legs of the three stirrups in the west beam are shown in Figures 5.28a and 5.28b respectively. The gauges on the side of the stirrups carried very little load with the exception of 5S. Gauges on the bottom leg of the stirrups recorded the greatest strains for the positive ductility factors when the west beam resisted the majority of the load in the specimen. Again some confinement is assumed to have been provided to the concrete in compression at the bottom of the beam.

5.3.4 Column and Joint Behaviour

Joint bar slip

Figure 5.29 plots the slip of a top bar in the joint against the column top shear force. Considerable similarities can be seen between this and the load-displacement relationship in Fig. 5.18 as the bar slip occurred readily with movement of the specimen. From the first run to + $0.5V_j$ the bond was lost and tension strains developed in the top bars in the east beam .

The slip of a bottom bar through the joint is shown in figure 5.30. Only the positive displacements produced large amounts of slip through the joint as the bar was anchored at the end of the east beam. The crack between the east beam and the column face offset the position of the bar in the joint giving positive slip at μ = -4/1. The loss of bond between the spliced bars prevented slip occurring during the negative displacement cycles.

Column Longitudinal and Joint Vertical Reinforcement

With the loss of bond around the beam bars only compression loads from the top of one beam and the bottom of the second beam were applied to the joint. The profile of the longitudinal column bar strains includes the results from the strain gauges on the vertical joint reinforcement. Two D12 bars were placed as joint reinforcement between the HD24 longitudinal column bars. Apart from a strain gauge at the lower beam face which was lost during casting, the gauges completed the test.

Figure 5.31 plots the bar strains at the beam faces above and below the joint. In each case the bar strains did not develop beyond those recorded for the $\pm 0.75V_j$ load cycle. The maximum

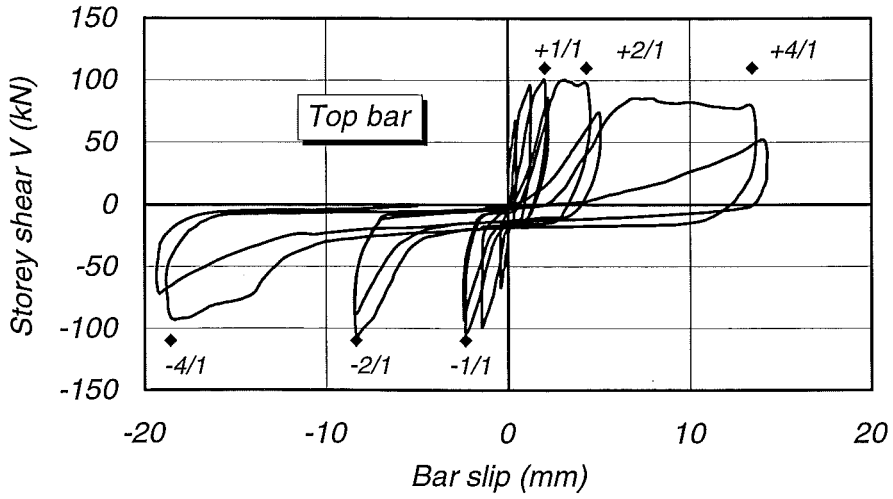

Fig. 5.29 Slip of a Top Longitudinal Beam Bar Through the Joint.

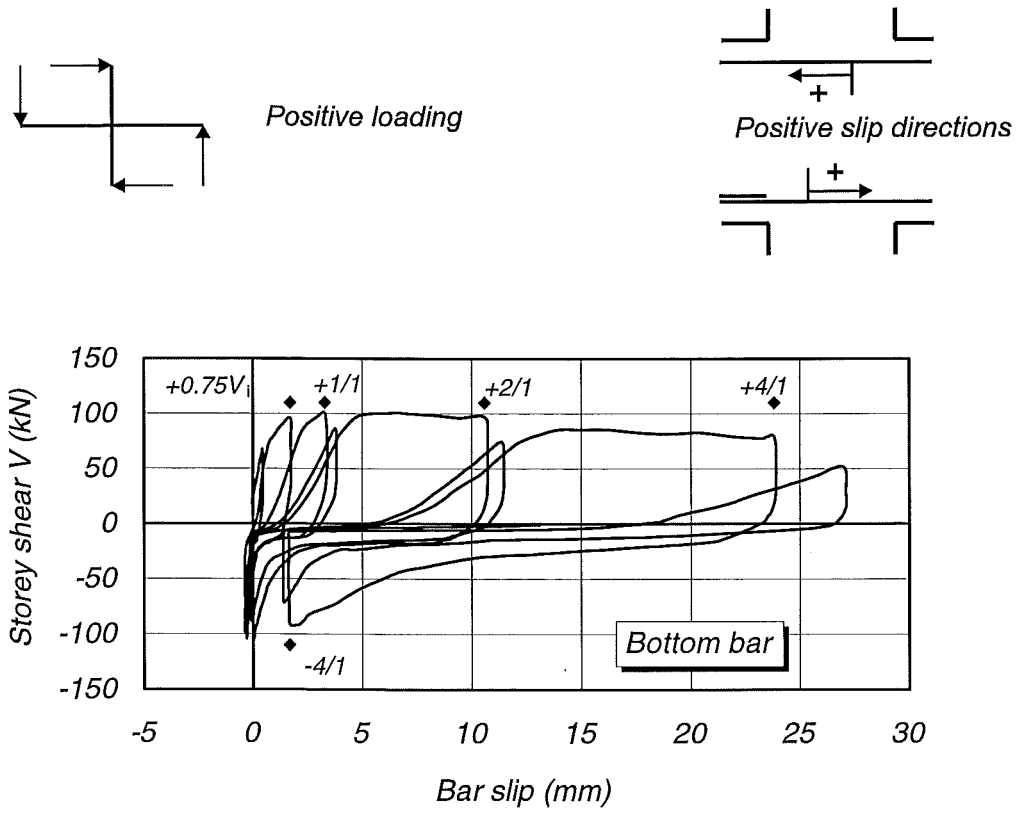

Fig. 5.30 Slip of a Bottom Longitudinal Beam Bar Through the Joint.

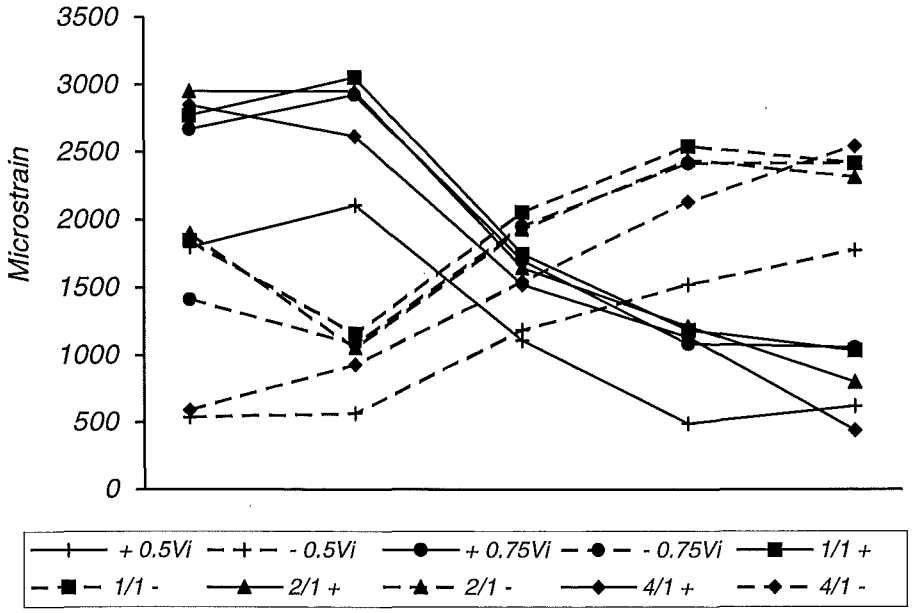

Above the joint.

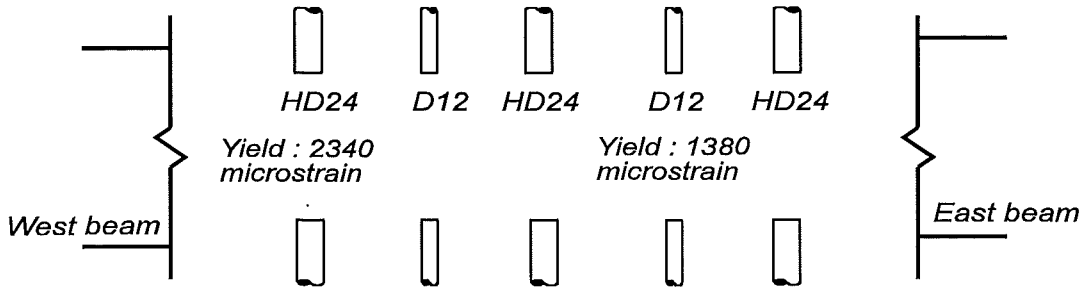

Below the joint.

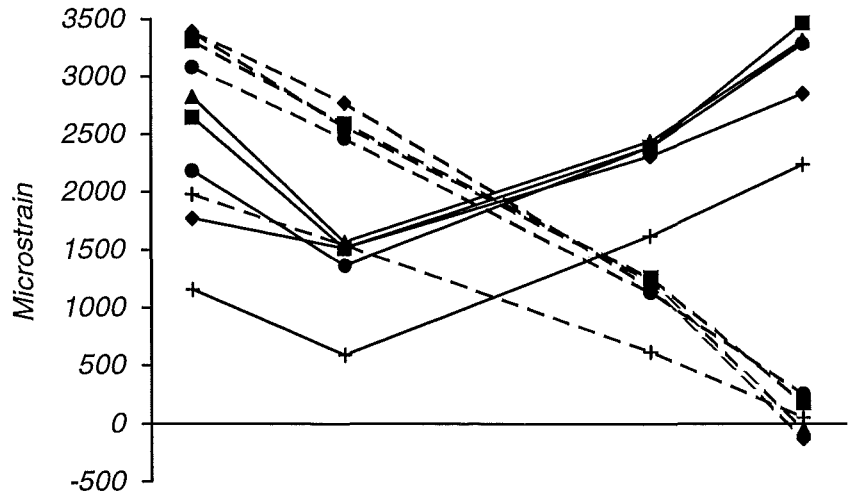

Fig 5.31 Strains Recorded From Column and Joint Reinforcing Bars.

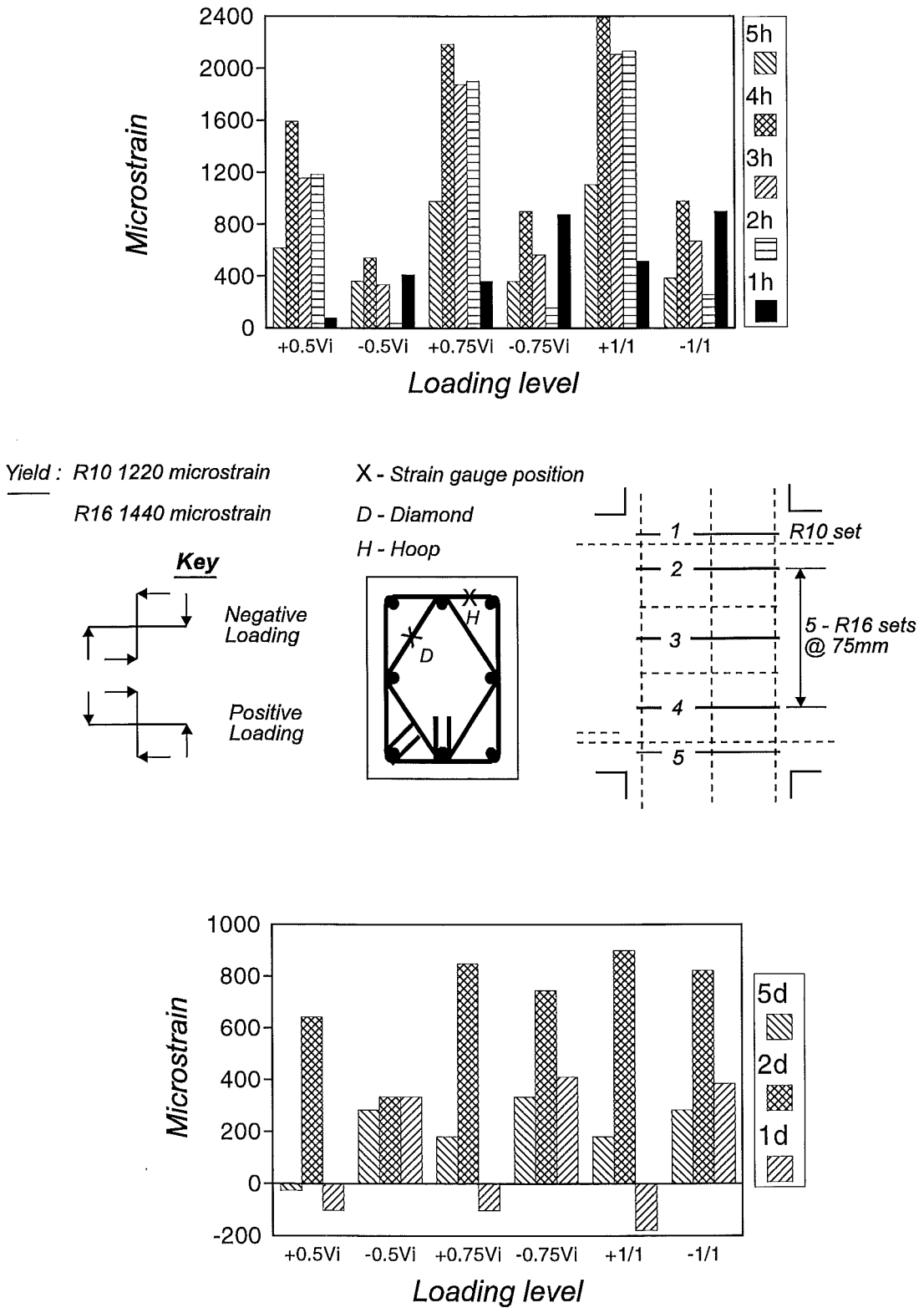

Fig 5.32 Strains Recorded by the Column and Joint Transverse Reinforcement.

bar strains recorded exceeded the yield strain of the bars. However, no strain gauges showed sign of inelastic strains. The maximum load resisted by the specimen was $0.79V_i$.

Column and Joint Transverse Reinforcement

Strain gauges were attached to diamonds and hoops of the column and joint transverse reinforcement. One set of column transverse reinforcement above and below the joint and three of the five sets in the joint were strain gauged. Figure 5.32 displays the strains recorded by the gauges. Two strain gauges on diamond transverse reinforcement in the joint were damaged during construction and did not begin the test. The remaining gauges completed the test but were affected by zero shift problems from other gauges.

The strains recorded by the gauges on the column transverse steel were low due to the moderate loads resisted by the column and the lack of column deterioration. The hoops which covered the width of the column recorded larger strains than the diamonds around the middle longitudinal bars.

The small joint depth left a steep angle for the diagonal concrete compression strut and cracking appeared in the joint from the first cycle. The lack of significant bond forces from the plain longitudinal beam bars minimised any further demands on the joint.

The joint reinforcement hoops which were monitored developed strains for the positive ductility factors twice as large as those for the negative ductility factors. It is assumed that some of the reinforcement not monitored with strain gauges took the greater proportion of strains during the negative displacements. The strains recorded by some of the bars exceeded the yield strain although, upon unloading, the results showed little sign of inelastic strain.

5.4 CONCLUSION

The splices of the deformed longitudinal beam bars in Specimen One resisted several cycles of increasing load, including two generating inelastic tensile strains, before they came apart due to the deterioration of the bond conditions in the splice. The specimen carried reduced loads during the subsequent negative displacements and its stiffness between the remaining displacements decreased.

The slip of the plain longitudinal beam bars through the joint of Specimen Two occurred from the first cycle of loading. An alternative lateral load resistance mechanism evolved for the specimen using the anchorage available from the test rig. A true test of the performance available with the plain longitudinal bars was not possible, but the results suggest there was a considerable lack of strength and stiffness in the specimen.

CHAPTER SIX

DISCUSSION AND CONCLUSIONS

6.1 GENERAL

A study of the seismic behaviour of two cruciform subassemblages containing lap splices in the beam potential plastic hinge regions has been conducted.

A discussion of each specimen's performance and the conclusions are presented in this chapter.

6.2 BEHAVIOUR OF SPECIMEN ONE

6.2.1 The Specimen

Specimen One was designed to the previous New Zealand concrete design code, NZS 3101:1982 [2], with the exception of the placement of two lap splices in the deformed longitudinal bars in the potential plastic hinge region of a beam. A review of the development length requirements from the present concrete code, NZS 3101:1995 [30] for deformed bar reinforcement has shown the required length of similar lap splices is unchanged.

6.2.2 Specimen Performance

The stiffness of the specimen differed for each direction of loading at $0.75V_i$. The displacement at the top of the column for the negative direction was 14.2 mm, 37% larger than the 10.4 mm displacement in the positive direction. An average slip of 0.15 mm was recorded in the two splices at the negative loading peak of this cycle. The potentiometers were placed 350 mm from the column face. The largest slip in the lap splices is likely to have occurred at the column face and this is considered to have been a factor in the greater column top displacement at - $0.75V_i$.

The column-top displacements at $\pm 0.75V_i$ were multiplied for the ductility factors that followed without being averaged. This maintained the larger displacements recorded for the specimen in the negative loading direction for the subsequent displacement controlled cycles.

The stiffness of the specimen changed with the displacements to $\mu = \pm 1$. The loads recorded in the positive displacement direction were $0.92V_i$ and $0.85V_i$, for the first and second cycle respectively. The load recorded for the negative displacement in the first cycle was - $1.1V_i$, the maximum lateral load resisted by the specimen to this point in the test. This established $0.88V_i$ as 80% of the maximum measured lateral load and the load criteria for determining the structural ductility factor [35] for the subassemblage. In the following displacement to $\mu = + 1/2$ the specimen resisted a maximum lateral load of $0.85V_i$, which failed to meet the required performance criterion. This may be unduly conservative as the two extremes of load resisted at $\mu = \pm 1$ would have been less if the original displacement values at $\pm 0.75V_i$ were averaged. The next ductility factor at which the load resisted by the specimen fell below $0.88V_i$ was at $\mu =$ - 4/1, when the lateral load resisted by the specimen was - $0.87V_i$. A review of the structural ductility available in the specimen is completed for both of these cases.

If the initial case is taken as critical, then the cumulative structural ductility factor $\sum \mu$ [35] will have been 2. If it is considered too conservative to judge the load at $\mu = + 1/2$ as critical, then a value for $\sum \mu$ of 18 is calculated for the loss of load during displacements to $\mu = - 4/1$. This figure indicates the available structure (displacement) ductility factor is $\mu_a = 2.25$. In each case the specimen has not demonstrated sufficient ductility to be categorised as a ductile structure.

For the negative displacements after $\mu = - 4/1$ the west beam carried less than one-third of its ideal strength. The load resisted by the specimen in subsequent negative displacements fell from - $0.78V_i$ at $\mu = - 4/2$ to - $0.36V_i$ at $\mu = - 8/2$. The east beam was forced to resist the majority of the load during the negative displacements. Minimal support was available from the west beam during positive loading until the previous limits of displacement were approached. This enabled the cracks in the bottom of the west beam to close and generate compression forces. By the end of testing the condition of the east beam had deteriorated severely. Without transverse reinforcement to resist the full shear force on the beam it would have failed.

The New Zealand loadings code NZS 4203:1992 [34] provides limits on interstorey deflections for the design of multistorey buildings. The maximum interstorey deflection allowed is a 0.02 fraction of the storey height which is equivalent to a drift angle of 2%. From the load displacement relationship the specimen passed a drift angle of 2% during displacements to the ductility factors $\mu = \pm 4$. A complete explanation for the lack of stiffness in the specimen is unable to be provided. However, as previously discussed, the slip in the splices during the loading at - $0.75V_i$ is one factor.

The lateral load resisted by the specimen at μ = - 2/2, before the failure of the splices was - $1.02V_i$. When the splices came apart at μ = - 4/1 the lateral load resisted by the specimen was - $0.87V_i$. Initially, the negative load resisted by the east beam increased with the failure of the splices, to offset the loss of west beam load capacity. The lap spliced reinforcement in the specimen represented one-third of the beam tension reinforcement available to resist lateral loads in the negative direction. If a larger portion of the reinforcement had been lap spliced the lateral load capacity of the specimen would have been further reduced.

6.2.3 Splice Performance

Horizontal cracking first appeared between the spliced bars during the two displacements to μ = - 1. Flexural cracks, especially at the free ends of the splices, increased the concrete circumferential tensile stresses around the bars, initiating the longitudinal splitting cracks.

Increasing negative displacements concentrated the curvature of the west beam at the end of the splice with the maximum bending moment. Strain gauge results show large inelastic tensile strains developed in both lower spliced bars at the column face during the two displacements to μ = - 2. The increased bond stresses and the dowel forces on the lower bar in each splice increased the cracking and the slip between the spliced bars.

Horizontal cracking between the bars covered 90% of the length of the splices at μ = - 2/2. At this point the stirrups surrounding the splices did not appear to have yielded. Regardless of this, a reduction in the spacing of the transverse reinforcing steel is likely to have provided further confinement to the splice length. Previous research [15] has revealed that splices with sufficient transverse steel are able to sustain a number of cycles after extensive splitting as bond transfer is improved, limiting the yield penetration of the bars into the splice.

The area of transverse steel provided for the splice exceeded the current code requirements for splice confinement by 30%. In concrete structures the function of the transverse reinforcement for splice confinement is to provide adequate clamping between the spliced bars, enabling the transfer of the bar forces by shear friction across a crack between two bars. These requirements are formed to ensure that lap splices in column members prepared to capacity design principles can satisfactorily sustain a number of reversed cyclic loads just below the ideal strength of the member. In these members the spliced bars will not be required to transmit yield forces [24]. Similarly detailed splices in beams are expected to demonstrate satisfactory behaviour as they are precluded from areas with the potential to develop inelastic reversing stresses.

During each of the displacement runs to μ = - 1 and - 2 the west beam exceeded 90% of its ideal member strength. The maximum load placing the splice in tension was 97% of the ideal member strength at μ = -1/1. Displacements to μ = - 4/1 split the remaining intact concrete cover around the splices and the anchorage for the spliced bars failed. The two previous displacements to μ = - 2 had generated yield forces at the end of the splices beside the column face. The number of these cycles the splices could resist was very limited. A concrete crack 5 - 6 mm wide formed between the spliced bars indicating some of the stirrups had yielded. This longitudinal splitting had occurred over the beam width on a line between the bars of each splice. The load resisted by the west beam began to drop steadily as the splices were pulled apart. A complete loss of load capacity did not occur in the west beam as the stirrups maintained some clamping force between the spliced bars. In the following negative displacements the west beam maintained approximately 30% of the ideal beam strength.

The slip between each pair of spliced bars as they came apart was the maximum recorded to that point in the test. The negative displacements since μ = - 1/1 had generated increasingly larger values of slip in the splices before the west beam supported the previous levels of load. As splitting progressed the length of the splices, the slip between the bars increased. The application of load in the opposite direction required the recovery of the slip before the bar deformations could bear upon concrete.

The lap splices responded differently in resisting the load at the end of the west beam. One splice was cast with 48 mm of concrete placed above the bars, the second lap splice was placed in the bottom of the beam formwork with 228 mm of concrete placed over the splice. The total depth of concrete cast for the beams was 300 mm. The splice cast in the top of the

beam consistently recorded the largest values of slip. When the load in the west beam began to decrease as the splices came apart, this splice was recording slip four times greater than the other splice.

The difference in the behaviour of the splices was reflected in the strains recorded at the column face from each bottom longitudinal bar. Initially, the bar cast in the bottom of the formwork developed greater strains at the column face. Better bond conditions concentrated the strains over a shorter bar length. Once the splitting increased in the splices this difference disappeared. Despite the differences in slip, both bars recorded inelastic tensile strains at the column face during the displacement peaks at $\mu = -2$.

In the casting of reinforced concrete members sedimentation and water gain is expected to increase under horizontally laid top-cast bars. In this specimen a soft and porous layer of concrete is likely to have formed as the concrete set beneath the top-cast lap splice. This will have limited the amount of bearing resistance from the concrete for the bar ribs and increased the possibility for bar slip.

Previous and current New Zealand concrete design codes [2,30] specify a 30% increase in bar development length where more than 300 mm of fresh concrete is cast beneath the bars. The depth of concrete cast in the beams was 300 mm so the requirement did not apply in the design. As lap splices and the development length of longitudinal bars are prohibited by the design codes from being placed in this region this is an unnecessarily rigorous examination of the top bar effect.

Initially, in compression the splices performed satisfactory. Little slip occurred in the splices before the maximum positive load was reached as most of this slip had been recovered as the beam unloaded from the previous negative displacement. The transfer of compression forces into the spliced bars was dominated by concrete bearing onto the bar ends. The spliced bars emerging from the joint recorded the largest compression strains. Strain gauges 65 mm from the end of these bars recorded up to 70% of the maximum compression strain developed in the bars over the splice length. Once the splices had come apart, the concrete cover at each end of the splices was loosened or lost, enabling the spliced bars to close further than they had previously. This contributed to a loss of stiffness in the west beam during the positive displacements.

The bond conditions [1] are superior for a bar in compression because of the absence of flexural cracks and the helpful effect of end bearing. For this reason, the development length for a bar in compression is less than the development length in tension. In the design of the splice the beneficial effects of transverse steel for controlling splitting cracks were used to reduce the development and splice lengths in tension. The splice length for the specimen was governed by the minimum length for a lap splice in compression. The testing of the specimen indicated the transverse steel was unable to maintain sufficient clamping force across the crack between the spliced bars.

6.3 BEHAVIOUR OF SPECIMEN TWO

6.3.1 The Specimen

Specimen Two modelled the lap splices in the plain round longitudinal bars in the potential plastic hinge region of the beam of a building constructed in the early 1960s. The column and joint designs complied with NZS 3101:1982.

6.3.2 Specimen Performance

Strain gauges on the longitudinal bars of Specimen Two recorded the gradual penetration of tensile strains through the joint and into the opposite beam as the specimen was loaded to $+ 0.5V_i$. In the subsequent cycles the specimen lost stiffness as the longitudinal bars slipped through the joint with each direction of loading. At $\mu = \pm 1$ a clip gauge indicated the yield strain had been exceeded in a top beam bar, 300 mm away from its anchorage at the end of the beam. Due to the loss of bond from the bars, the testing of the specimen had become dominated by the anchorage that was available for the bars from the test rig and further results were of limited value.

The interstorey deflection limits in the New Zealand loadings code NZS 4203:1992 [34] for the design of multistorey buildings allow a maximum drift angle of 2%. For displacements in the positive direction this limit was passed as $\mu = + 1$ was reached. Due to the difference in the ductility factors the displacement at $\mu = - 1$ was equivalent to a drift angle of 1.80%. These figures indicate insufficient stiffness existed in the specimen.

Slip occurred in the splices to accommodate the fixed end rotations of the beams and yielding in the top longitudinal bars. The lap splices are considered to have contributed to the lack of stiffness in the specimen. It is suggested that without the lap splices a similarly tested specimen would have lost bond from the top and bottom sets of longitudinal beam steel. The loss of bond is unlikely to have been as rapid as both sets of bars would have been able to develop tension strains. With a probable increase in the load resistance of the specimen, the displacements required to reach the $\pm 0.75V_i$ loading levels may have been reduced.

Any statements or values describing the performance of Specimen Two are given tentatively as they are not intended to indicate a satisfactory test. As the test rig is assumed to have improved the performance of the specimen, the results should be viewed in that light. Any results during and after $\mu = \pm 1$ are thought to have been influenced by the test rig. Strains just below the bar yield strain were recorded at one clip gauge location at $\pm 0.75V_i$. At this level it is debatable whether the top beam bars were receiving excessive anchorage from the end plate of the west beam.

The loads at $\pm 0.75V_i$ may be considered the maximum loads recorded by the specimen. The specimen was unable to exceed this during displacements at $\mu = \pm 1$. The maximum load recorded during the test, $- 0.79V_i$, was achieved with the influence of the test rig. Higher levels of load might have been possible if the initial load cycles had been higher when bond deterioration was at a minimum.

The presentation of any values defining the ductility available from the specimen is avoided as it would represent test data generated with the benefits of the test rig. Viewing the lateral load-displacement relationship of the specimen, and considering the method in which it was obtained, the specimen is considered to have low levels of displacement ductility and lateral load resistance.

6.3.3 Bond Considerations for Plain Bars

The loss of bond from the plain bars began during displacements to the first loading peak, before any load reversals. Loading the specimen to $+ 0.5V_i$ placed the lap splices in compression. The loss of bond from the top longitudinal beam bars was not attributed to the presence of the lap splices. The use of plain bars for longitudinal reinforcement is

discouraged because of the effects of cyclic loading on bond for the bars. In this case cyclic loading was not a factor; the bars slipped through the joint because they had insufficient anchorage.

A bar slipped once the bond stresses at a point exceeded the adhesion capacity between the bar and the surrounding concrete. The only component of bond resistance left at that point of the bar was frictional resistance to slip. The bond deterioration continued along the bars as this component was insufficient to resist the bond stresses. Once the loss of bond transfer began, the inverted concrete arch mechanism would have started to form. The transition from beam action to arch action was gradual as the bar slip increased to allow the full extent of the arch action to develop.

The original column width of 305 mm was increased to 340 mm so that the design of the columns and joint met the capacity design requirements of NZS 3101:1982. This column depth left a h_c / d_b ratio of 14.2 for the longitudinal beam bars through the joint. A ratio of 20.7 is considered suitable [30] for Grade 300 deformed bars to ensure they do not prematurely slip through a joint during intense cyclic loading, when plastic hinging can develop at the column faces and with f'_c = 30 MPa. The rapid loss of bond for the plain bars through the joint is understandable.

Splitting cracks are a typical sign of the loss of anchorage for a deformed bar without large amounts of concrete cover. The plain bars did not give any visible signs of a loss of anchorage as the energy required to break the adhesion did not crack the surrounding concrete. Transverse reinforcement is used in the calculation of the development lengths for deformed bars as they represent a confining force across any splitting cracks around a developing bar. As little longitudinal splitting is associated with the loss of anchorage for the plain bars the influence of the transverse reinforcement for bond resistance is minimal.

The lack of an external axial load on the column provided conservative conditions for the longitudinal bars through the joint. Additional confinement from compressive forces normal to the bars might have limited the rate of bond deterioration by providing an increase in the frictional bond resistance. However, as bond was lost early in the test any such confinement for the bars may have been overcome with higher levels of load in the bars.

The strain gauged top longitudinal bar which displayed the loss of bond at + $0.5V_i$ was cast 180 mm below the top of the concrete. With a total depth of concrete cast of 300 mm the bar should not have been experiencing any bond problems associated with the top bar effect.

Several research projects [35,36] completed at the Civil Engineering Department of the University of Canterbury have investigated the behaviour of subassemblages reinforced with plain longitudinal reinforcement. Inadequate bond between the longitudinal bars and the concrete, low displacement ductility factors, and significant reductions in strength during testing are common characteristics of these tests. This behaviour was apparent in the test results of Specimen Two. The rate of bond deterioration from the plain bars was surprisingly rapid and led to unanticipated cooperation between the specimen and the test rig to resist the applied lateral load.

Any future testing investigating existing structures with plain longitudinal reinforcing bars should be prepared so that results obtained from the testing are not affected by the behaviour of the test rig. The problem of providing suitable anchorage at the member ends of the specimen to reflect the actual conditions in an structure will require attention. One possibility is the use of a hook to anchor each bar, especially if hooks have been used for the termination of the bars in the existing structure. This method would not be suitable where bars have been lapped in an existing structure. When the anchorage for testing involves the welding or bolting of the longitudinal bars to plates at the end of a member, the bars should be monitored near the connections to indicate the level of any restraint developed.

Specimen Two tested plain bar lap splices located in the potential plastic hinge region of a beam. Bond was lost from the top longitudinal bars over a beam length of 1585 mm during the first three cycles of moderate loading. The amount of bond which may be lost during a couple of severe seismic cycles could involve considerably greater lengths of bar. This may expose lap splices located beyond the potential plastic hinge regions of members. Of particular concern is any members in which all or a large portion of the longitudinal steel is lap spliced at a cross section. Any members required to resist tensile loads across a set of lap spliced plain bars may separate if the bond has deteriorated over the splice lengths.

6.4 CONCLUSIONS

A beam-column subassemblage designed to NZS 3101:1982 but containing lap spliced deformed bar reinforcement in a beam potential plastic hinge region displayed low specimen ductility during simulated seismic loading. Deteriorating behaviour in the splices began during the initial negative displacement ductility factors and the splice failures led to a loss of beam and specimen load capacity. The potential for a large loss of lateral load capacity existed if the lapped spliced reinforcement represented a significant portion of the total tension beam reinforcement.

The present transverse reinforcing steel requirements for the confinement of deformed bar lap splices are not sufficient to allow ductile behaviour from members containing splices in regions of inelastic reversing stresses.

Current code requirements prevent the placement of lap splices in potential plastic hinge regions. On the basis of this testing these requirements should not be changed.

A beam-column subassemblage examining the behaviour of lap splice beam details for plain round bars from a building constructed in the early 1960's displayed insufficient stiffness, ductility and strength during simulated seismic loading.

Bond for plain longitudinal beam bars was lost from the first loading cycle due to insufficient anchorage within the beam-column joint depth. Further load cycles increased the loss of bond and enabled the specimen to obtain unanticipated anchorage from the testing rig.

Any further research into the performance of plain bar reinforced subassemblages should attempt to replicate the type of anchorage available for the bars in a prototype structure, or at least monitor the restraint obtained at the member end connections.

APPENDIX : NZS 3101:1982 AND NZS 3101:1995 LAP SPLICE REQUIREMENTS

The design of Specimen One was completed with NZS 3101:1982 including Amendment No. 1 produced in December 1989. The following calculations give a comparison of the development length and lap splice requirements from NZS 3101:1982 and the more recent design code NZS 3101:1995.

NZS 3101:1982 Requirements

Basic Development Length in Tension $l_{db} = \dfrac{380 A_b}{c\sqrt{f_c'}}$ [NZS 3101:1982, Eq. 5-6]

Longitudinal beam D24 bars.

$$l_{db} = \frac{380 \times 452}{60 \times \sqrt{30}} = 523\ mm$$

Modification factors: [NZS 3101:1982, Cl. 5.3.7.3]

Longitudinal and transverse bar yield strengths = 300 MPa.

Beam cast on its side, all bars with less than 300 mm of fresh concrete beneath.

Transverse reinforcement factor. $\dfrac{c}{c + k_{tr}}$ where $k_{tr} = \dfrac{A_{tr} f_{yt}}{10s}$

R10 bars at 120 mm centres. $= \dfrac{78.5 \times 300}{10 \times 120} = 19.63$

$c \le c_c = c_s = 60\ mm$

$c,\ c + k_{tr} \not> 3d_b = 72\ mm$ $\qquad \dfrac{c}{c + k_{tr}} = \dfrac{60}{72} = 0.83$

Development Length in Tension [NZS 3101:1982, Cl 5.3.7.1]

$$l_d = 0.83 \times 523\ mm = 434\ mm$$

Basic Development Length in Compression

[NZS 3101:1982, Amendment No.1, Dec. 1989, Cl 5.3.9.2]

$$l_{db} = \frac{0.22 d_b f_y}{\sqrt{f_c'}}$$

Longitudinal beam D24 bars.

$$l_{db} = \frac{0.22 \text{x} 24 \text{x} 300}{\sqrt{30}} = 289 \ mm$$

Modification Factor: [NZS 3101:1982, Cl 5.3.9.3]

Transverse Reinforcement Factor $\frac{A_{tr}}{s} \geq \frac{A_b}{1000}$

R10 bars at 120 mm centres. $\frac{78.5}{120} \geq \frac{452}{1000}$ $0.65 \geq 0.45$

Multiplication factor : 0.75

Development Length in Compression [NZS 3101:1982, Cl 5.3.9.1]

$$l_d = 0.75 \text{x} 289 \ mm = 217 \ mm$$

Lap Splices of Bars in Tension [NZS 3101:1982, Cl 5.3.18.1]

The minimum length for lap splices in tension was the development length $l_d = 434 \ mm$.

Lap Splices of Bars in Compression

[NZS 3101:1982, Amendment No.1, Dec. 1989, Cl 5.3.20.1]

The minimum length of a lap splice in compression was the development length in compression $l_d = 217 \ mm$, but not less than $0.067 f_y d_b$ for f_y of 430 MPa or less.

$0.067 f_y d_b = 0.067 \text{x} 300 \text{x} 24 = 482 \ mm$ Critical, use a splice length of 485 mm.

NZS 3101:1995 Requirements

Basic Development Length in Tension $L_{db} = \dfrac{0.5\alpha_a f_y}{\sqrt{f'_c}} d_b$ [NZS 3101:1995, Eq. 7-2]

Longitudinal beam D24 bars, $\alpha_a = 1.0$ for reinforcement cast with 300 mm or less of fresh concrete cast beneath.

$$L_{db} = \frac{0.5 \times 1.0 \times 300 \times 24}{\sqrt{30}} = 657 \text{ mm}$$

Development Length in Tension [NZS 3101:1995, Eq. 7-3]

$$L_d = \frac{\alpha_b}{\alpha_c \alpha_d} L_{db} \geq 300 \text{ mm}$$

For a member subjected to seismic forces $\alpha_b = 1.0$.

Cover to the bars = 48 mm ($> 1.5 d_b$) $\alpha_c = 1 + 0.5\left(\dfrac{c_m}{d_b} - 1.5\right)$

$$= 1 + 0.5\left(\frac{48}{24} - 1.5\right) = 1.25$$

Assuming four R10 stirrups spaced at 120 mm centres transverse to the spliced bars.

$$\alpha_d = 1 + \sqrt{\frac{A_{tr}}{s}\frac{f_{yt}}{80 n_L d_b}} = 1 + \sqrt{\frac{78.5}{120}\frac{300}{80 \times 4 \times 24}} = 1.16$$

Development Length $L_d = \dfrac{1.0}{1.25 \times 1.16} \times 657 \text{ mm} = 453 \text{ mm}$

Basic Development Length in Compression [NZS 3101:1995, Eq 7-6]

$$L_{db} = \frac{0.22 f_y}{\sqrt{f'_c}} d_b$$

Unchanged from NZS 3101:1982 = 289 mm

Development Length in Compression $L_d = \alpha_b \alpha_e L_{db}$ [NZS 3101:1995, Eq 7-8]

For a member subjected to seismic forces $\alpha_b = 1.0$.

Transverse reinforcement factor, $\alpha_e = 0.75$ where $\frac{A_{tr}}{s} \geq \frac{A_s}{600}$

$\frac{78.5}{120} \not\geq \frac{4x452}{600}$ therefore $\alpha_e = 1.0$.

$$L_d = 1.0x1.0x289\ mm = 289\ mm$$

Lap Splices of Bars in Tension [NZS 3101:1995, Cl 7.3.17.1]

The minimum length of lap splices in tension is the development length
$L_d = 453\ mm$

Lap Splices of Bars in Compression [NZS 3101:1982, Cl 7.3.19.1]

The minimum length of a lap splice in compression is the development length in compression, $L_d = 289\ mm$ but not less than $0.067 f_y d_b$ for f_y of 430 MPa or less. Unchanged from NZS 3101:1982, the minimum splice length = 482 mm and remains critical for splice length.

REFERENCES

1. Park, R. and Paulay, T., "Reinforced Concrete Structures", John Wiley and Sons, New York, 1975.

2. New Zealand Standard Code of Practice for the Design of Concrete Structures, NZS 3101, Part 1 : 1982.

3. ACI Committee 318, "Building Code Requirements for Reinforced Concrete (ACI 318-89)" , American Concrete Institute, Detroit, 1992.

4. Lutz, L.A. and Gergely, P., "Mechanics of Bond Slip of Deformed Bars in Concrete", ACI Journal, Vol. 64, No. 11, Nov. 1967, pp.711-721.

5. Orangun, C.O., Jirsa, J.O. and Breen, J.E., "A Re-evaluation of Test Data on Development Length and Splices", ACI Journal, Vol. 74, No. 3, March 1977, pp. 114-122.

6. ACI Committee 408, "Abstract of : State-of-the-Art-Report : Bond Under Cyclic Loads", ACI Materials Journal, Vol 88, No. 6, Nov-Dec. 1991, pp.669-673.

7. Chinn, J., Ferguson, P.M. and Thompson, J.N., "Lapped Splices in Reinforced concrete Beams", ACI Journal, Vol. 52, Oct. 1955, pp.201-214.

8. Tepfers, R., "A Theory of Bond Applied to Overlapped Tensile Reinforcement for Deformed Bars", Publication 73:2. Division of Concrete Structures, Chalmers University of Technology, Sweden, 1973.

9. Morita, S. and Kaku, T., "Splitting Bond Failures of Large Deformed Reinforcing Bars", ACI Journal, Vol. 76, No. 1, Jan. 1979, pp.93-110.

10. Rezansoff, T., Zacaruk, J.A. and Topping, R., "Tensile Lap Splices in Reinforced Concrete Beams under Inelastic Cyclic Loading", ACI Structural Journal, Vol. 85, No.1, Jan-Feb 1988, pp.46-52.

11. Rezansoff, T., "Performance of Lapped Splices in Reinforced Concrete Loaded Beyond Yielding of the Steel", Canadian Journal of Civil Engineering, Vol. 5, No. 4, Dec. 1978, pp 489-496.

12. Goto, Y., "Cracks Formed in Concrete Around Deformed Tension Bars", ACI Journal, Vol. 68, No. 4, April 1971, pp.245-250.

13. Sivakumar, B., Gergely, P. and White, R.N., "Suggestions for the Design of R/C Lapped Splices for Seismic Loading", Concrete International, Vol. 5, No. 2, Feb. 1983, pp.46-50.

14. Ferguson, P.M. and Breen, J.E., "Lapped Splices for High Strength Reinforcing Bars, ACI Journal, Vol.62, No.9, Sept. 1965, pp.1063-1078.

15. Gergely, P. and White, R.N., "Seismic Design of Lapped Splices in Reinforced Concrete", Proceedings of the 7th World Conference on Earthquake Engineering, Istanbul, 1980, Vol. 4, pp.281-288.

16. Tocci, A.D., Gergely, P. and White, R.N., "The Behaviour and Strength of Lapped Splices in Reinforced Concrete Beams Subjected to Cyclic Loading", Report No. 81-1, Department of Structural Engineering, Cornell University, Ithaca, 1981.

17. MacKay, B., Schmidt, D. and Rezansoff, T., "Effectiveness of Concrete Confinement on Lap Splice Performance in Concrete Beams Under Reversed Inelastic Loading", Canadian Journal of Civil Engineering, Vol. 16, No. 1, Feb. 1989, pp.36-44.

18. Lukose, K., Gergely, P. and White, R.N., "Behaviour of Reinforced Concrete Lapped Splices for Inelastic Cyclic Loading", ACI Journal, Vol.79, No. 5, Sept-Oct 1982, pp.355-365.

19. Rehm, G. and Eligehausen, R., "Bond of Ribbed Bars Under High Cycle Repeated Loads", ACI Journal, Vol.76, No.2, Feb. 1979, pp.297-309.

20. ACI Committee 408, "Suggested Development, Splice and Standard Hook Provisions for Deformed Bars in Tension", Report No. ACI 408. IR-79, Concrete International, Vol. 1, No. 7, July 1979, pp.44-46.

21 Fagundo, F., Gergely, P. and White, R.N.,"The Behaviour of Lapped Splices in R/C Beams Subjected to Repeated Loads", Report No.79-7, Department of Structural Engineering, Cornell University, Ithaca, 1981.

22. Sparling, B. and Rezansoff, T., "Effect of Confinement on Lap Splices in Reversed Cyclic Loading", Canadian Journal of Civil Engineering, Vol.13, No. 6 Dec. 1986, pp.681-692.

23. Panahshahi, N., White, R.N. and Gergely, P., "Reinforced Concrete Compression Lap Splices Under Inelastic Cyclic Loading", ACI Structural Journal, Vol.89, No. 2, Mar-Apr. 1992, pp.164-175.

24. Paulay, T., "Lapped Splices in Earthquake - Resisting Columns", ACI Journal, Vol. 79, No. 6, Nov-Dec. 1982, pp.458-469.

25. Paulay, T., Zanza, T.M., and Scarpas, A., "Lapped Splices in Bridge Piers and in Columns of Earthquake Resisting Reinforced Concrete Frames", Research Report No.81-6, Department of Civil Engineering, University of Canterbury, Christchurch, 1981.

26. Jirsa, J.O., Lutz, L.A. and Gergely, P., "Rationale for Suggested Development, Splice, and Standard Hook Provisions for Deformed Bars in Tension", Concrete International, Vol. 1, No. 7 July 1979, pp;47-61.

27. Draft New Zealand Standard Code of Practice for the Design of Concrete Structures, DZ 3101:1978.

28. New Zealand Standard Commentary on the Design of Concrete Structures, NZS 3101, Part 2: 1982.

29. New Zealand Standard Model Building Bylaw, NZS 1900 Chapter 9.3:1964.

30. New Zealand Standard Code of Practise for the Design of Concrete Structures, NZS 3101: Part 1: 1995

31. Bull, D.K., "Bond and Anchorage of Reinforcement in Concrete - A New Zealand Perspective",

32. Sozen, M.A. and Moehle, J.P.., "Development and Lap-splice Lengths for Deformed Reinforcing Bars in Concrete", Portland Cement Association and Concrete Reinforcing Steel Institute, 1990.

33. "Building Code Requirements for Reinforced Concrete and Commentary (ACI 318-89)", American Concrete Institute, Detroit, 1989.

34. General Structural Design and Design Loadings for Buildings, NZS 4203, 1992.

35. Park, R., "Evaluation of Ductility of Structures and Structural Assemblages From Laboratory Testing", Bulletin of the New Zealand National Society for Earthquake Engineering, Vol. 22, No.3, Sept. 1989.

36. Park, R. and Rodriguez, M., "Retrofitting of Reinforced Concrete Bridge Piers For Seismic Resistance", Seismic Assessment and Retrofit of Concrete Structures, Technical Report No. 12, New Zealand Concrete Society, May 1992.

37. Park, R. and Rodriguez, M., "Seismic Load Tests of Reinforced Concrete Columns Strengthened by Jacketing", Seismic Assessment and Retrofit of Concrete Structures, Technical Report No. 12, New Zealand Concrete Society, May 1992.